EXTRA-TROPICAL CYCLONE CLIMATOLOGY AND SHIFTS IN CLIMATE REGIME IN THE NORTHERN HEMISPHERE

by

ANDREW P. GRANT

B.Sc (Hons.) The University of Melbourne, 2000

A THESIS SUBMITTED IN PARTIAL FULFILMENT OF
THE REQUIREMENTS FOR THE DEGREE OF

MASTER OF SCIENCE

in

THE FACULTY OF GRADUATE STUDIES

Department of Earth and Ocean Sciences, Atmospheric Science Programme

We accept this thesis as conforming
to the required standard

THE UNIVERSITY OF BRITISH COLUMBIA

April, 2004

Library Authorization

In presenting this thesis in partial fulfillment of the requirements for an advanced degree at the University of British Columbia, I agree that the Library shall make it freely available for reference and study. I further agree that permission for extensive copying of this thesis for scholarly purposes may be granted by the head of my department or by his or her representatives. It is understood that copying or publication of this thesis for financial gain shall not be allowed without my written permission.

ANDREW GRANT — 22/04/2004

Name of Author *(please print)* — Date (dd/mm/yyyy)

Title of Thesis: Extra-tropical cyclone climatology and shifts in climate regime in the Northern Hemisphere

Degree: MSc Year: 2004

Department of Earth and Ocean Science.

The University of British Columbia
Vancouver, BC Canada

Abstract

Extra-tropical cyclones are an important feature of mid-latitude weather and climate. The interdecadal variability of extra-tropical cyclones is assessed here. This is undertaken with respect to changes in Northern Hemisphere atmospheric circulation associated with a shift in climate regime around 1976/77.

Data from the Goddard Institute of Space Studies (GISS) Atlas of Extra-tropical Cyclones and National Snow and Ice Data Centre (NSIDC) Arctic Cyclone Track Data Set are used to construct a climatology of cyclones and intense cyclones (those reaching a minimum sea level pressure less than 980hPa) in the Northern Hemisphere. Time series of cyclone data in various regions are analysed to assess relationships with indices representing the 1976/77 shift and changes in trend over the period investigated. The possibility of a second shift around 1989 is also investigated. Indices used are based on phases of the Pacific Decadal Oscillation (PDO). Emperical Orthogonal Function (EOF) analyses are also used to examine possible relationships with other climate indices such as the Arctic Oscillation (AO), North Atlantic Oscillation (NAO) and Southern Oscillation Index (SOI).
Analyses limited to specific regions are also undertaken to assess reliability of the data and the importance of specific regions to cyclone occurrence in the North Pacific.
Shifts in climate regime are also assessed with respect to changes in atmospheric circulation in the Northern Hemisphere. This is undertaken by analysing variability in a major feature of the circulation, the Siberian High.

The nature of the Siberian High is observed to change around the 1976/77 shift. Similar changes are also observed in cyclone frequency between different climate regime phases. Additionally, significant trends over the time period investigated are observed in cyclone and intense cyclone frequency in most regions of the Northern Hemisphere. These trends are most prevalent in intense cyclone frequency.
It is concluded that changes in atmospheric circulation associated with the 1976/77 regime shift affected the frequency of cyclones and intense cyclones in the Northern Hemisphere. Evidence suggests that this occurs on a hemispheric scale, though it is likely that effects of the 1989 event are limited to the Pacific region.

Table of Contents

Index of Tables and Figures

Acknowledgements

I would like to acknowledge the assistance and insight of my supervisor, Lionel Pandolfo, in the research and construction of this dissertation.

I would also like to thank William Hsieh for help with research-related questions and providing comments on a draft version of this thesis; and Roland Stull for acting as an external examiner.

Aiming Wu provided assistance and valued advice on methods of EOF analysis with respect to the North Pacific region.

I am also grateful to the Department of Earth and Ocean Science and School of Graduate Studies at the University of British Columbia for support and financial assistance.

1. Introduction.

Extra-tropical cyclones are an important and prominent feature of mid-latitude weather and climate. Variability in properties associated with cyclone development and propagation have been linked to a range of important climatic factors such as precipitation and the hydrologic cycle (Cayan and Peterson, 1989; Chen et al., 1996), as well as temperature and wind patterns (Dettinger and Cayan, 1995). In turn, the influence of cyclones on these parameters can lead to severe weather-related events such as flooding and landslides (as outlined by Droegemeier et al., 2000).

In addition to influencing sensible weather, mid-latitude cyclones are also closely linked to the state of mid-latitude, atmospheric flow (Cai and Mak, 1990) and are instrumental in transporting energy from the sub-tropics to higher latitudes (see Holton, 1992). This means that variability in cyclones and the mid-latitude storm tracks is closely linked to large-scale climate variations such as inter- to multi-decadal shifts in regimes of global climate circulation (Trenberth and Hurrell, 1994).

As such, knowledge of storm climatology has broad implications for a wide range of socio-economic, political, environmental and human welfare issues.

Considerable work has been undertaken to assess interannual and seasonal variability in extra-tropical cyclone occurrence on both regional and global scales. In recent times, much of this work has also focused on the analysis of long-term trends in various mid-latitude cyclone variables (eg. Lambert, 1996; Key and Chan, 1999; Geng and Sugi, 2001; Graham and Diaz, 2001; Gulev et al., 2001; and Paciorek et al., 2002). In some instances, analyses have been with regard to possible changes in cyclone frequency, intensity and location of formation associated with increased atmospheric CO_2 levels in a "Global Warming" scenario (eg. Held, 1993; Carnell et al., 1996).

Much less work has been undertaken to describe the interdecadal variability in extra-tropical cyclone occurrence, particularly with respect to changes in the general state of climate and atmospheric circulation. These are referred to here as 'climate regimes' and shifts thereof.

1.1. Overview of extra-tropical cyclone variability and characteristics in the Northern Hemisphere.

Most cyclones in the Northern Hemisphere occur along "storm tracks" in the North Pacific and North Atlantic regions, with other lesser maxima in storm occurrence over areas such as eastern North America (see Chang et al., 2002; GISS Atlas of Extratropical Storm Tracks, http://www.giss.nasa.gov/data/stormtracks).

Numerous studies on extra-tropical cyclone variability in the Northern Hemisphere and regions therein have yielded an array of results which are not necessarily all in agreement. For instance, while many studies have reported a decrease in mid-latitude cyclones over recent decades (eg. Key and Chan, 1999), others have observed either no change in trend (eg. Paciorek et al., 2002) or have noted variable changes in trend depending on the decades analysed (eg. Gulev et al. 2001; Nakamura et al., 2002; Harnik and Chang, 2003). It should also be noted, that in addition to a decrease in cyclone frequency in mid-latitudes, several studies have also observed a simultaneous increase in cyclones poleward of 60°N (eg. Serreze et al., 1997; Key and Chan, 1999). The Serreze et al. (1997) study also highlighted the existence of centres of localised cyclone occurrence which exhibit specific trends. Serreze et al. (1997) demonstrated this in the area underneath the Icelandic Low, although similar studies have focused on other regions as well (eg. Graham and Diaz, 2001).

Many of the studies investigating large-scale cyclone variability have drawn a distinction between variability occurring only in intense cyclones as opposed to that occurring in all cyclones. In many cases, including those where no significant change in trend has been found in the complete cyclone record, a positive trend has been observed in intense cyclones (eg. Lambert, 1996 – although only after 1970; Paciorek et al., 2002). It has been hypothesised that this may signify an intensification of Northern Hemisphere winter cyclones over the various periods investigated (eg. Geng and Sugi, 2001; Graham and Diaz, 2001; Chang and Fu, 2002). Some studies have also pointed out that variability and changes in storm track location are likely to be responsible for much of the variability observed in cyclone numbers. For example, a common prediction associated with a global warming scenario is for a decrease in the meridional temperature gradient resulting from warming at higher latitudes that could produce storm tracks

which form further poleward (eg. Held, 1993; Carnell et al., 1996). This is similar to the observed effect of an El Niño phase of the El Niño Southern Oscillation (ENSO) on North Pacific storm tracks, where the occurrence of such an event is accompanied by an equatorward and downstream shift in the Pacific storm track (Straus and Shulka, 1997).
A close link has also been established between cyclone variability and changes in the mean atmospheric flow (eg. Metz, 1989). Mid-latitude cyclones form as eddies in the mean flow (refer to Peixoto and Oort, 1992; also Holton, 1992), so it follows that variations in the properties of the mean flow may also translate to variability in eddy formation.

Studies comprising investigations of interdecadal-scale cyclone variability per se are less common than analyses of changes or trends over several decades, and many of the studies that have focussed on variability have often been hampered by either a lack of data or lack of homogeneity in earlier data. Some of the studies undertaken observed certain periods where anomalies in a range of cyclone variables occurred. For instance, Chang and Fu (2002) found differences in the strength of both Atlantic and Pacific storm tracks in different parts of the record. Those observations were of a similar nature to observations made by Nakamura et al. (2002) in the north-west Pacific, where an enhanced storm track was observed in the 1980's. This enhancement of the Pacific storm track was found to be related to changes in midwinter storm activity. Both the Nakamura et al. and Chang and Fu 2002 studies linked storm track changes to interdecadal variability in the mean atmospheric flow. In the case of Nakamura et al. (2002), changes in seasonal cyclone progression in the Pacific storm track were observed to accompany a weakening of features in the mean flow such as the Siberian High and Aleutian Low. Chang and Fu (2002) suggested that a similar change existing in both Pacific and Atlantic storm tracks might indicate the influence of mean flow variability. In that study, a leading mode of with the interdecadal variability of mid-winter (December-January) cyclones in the Northern Hemisphere was observed which was not completely explained by influence of the Arctic Oscillation (AO) or interdecadal ENSO-like variability. This grey area allows the possible influence of other major changes in Hemispheric atmospheric circulation to be considered as a factor in cyclone variability.

1.2. The 1976/77 and 1989 climate regime shifts.

The 1976/77 shift in Northern Hemispheric climate is well documented and is observed in a number of climate-related variables and indices as a distinct 'shift' in the general state of physical climate in the Northern Hemisphere. The 'shift' can be readily observed in a range of climate-related variables which include changes in atmospheric circulation and marked effects on various animal and plant species.

The 'regime shift', as it has become known, was described early on by Ebbesmeyer et al. (1991; as reviewed by Hare and Mantua, 2000; see also Minobe, 2000) as a statistically significant "step" in a composite of indices constructed from numerous biological and physical environmental variables.

Trenberth and Hurrell (1994) followed with an in-depth discussion on physical changes in North Pacific atmospheric and oceanic climate associated with a "decade-long change... lasting from 1976 to 1988". Characteristics of the changes noted in that study included a deepening and eastward shift of the wintertime Aleutian Low and related changes in North Pacific Sea Surface Temperatures (SSTs), rainfall and sea-ice in the Berring Sea.

Along with the physical changes, Trenberth and Hurrell (1994) also noted a range of biological changes. This effect on biological changes was also well defined, and used as evidence for the possible oscillatory nature of regime shift events, by Mantua et al. (1997). Following Zhang, Wallace and Battisti (1997), who described an ENSO-like interdecadal mode of variability in Pacific SSTs of which the 1976/77 regime shift was a major feature, Mantua et al. (1997) used similarities between air temperature in the Gulf of Alaska, SSTs along the North American Pacific Northwest coast and catch records of several species of Pacific salmon to describe recurring regime shift events as a quasi-decadal oscillation, which they coined the Pacific Decadal Oscillation (PDO). The existence of the semi-periodical nature of regime shift events was confirmed by a concurrent study conducted using various north-west Pacific SST indices by Minobe (1997). The Minobe (1997) study also suggested a continued oscillation throughout the previous 300 years as observed in dendroclimatological records used as a proxy for temperature and rainfall over the western North American continent.

Since then, the regime shift has been either identified, associated with or defined using a wide range of physical climate parameters (eg. Zhang, Sheng and Shabbar, 1997; Bond and Harrison, 2000; Jones and Moberg, 2003), biological indices (eg. Hare and Mantua, 2000; Miller and

Schneider, 2000; Minobe, 2000) and geological indices such as changes in glacial mass balance (Hodge et al., 1998).

The causes of the identified regime shifts are not certain. Much of the work already undertaken has focused on the Pacific region, including not only the northern Pacific represented by the PDO, but also the tropical Pacific. For example, in addition to the PDO signal being observed in ENSO, the nature of ENSO has also changed since the late 1970's in such a way that El Niño events have been more common and generally more severe than La Niña events during this time (Trenberth and Hurrell, 1994). Via teleconnections, this phenomenon in itself is sufficient to influence a wide range of ENSO-related climate variables such as global rainfall and temperature patterns (eg. Gershunov and Barnett, 1998; McCabe and Dettinger, 1999; Power et al., 1999). Fewer studies have investigated the climate regime shift signal in other regions, however some evidence for the shift in other parts of the Northern Hemisphere does exist. For instance, in a summary and update of numerous Northern Hemispheric surface air temperature analyses, Jones and Moberg (2003) showed that warming and cooling periods in most regions of the globe over the last century change depending on the climate regime at hand. Hurrell and Van Loon (1997) and Lu and Greatbatch (2002) also noted changes in the nature of the North Atlantic Oscillation (NAO) beginning around the 1976/77 date. While those papers discussed ways by which this change could be influenced by the state of North Pacific climate, the notion of regime shift affects being identified in a primarily Atlantic region phenomenon suggests a more Hemispheric scale of the variability.

While other likely climate regime shifts have been observed during the 1920's and 1940's (for a review refer to Minobe, 2000), there is also the possibility of a more recent shift around 1989. The 1989 shift coincides with a brief negative phase of the PDO around that time (see figure 2.2) during which numerous changes were observed in North Pacific regional climate and biological indices. These changes separated the general climatic state of 1976/77-1989 from that of 1989-1997 (Hare and Mantua, 2000). However, the change in various climate variables observed across 1989 was not as clearly defined as that of the 1976/77 shift and several studies have argued that the post 1976/77 state has continued into the 1990's (eg. Mantua et al., 1997). One explanation for the lesser degree of recognition of the 1989 event lies in the possibility of at least two modes of inter- to multi-decadal variability in the Pacific region. These can combine in different ways during different parts of the record (Minobe, 1999; Enfield and Mestas-Nuñez, 1999). This explanation observes the two modes (one at 50-70 years, the other at 15-20 years) becoming superimposed around periods of regime shift (Minobe, 1999). Hare and Mantua

(2000) note that their evidence implies that only the shorter of the two Pacific modes of interdecadal variability changes phase around 1989, perhaps suggesting only a partial shift in climate regime rather than a more complete shift as with the 1976/77 event.

This investigation addresses the variability of extra-tropical cyclones in the Northern Hemisphere with specific reference to changes over multiple decades in global-scale atmospheric circulation and shifts in climate regime. The existence and effect of the 1976/77 and 1989 regime shifts with respect to extra-tropical cyclone occurrence and features in mean Northern Hemisphere flow will also be investigated.

This will be undertaken by examining spatial and temporal variability in cyclone climatology for the Northern Hemisphere and various regions therein. Variability in the mean flow, and how it relates to cyclone variability, will be assessed using observed variability in features of the mean flow such as the Siberian High.

Chapter two details the data and methods used to conduct the investigation, as well as outlining some of the statistical tools upon which analyses were based.

Chapter three provides a summary and analysis of Northern Hemisphere cyclone climatology and variability over the time period investigated as well as a comparative-based critique of the data used.

Chapters four and five comprise findings from various aspects of the investigation and discussions concerning the implications of the findings to climate variability and with regard to other previous studies. Presented in these chapters are analyses of specific regions seen to significantly contribute to the observable variability of cyclone statistics and circulation in larger, hemispheric and semi-hemispheric scale regions.

Chapter six summarises the findings of the study.

2. Data and Methods.

2.1. Northern hemisphere cyclone analysis.

Storm data were taken from the Goddard Institute of Space Studies (GISS) Atlas of Extra-tropical Cyclones. The data in the GISS dataset detail cyclone tracks and statistics on a 2.5°x2.5° latitude/longitude planetary grid from 1961 to 1998. The cyclone, or "storm" tracks in the GISS dataset are derived using an algorithm which identifies and tracks Sea Level Pressure (SLP) minima from 12-hourly 500Hpa and 1000Hpa geopotential heights of the National Centres for Environmental Prediction (NCEP)/National Centre for Atmospheric Research (NCAR) Reanalysis project (Kistler et al., 2001 – hereafter known as Reanalysis data).

Data from the National Snow and Ice Data Centre (NSIDC) Arctic Cyclone Track Data Set (hereafter known as the ARCSS dataset) from 1966-1993 (Serreze, 1996) were also used concurrently with the GISS data. The ARCSS data consist of 12-hourly cyclone statistics for the Northern Hemisphere from May 1966 to December 1993 and are derived from National Meteorological Centre (NMC) SLP fields on a 47x51 octagonal grid. Seeing as the ARCSS data are derived using a different algorithm for cyclone identification than most other studies, the data provide a check for the GISS and other Reanalysis-based datasets, allowing for comparisons to be made with the aim of assessing data reliability.

For both data sets, Northern Hemisphere cyclone data were evaluated from 30°N to 80°N for the months of an extended Northern Hemisphere 'winter', from November through April. In all cases, a given season includes data from January through April of that year as well as November and December data from the previous year.

Cyclones forming north of 80°N were scarce and deemed to not be important to this study of extratropical cyclones. Above 80°N there is also the increasing possibility of inaccuracies in the analysis due to the distortion of storm track density with changes in area covered by the equal area grid boxes (as noted by Hayden, 1981; Taylor, 1986; and Gulev et al., 2001) . Since the area of the equal-area boxes is standardised at 60°N in the ARCSS data set and minimal analysis

was required north of this latitude, it was assumed spatial distortion would not be an overly significant problem. 30°N was chosen as the southern limit as this latitude is within the 25°N limit recommended in the ARCSS dataset documentation (accessible online at http://nsidc.org/data/arcss003.html). This latitude was suggested as a limit due to reservations concerning edge effects on cyclogenesis and cyclolysis data. 30°N was also considered far enough north to not include most hurricanes, typhoons or other tropical storms. Tropical storms, or low pressure systems left over from tropical storms, that did progress north of this latitude were considered to contribute to the climates of the regions in question and were thus included.

Cyclone data were analysed for several regions of the Northern Hemisphere (see figure 2.1). Region 1 encompasses most of the Northern Hemisphere Pacific Ocean within 30°N to 80°N and 135°E to 120°W. Region 2 includes most of the North American continent and the northern Atlantic Ocean, from 30°N to 80°N and 120°W to 0°. Region 3 covers the Eurasian continent, from 30°N to 80°N and 0°E to 135°E.

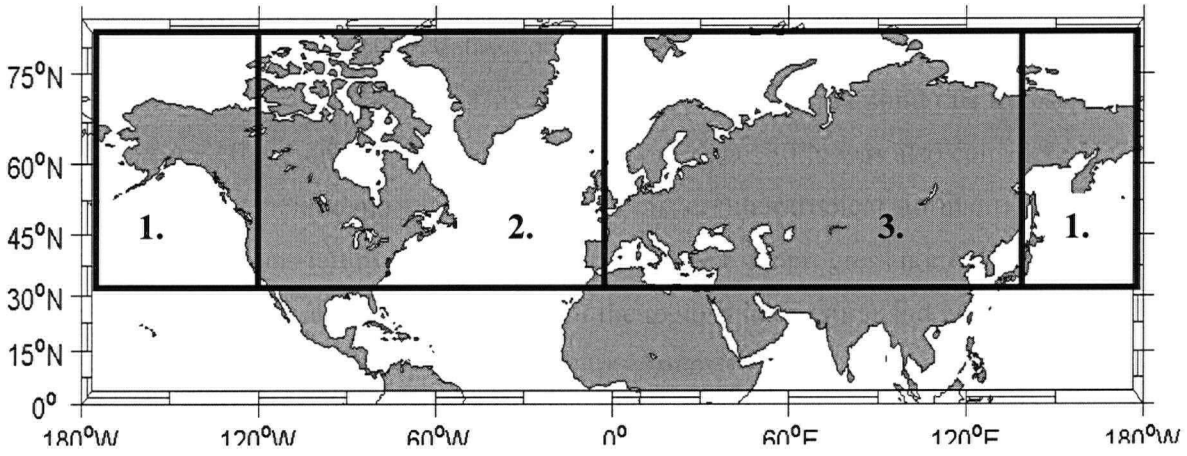

Figure 2.1 - Regions of study. Region 1: Pacific Ocean (30°N to 80°N, 135°E to 120°W); Region 2: North America/North Atlantic Ocean (30°N to 80°N, 120°W to 0°); and Region 3: Europe/Asia (30°N to 80°N, 0° to 135°E).

Having the maximum and minimum latitudes vary to this degree was assumed to accommodate any possible meridional variability of the storm track over the time period investigated. This allowed for an assessment of cyclone numbers without risk of error due to the possibility of the storm track shifting outside of the sample area due to climate trends or variability.

Further analyses were also conducted on storms in the North American (30°N to 80°N, 120°W to 70°W) and North Atlantic (70°W to 0°W) regions separately, as well as the Gobi Desert region in northern China/Mongolia (40°N to 50°N, 100°E to 110°E). The Gobi Desert region was chosen because of the intriguing nature of storm variability observed there during analysis of the whole Eurasian continent. It was also selected as a focus due to its significance as a 'birthing ground' for dust storms that affect Beijing and the surrounding areas of China (Qian et al., 2002; after Iwasaka et al., 1983). From searches of relevant literature there appeared to be a relative lack of analyses undertaken in this area. Dust storms in this area are associated with cyclone occurrence, the variability of which is linked to the Siberian High (Watts, 1969). It was hypothesised that possible relationships between the Siberian High and Northern Hemisphere mean wave flow might exhibit a variability related to longer timescale changes in the latter, which could show up in the cyclone frequency of the immediate area.

An index for variability in the Siberian High (dubbed the Siberian High Index, or SHI) was constructed using NCEP/NCAR Re-analysis monthly mean Sea Level Pressure (SLP) data from November 1948 to April 2003. Seasonal means were calculated from November to April at 50°N, 90°E. This point was observed to be within the usual position of the mid-winter centre of the Siberian High over the time period investigated. This centre was determined using data obtained from the NOAA-CIRES Climate Diagnostic Centre (CDC) Reanalysis website (http://www.cdc.noaa.gov). A comparison of the SHI with variability in the mean seasonal position of the Siberian High suggested that the SHI is a fairly good representation of variability in Siberian High intensity.

Empirical Orthogonal Function (EOF) analyses were also undertaken using Siberian High data. In these cases, data were obtained in a similar manner to when constructing the SHI, except the region analysed was extended to encompass mid-winter (January) mean SLP values of greater than 1016hPa. These values were predominantly within 40°N to 60°N, 60°E to 110°E. This is in the north-west Asian region usually occupied by the Siberian High during the Northern Hemisphere winter.

Storm variability was assessed in terms of cyclone frequency and cyclogenesis in 5° by 5° latitude-longitude grid points within sample areas. The spacing of the latitude-longitude grid points was deemed adequate, as the typical horizontal scale of a cyclonic system means that it is unlikely for more than one storm to occupy a 5° by 5° space at any time. Grid points were used

for ease of calculation and to reduce bias toward higher storm frequency counts at higher latitudes that could be introduced by the area normalisation of grid boxes (see Changon et al., 1995; Paciorek et al., 2002). Spatial occurrence of the cyclone variables was also assessed. Cyclone frequency is defined as the number of cyclone observations at any point over a November-April 'season'. Cyclogenesis, on the other hand, better represents the actual number of individual cyclones observed in a region. The implication of this distinction is that in the case of cyclone frequency it is possible a cyclone may be observed more than once within a region. Whereas in the case of cyclogenesis each storm is counted only once. The main setback associated with cyclogenesis as a means for assessing actual cyclone counts, is that it does not allow the inclusion of cyclones entering the region from elsewhere. The degree to which this setback introduced error to the analysis was assessed by comparing cyclone numbers from a cyclogenesis event tally to the total number of cyclones calculated by removing multiple observations of individual storms from a cyclone frequency analysis. By careful selection of sample regions (ie. by taking into account where primary areas of cyclogenesis occur), error associated with cyclogenesis events being used to estimate finite storm numbers was kept minimal.

Cyclone frequency, cyclogenesis events and spatial occurrence were also analysed in the case of intense cyclones. Intense cyclones included only those cyclones which reached a central low SLP of 980hPa or less. 980hPa was chosen as a threshold as it was a value that seemed to fall roughly around those used by other studies where cyclone intensity was assessed (eg. Carnell et al., 1996; Lambert, 1996; Geng and Sugi, 2001; Graham and Diaz, 2001; and Paciorek et al. 2002). It should be noted, that while studies such as those by Carnell et al. (1996), Lambert (1996) and Graham and Diaz (2001) used intense cyclone cut-offs of 970hPa and 975hPa, it is noted by Paciorek et al. (2002) that 970hPa and 980hPa storms occur to a similar frequency in locations with a sufficient number of storms for analysis. Since the regions investigated all include the higher mid-latitude storm tracks of the Northern Hemisphere where cyclone occurrence is most common, it was assumed that there would be a sufficient frequency of storms that a cut-off of 980hPa could be used. This also allowed higher degrees of freedom and better statistics than would have been possible with the lower frequency of storms associated with a lower cut-off.

It was also noted during the course of the investigation that there is a tendency for the central pressure of cyclones to decrease poleward. This could lead to a degree of bias in the number of

intense cyclones occurring in the northern regions of the area analysed. However, since most storms investigated tended to form in similar latitudes of the sample area, these were considered relatively minor issues and not pursued.

In each of the sample areas for all variables, cyclone statistics were compared between different phases of climate regime. The climate regimes were generally defined around the well-documented 1976/77 regime 'shift' (eg. Nitta and Yamada, 1989; Trenberth, 1990; Trenberth and Hurrell, 1994; Mantua et al., 1997; Hodge et al., 1998; Hare and Mantua, 2000; Miller and Schneider, 2000). Additional analyses were also conducted with a possible second shift of climate regime around 1989 (Hodge et al., 1998; Hare and Mantua, 2000; and Miller and Schneider, 2000) added to the better documented 1976/77 event. Analyses were also made using the Pacific Decadal Oscillation (PDO; Mantua et al., 1997) as a proxy for climate regime phases in the North Pacific region. The PDO is an index which describes long time scale variability in North Pacific ocean SSTs, of which the change in the late 1970's is a prominent feature. It was initially conceived as an index to describe climate regime shifts as an oscillation (Zhang et al., 1997; Mantua et al., 1997). In figure 2.2, the major shift near 1976/77 in the PDO can be observed. Another, shorter-lived period of negative-phase PDO can also be seen near 1989.

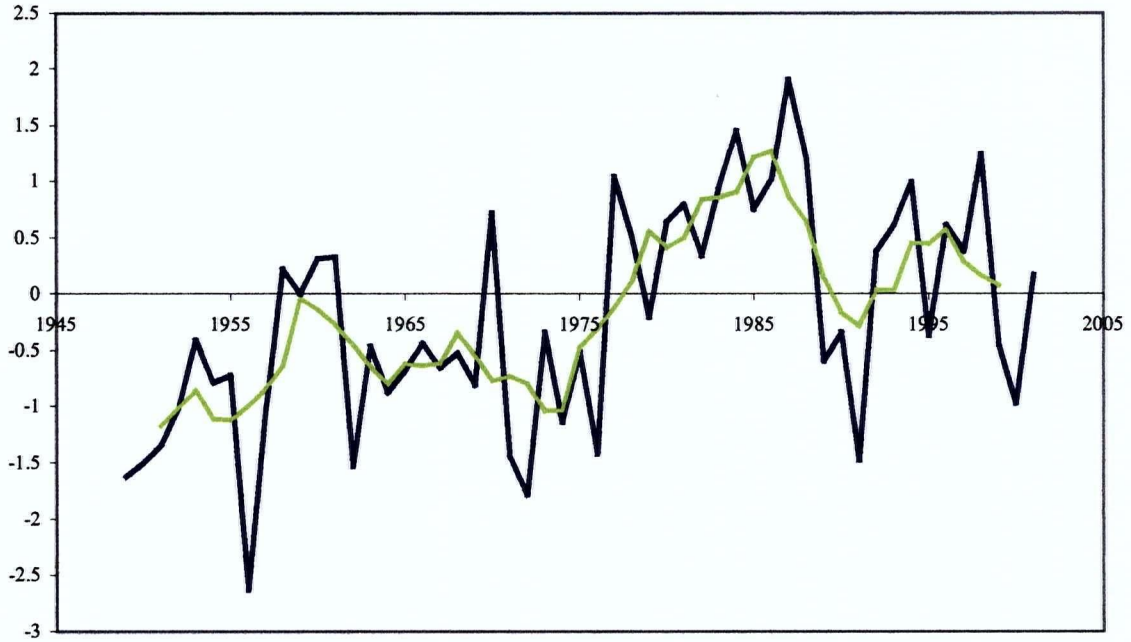

Figure 2.2 - NDJFMA Pacific Decadal Oscillation (PDO), 1948/49 to 2002/03 with 5 year running mean (green line).

In order to maintain consistency, regimes were defined positive or negative in accordance with positive and negative phases of the PDO around 1977. So, in the case of the single regime shift scenario, dates prior to the 1976/77 season are defined negative with seasons 1976/77 and after being defined as positive. In the case of the double regime shift scenario, seasons 1989 and after are negative again (referred to here as the 77/89 regime index), despite the predominantly positive state of the PDO in the mid to late 1990's. This definition was made to remain consistent with the definition of a 'regime shift'. That is, a regime shift results in a transition to a different global circulation and climate phase, rather than the more conventional oscillation in conditions such as that represented by the PDO. It should be noted, that from a PDO-definition of climate regime shift alone, it is arguable that the continued positive general state of the PDO into the 1990's suggests that the 1989 event is not a climate regime shift in the same sense as the major 1976/77 event, despite some physical and biological evidence to the contrary (see Chapter 1).

Cyclone variables were analysed to assess the possible existence of major changes near the regime shift dates. Trends over the period were also examined. Trends were analysed and assessed for significance using a simple z-test for testing hypotheses with standard errors (refer to Moore and McCabe, 1993). Analyses were also tested using a more stringent Student's t-test (Moore and McCabe, 1993). However the nature of the results meant that occasions where the two tests yielded different designations of significance/non-significance were rare.

With only 38 seasons and 28 seasons available in the GISS and ARCSS datasets respectively, poor statistics and lack of degrees of freedom made it difficult to assess relationships between cyclone variables and the regime shift indices with any degree of confidence. Data could be smoothed to assess trends or filtered to exclude minor fluctuations, but smoothing of the data resulted in very large degrees of autocorrelation between time series points. Reducing degrees of freedom to correct for the autocorrelation (refer to Wilks, 1995), as was undertaken for all analyses involving filtering or smoothing of data, made it even more difficult to obtain a confident assessment of cyclone/regime relationships. As an alternative to merely performing simple correlation analyses, the differences in cyclone variables between the positive and negative phases of the various regime shift indices were examined. The differences in cyclone variables between regime phases were compared and tested for significance using a two-sample z-test for means (refer to Moore and McCabe, 1993).

2.2. North-west Pacific cyclone frequency and vertical wind shear.

Following relationships between vertical wind sheer and cyclone/eddy development in the mean atmospheric flow resulting from thermal wind theorem (refer to Holton, 1992), it was suggested by Graham and Diaz (2001) that variability in the occurrence of cyclones forming between 30°N to 35°N in the mid-Pacific Ocean is related to the difference in velocity between upper and lower level atmospheric winds, or vertical wind shear. The authors of this study also suggested that variability in vertical wind shear was due primarily to variability in the upper, 200hPa winds. This study also suggests, based on findings by Hoskins and Karoly (1981), Hoerling and Ting (1994) and Lau (1997), that variability in mid-latitude upper level winds results from changes in equatorial Pacific SST.

It was thus hypothesised that a relationship might exist between vertical wind shear variability and cyclone formation in the north-west Pacific region. From the observation of Pacific Ocean storm tracks using the GISS Atlas of Extra-Tropical Cyclones, this region appears to be a major 'birthing ground' for North Pacific cyclones. In this case, variability in the number of cyclones forming in the north-west Pacific region would be an important factor in the variability of all northern hemisphere Pacific region cyclones.

To investigate this hypothesis, cyclone frequency and intense cyclone frequency in the north-west Pacific region (30°N to 60°N, 130°E to 175°E) were compared to vertical wind shear in that region. To assess the degree to which variability in this 'birthing region' might also affect regional Pacific cyclones, cyclone frequency and intense cyclone frequency in the whole region were also compared.

Following the conjecture that most of the variability in vertical wind shear occurs in the upper levels of the atmosphere, winds at 200hPa were used for this analysis. Observation of monthly mean wind fields in NCEP/NCAR reanalysis data (http://wesley.wwb.noaa.gov/reanalysis.html) shows that the v-direction (north-south) component of mean monthly 200hPa winds is much less than the u-direction (east-west) component. It was thus assumed that most of the variability in NDJFMA 200hPa winds also occurs mainly in the u-direction. Hence, only the u-direction component (hereafter known as u-wind) was used in the analysis. An EOF analysis of u-wind was used to assess modes of variability influencing cyclone frequencies.

To further assess the validity of assuming that all variability occurs at the 200hPa level in this instance, an analysis was also briefly made using a more intuitive definition of vertical wind shear. In this case, vertical wind shear is defined as the difference in wind speed between 200hPa and 925hPa winds. 925hPa was selected as a lower level as it is assumed to be representative of near-surface winds while also being at a sufficient altitude above the surface to avoid significant surface effects. Again, only the u-wind component was analysed.
Wind shear and 200hPa wind data were calculated for November-April winter 'seasons' from November 1961 to April 1998 using monthly mean wind velocity data from the NCEP/NCAR Reanalysis. For this part of the analysis, cyclone variables were evaluated over 2.5°x2.5° latitude-longitude grid boxes to remain consistent with the 2.5°x2.5° grid of the global Reanalysis data. As a control, cyclone frequency in this 2.5°x2.5° format was also compared to the 5°x5° grid frequency analysis to ensure that no major discrepancies arose from the implementation of the two different methods.

3. Key characteristics of the ARCSS and GISS cyclone datasets and a Northern Hemisphere cyclone climatology, 1961/62-1997/98.

3.1. Variability between datasets and cyclone climatology.

Both the ARCSS and GISS data sets generally capture the main features of the northern hemisphere storm tracks quite well. The Pacific and Arctic storm track locations are particularly well represented (see figures 3.1a and 3.1b).

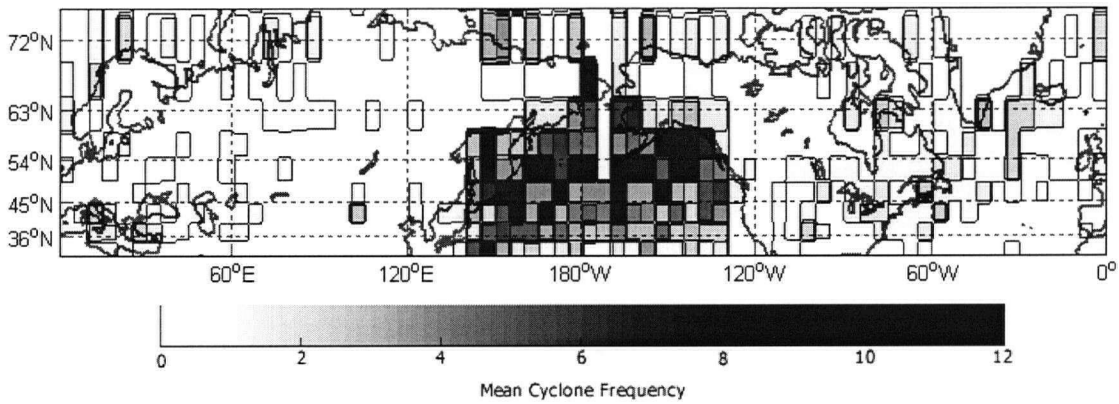

Figure 3.1a – Mean NDJFMA cyclone frequency from ARCSS data for the northern hemisphere between 30°N and 75°N, 1966/67-1992/93. Cyclone frequency is calculated in 5° x 5° latitude-longitude boxes.

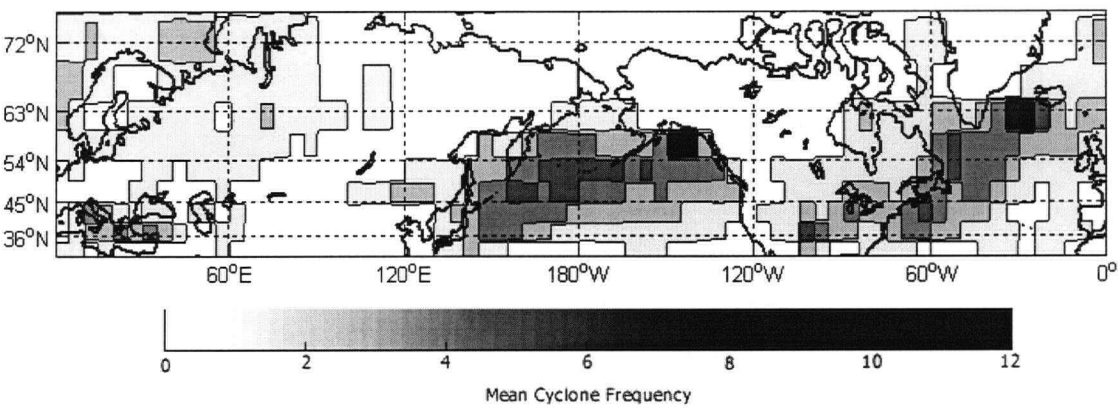

Figure 3.1b – Mean NDJFMA cyclone frequency from GISS data for the northern hemisphere between 30°N and 75°N, 1961/62-1997/98. 5° x 5° latitude-longitude boxes.

While the GISS data appear to represent the North Pacific and North Atlantic storm tracks evenly, the ARCSS data contain far more Pacific storms than Atlantic. Both sets of data make use of 12 hourly observations, so it can be assumed that major differences are related more to the nature of the modelled data from which the datasets are built and from the different algorithms used to identify cyclones.

Documentation accompanying the ARCSS data (ftp://adcc.colorado.edu/pub/projects/arcss003/readme.txt) gives a summary of known 'quality control' issues for that dataset. It is noted that smoothing in the NMC grid, upon which the dataset is based, results in loss of detail and over-estimated frequency closer to polar latitudes. Indeed, cyclone frequency is better represented above 60°N in the ARCSS dataset compared with analyses from the GISS data in the Pacific region. However, in far-north European latitudes the GISS dataset appears to contain more storms.

It is also interesting to note, that despite the smoothing 'disclaimers' in ARCSS documentation, the GISS data appear more smoothed. This is likely due to the algorithm used in cyclone identification in the GISS data actively smoothing data between separate observations of the same storm (see http://www.giss.nasa.gov./data/stormtracks/). The algorithms used for both sets of data contain distance thresholds when linking subsequent observations of cyclone pressure systems. Although the GISS algorithm allows for a potentially larger distance travelled by a cyclone in one 12 hour observation segment (1440km as opposed to 1200km with the ARCSS algorithm), it is not likely that such a relatively minor discrepancy would allow for the difference in 'patchiness' observed in the respective frequency maps above.

Perhaps a more relevant feature of the GISS data, is the assertion that extra-tropical storms do not tend to 'double back' on themselves and measures taken within the algorithm prevent such events from developing in the output. These measures, such as the exclusion of two storm track observations that are greater than an angle of 85° to one another. In the GISS cyclone identification algorithm it is assumed that two observations occurring along a path displaying such an angle result from multiple observations of the same storm. These observations are removed and thus would result in the smoother representation of the storm track regions of cyclone occurrence observed in figure 3.1b. The ARCCS algorithm, on the other hand, appears to allow the inclusion of any observation near to the previous one. This occurs in order to account for slow-moving and stationary cyclones. In a region such as the north-east Pacific Ocean, where cyclones are 'blocked' against the North American continent, this could lead to a higher frequency of cyclones observed than in the GISS data. This does appear to be the case

from a comparison of figures 3.1a and 3.1b and might also account for the patches of higher cyclone frequency observed across the whole Pacific region in the ARCSS dataset. Whether this is a more accurate representation of the North Pacific storm track is unclear.

Additional smoothing in the GISS algorithm could also explain the more consistent storm frequency values across much of Europe and the Atlantic region. This does not necessarily explain the higher frequency of cyclones recorded in GISS data in the Atlantic region unless cyclones are travelling quickly along the Nth Atlantic storm track. Purely cumulating the frequency of each storm per 5° block would result in missed storms if the cyclones are moving fast enough to completely pass through an adjacent latitude-longitude block in the 12 hour time period between observations. Additional smoothing between observations, on the other hand, would 'fill in the gaps' and compensate for fast moving storms.

Areas where cyclone frequency is most intense are similarly well represented for both datasets in the north-east Pacific, although the ARCSS data include several more 5° x 5° blocks in this 'hotspot' than the GISS data do. In the north-west Pacific however, areas of intense cyclone frequency observed in ARCSS data are not found in the GISS data. In this case, the hypothesis that Nth Atlantic storms are missed in the ARCSS data due to speed of propagation does not apply, or is reversed in the case of the Pacific region. That is, the nature of the differences between the two sets of data appears to be inconsistent and dependent upon region.

In the case of the ARCSS data, it is not clear if the inconsistencies in representation of the Atlantic and Pacific regions are because the Pacific region is over-represented and more accurately depicted, or if they are due to the nature of the algorithm used.

Another ambiguity in the ARCSS data is a lack of storms near the dateline in the Pacific Ocean. One possibility for this 'gap' in the storm track could result from some effect on cyclone paths related to land influences associated with either the Aleutian chain of islands and south-western Alaskan Coast which is not apparent in the GISS data due to smoothing. There are some documented observations of storm propagation of such nature in this region from accumulated observations by voluntary observing ship programs (eg. Mariner's Weather Log, National Weather Service, http://www.nws.noaa.gov). However, an assessment of the accuracy of such weather logs is not within the scope of this investigation.

A more likely explanation might be linked to the proximity of the 'gap' to the dateline. The 'gap' occurs along the interface between the 180°E-175°W and 175°W-170°W longitudinal columns. This coincidence might suggest a temporal discontinuity in the ARCSS data which is exploited by the methods of analysis used here. Although, since identical methods of analysis

were used for both datasets and the 'gap' is not apparent in the GISS analysis, it is unlikely that the discontinuity was produced by method error alone. The 'gap' only occurring north of 50°N could also suggest that increasing distortion effects with latitude are also a factor in the discontinuity. It is also possible that the smoothing in the GISS algorithm might be the correcting factor in that dataset, especially at higher latitudes where grid-spacing becomes a more important issue.

Table 3.1 displays trend analyses of cyclone frequency and intense cyclone frequency for the regions investigated. Figures 3.2 through 3.13 show time series analyses for regional cyclone frequency with linear regression lines inserted to illustrate trends.

In nearly all cases a significant trend was found in cyclone and intense cyclone frequency using ARCSS data. Using GISS data, significant trends were found for all cases. From the Difference Index in table 3.1, it can be seen that in most cases trends found using the GISS data were more significant than those from ARCSS data, the exceptions being north Pacific frequency, combined North American and north Atlantic frequency, cyclone frequency across the Eurasian continent and Eurasian intense cyclone frequency. A possibility for the stronger trends in GISS data could be related to the more even spatial coverage of cyclone frequency mentioned previously.

For most regions, trends were the same sign for both datasets. However, in the cases of North American and North Atlantic intense cyclone frequency, trends of opposite sign were found. In the case of North American intense cyclone frequency, a significant trend was not found using ARCSS data. However, the slight trend apparent is negative in nature, as opposed to a significant positive trend in the GISS data. In the case of North Atlantic intense cyclones, the ARCSS data yield a significant positive trend, while a significant negative trend was found using GISS data. A similar discrepancy between the two sets of data is apparent in the analyses of Gobi Desert cyclone frequency, except in this case the difference in magnitude of trends between datasets is very large.

Table 3.1 – Cyclone and intense cyclone (designated here by the inclusions of "980", representing the threshold SLP used to designate a cyclone being 'intense') trend analyses for the regions of study. Values are z-statistics associated with the significance of the trend. A positive z-statistic denotes a positive trend, and negative z-statistic a negative trend. The Difference Index represents the difference in magnitude between ARCSS and GISS z-statistics. Dark shading denotes a trend which is significant at the 95% level – orange for significant positive and blue for significant negative. Pale shading denotes significance at the 90% level.

	z-statistic		
	ARCSS	GISS	Diff index
Nth Hem:	-1.78	-4.48	2.7
Nth Hem 980:	8.6	12.97	4.37
Pacific:	2.75	1.97	-0.78
Pacific 980:	5.64	7.97	2.33
Eurasia:	-5.63	-3.83	-1.8
Eurasia 980:	8.67	6.67	-2
Nth Am/Atl:	-5.61	-5.4	-0.21
Nth Am/Atl 980:	3.65	4.66	1.01
Nth America:	-3.25	-2.15	-1.1
Nth Am 980:	-0.18	-3.01	2.83
Atlantic freq:	-5.6	-4.23	-1.37
Atlantic 980:	3.67	-1.73	-1.94
Gobi Desert:	6.03	-4.54	-1.49

The reason for the difference in North American and north Atlantic cyclone trends is not clear. Taking into account variations between figures 3.1a and 3.1b, it is likely that the differences are again related to the apparently more complete coverage of cyclones in the GISS data for this region. Neither is it clear how the relatively moderately significant trends in the intense cyclone frequency of the various regions combine as such a highly significant trend in the full Northern Hemisphere intense cyclone record.

It is interesting to note that while trend direction is generally consistent across all analyses in the North America/Atlantic region, GISS intense cyclones forming only in the north Atlantic region

(with North America excluded) exhibit an opposite trend to that of cyclone frequency in the combined region. This could suggest that the overall positive trend in intense cyclones in the combined North America/Atlantic region is due largely to the increase in North American intense cyclones.

It is also interesting to note that in all cases except for Pacific region storms, intense cyclone frequency trends over the sample period are of opposite sign to trends associated with overall cyclone frequency. This is in agreement with other studies (eg. Graham and Diaz, 2001; Paciorek et al., 2002) which have suggested, in various forms, a difference in the way current climate change trends affect intense cyclones as opposed to all cyclones. What is consistent across nearly all regions (cyclones occurring over North America being the exception), however, is that the trends in intense cyclone frequency are significantly (at the 95% level) more positive than for all cyclones. Thus, in most regions of the Northern Hemisphere the percentage of cyclones reaching a severity which is considered here to be 'intense', has increased during the time period investigated. While Northern Hemisphere cyclone frequency has decreased since 1961/62, the frequency of intense cyclones has increased. In both data sets, and particularly in the GISS data, this positive trend is very large. In the case of the North American region, the trend is more negative, highlighting that variability in cyclone frequency and other climate variables are not uniform around the globe under a Global Warming scenario. In this case, it can be noted that the trend seen in intense cyclone frequency is still more significant than that observed in the complete North American record.

The time series analysis of Northern Hemisphere cyclone frequency (figure 3.2) shows that for all regions combined, the ARCSS and GISS records are in fairly good agreement after 1975/76. Although the GISS data show a larger number of cyclones, the magnitude of variability relative to the dataset is similar, as is the timing of positive and negative anomalies in the record. The biggest difference between the two sets of data occurs around 1970 and, as would be expected if more recent parts of the record are assumed to be more accurate, decreases slightly towards the latter part of the record. The 1970 difference coincides with a large negative anomaly observed in the ARCSS data, but not the GISS data. Both datasets feature a negative anomaly in the frequency of cyclones around 1976/77, followed and preceded by a greater number of positive anomaly frequency seasons. This 'dip' in cyclone frequency also occurs in Pacific (figure 3.4) and Eurasian (figure 3.12) regional time series. It also occurs to a lesser degree in the North American record and in the Atlantic a negative period can also be observed around that time. The North American and North Atlantic combined analyses only show the 1976/77 anomaly in

the GISS data. The more prominent existence of the anomaly at this time in the Pacific and Eurasian regions might suggest that the reasons for this anomalous season are related to mechanisms which also influence Eurasian and Pacific cyclone frequency.

It can be noted, that this anomaly also coincides with the 1976/77 regime climate shift and around a change-of-phase period in the PDO (see figure 2.2).

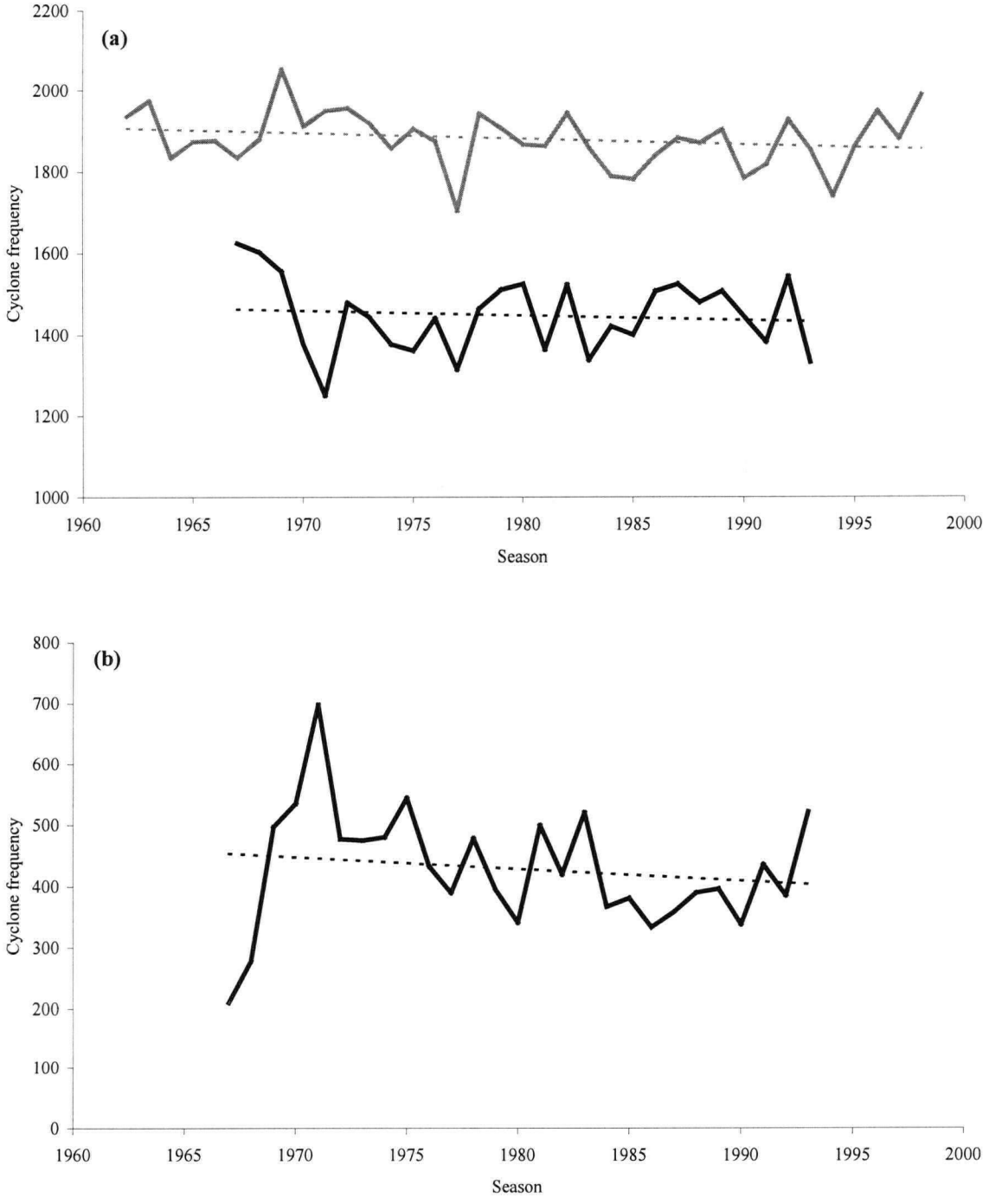

Figure 3.2 – Northern Hemisphere NDJFMA cyclone frequency: (a) shows cyclone frequencies: GISS data (1961/62-1997/98) are represented by grey lines, while the dark lines represent ARCSS data (1966/67-1992/93); and (b) shows the difference in frequency observed between the two datasets. Thin, dashed lines represent a linear regression trend in each case.

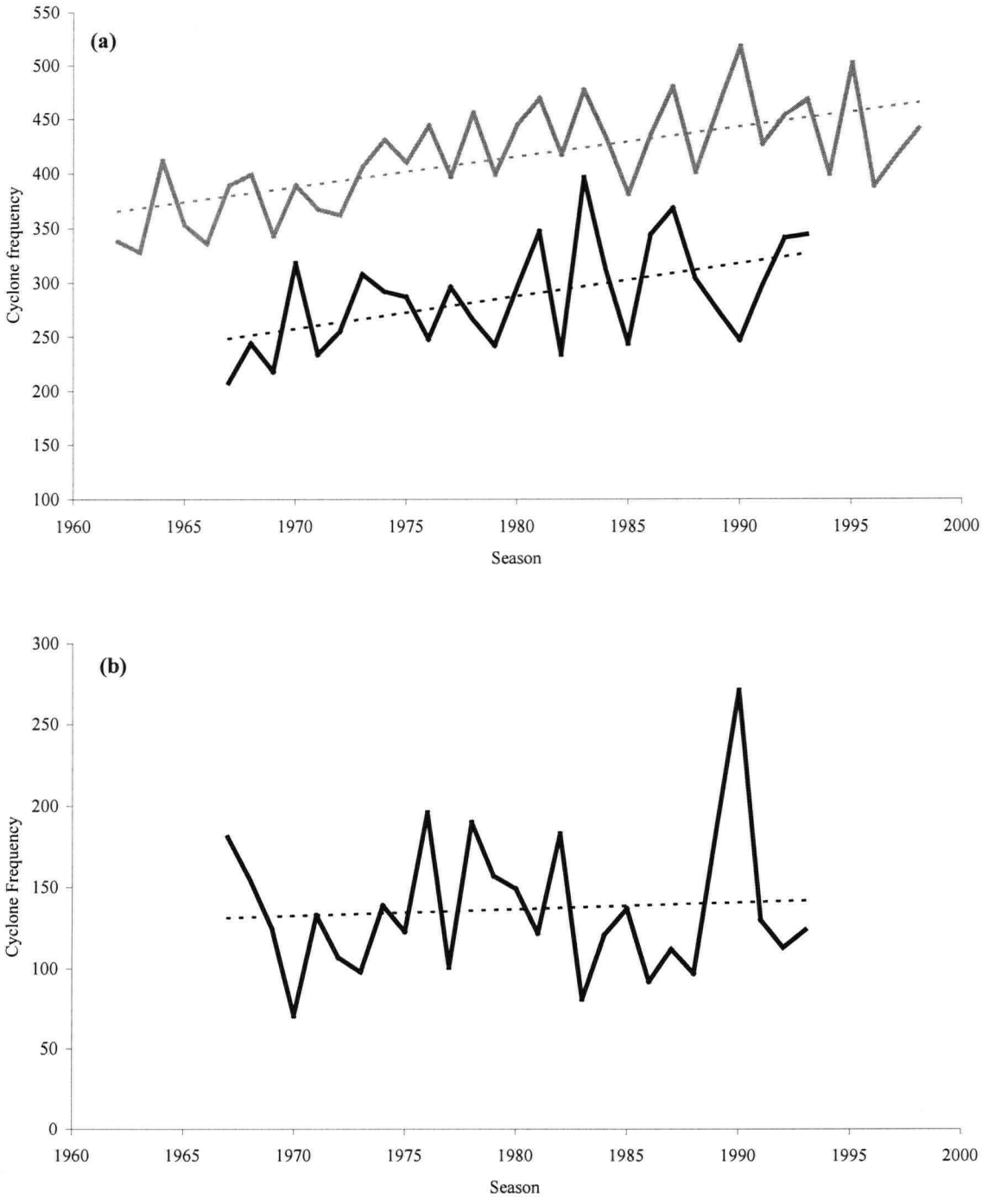

Figure 3.3 – Northern Hemisphere NDJFMA intense cyclone (<980hPa) frequency: (a) shows cyclone frequencies: GISS data (1961/62-1997/98) are represented by grey lines, while the dark lines represent ARCSS data (1966/67-1992/93); and (b) shows the difference in frequency observed between the two datasets. Thin, dashed lines represent a linear regression trend in each case.

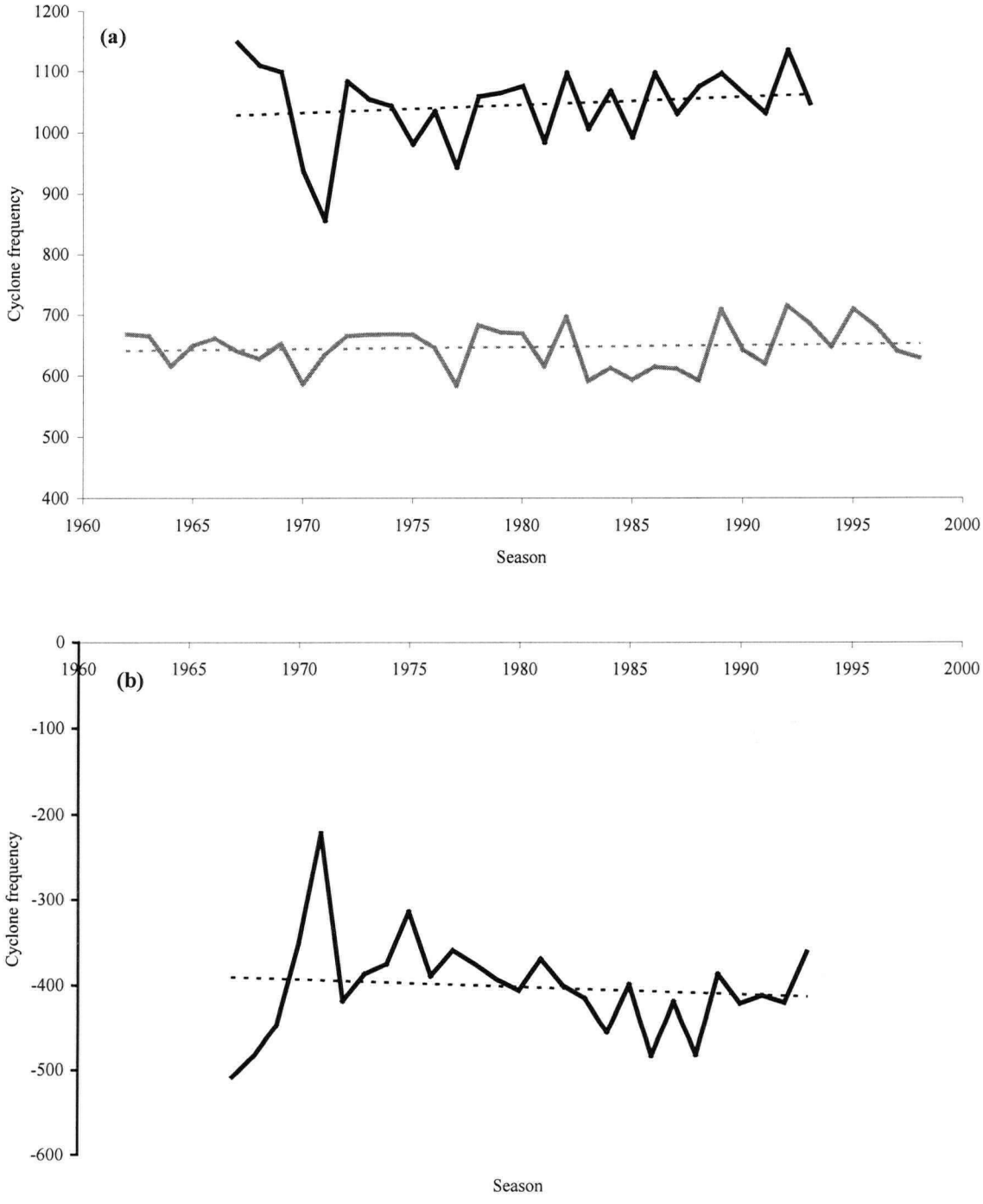

Figure 3.4 – North Pacific (30°N to 80°N, 135°E to 120°W) NDJFMA cyclone frequency: (a) shows cyclone frequencies: GISS data (1961/62-1997/98) are represented by grey lines, while the dark lines represent ARCSS data (1966/67-1992/93); and (b) shows the difference in frequency observed between the two datasets. Thin, dashed lines represent a linear regression trend in each case.

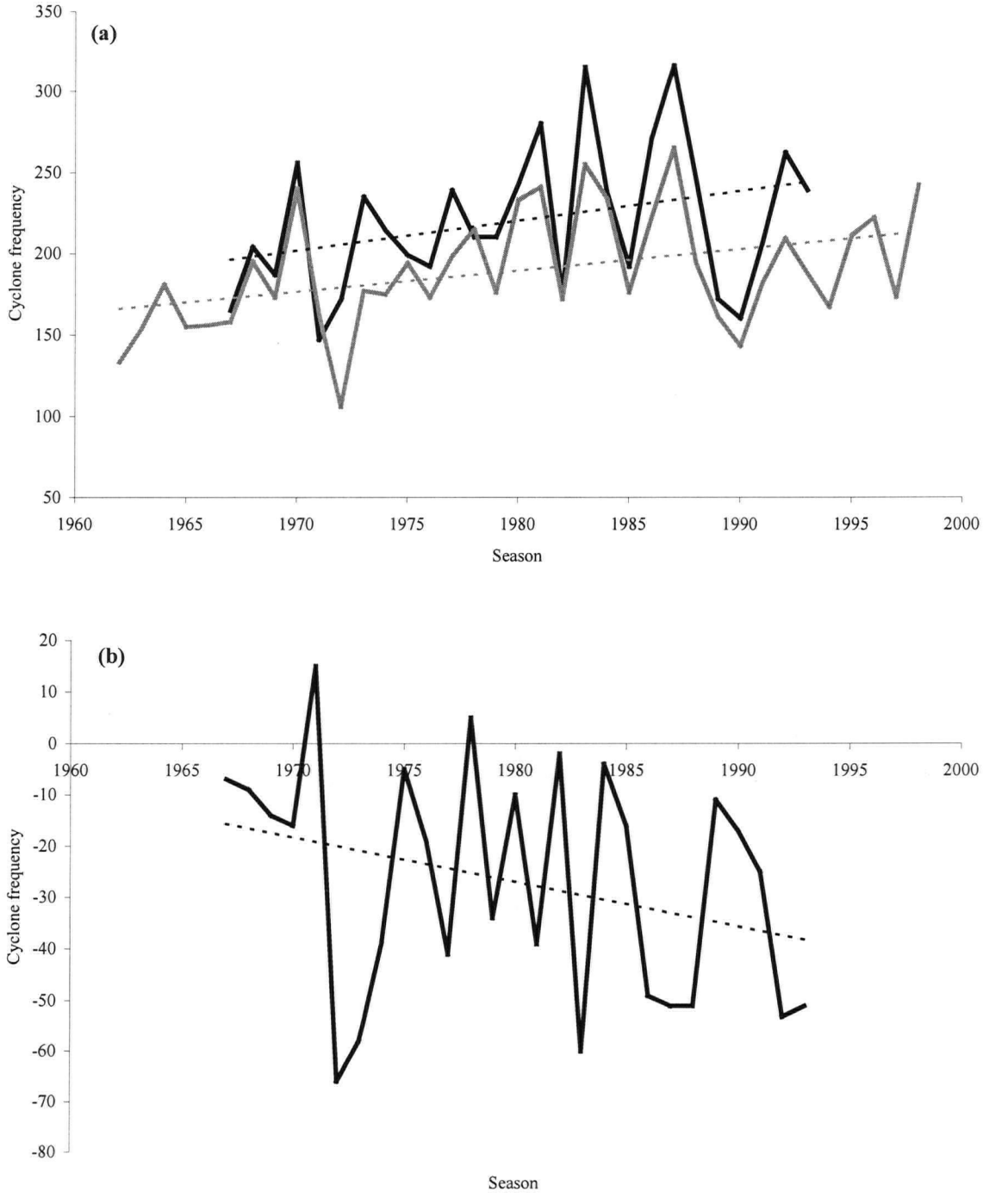

Figure 3.5 – North Pacific (30°N to 80°N, 135°E to 120°W) NDJFMA intense cyclone (<980hPa) frequency: (a) shows cyclone frequencies: GISS data (1961/62-1997/98) are represented by grey lines, while the dark lines represent ARCSS data (1966/67-1992/93); and (b) shows the difference in frequency observed between the two datasets. Thin, dashed lines represent a linear regression trend in each case.

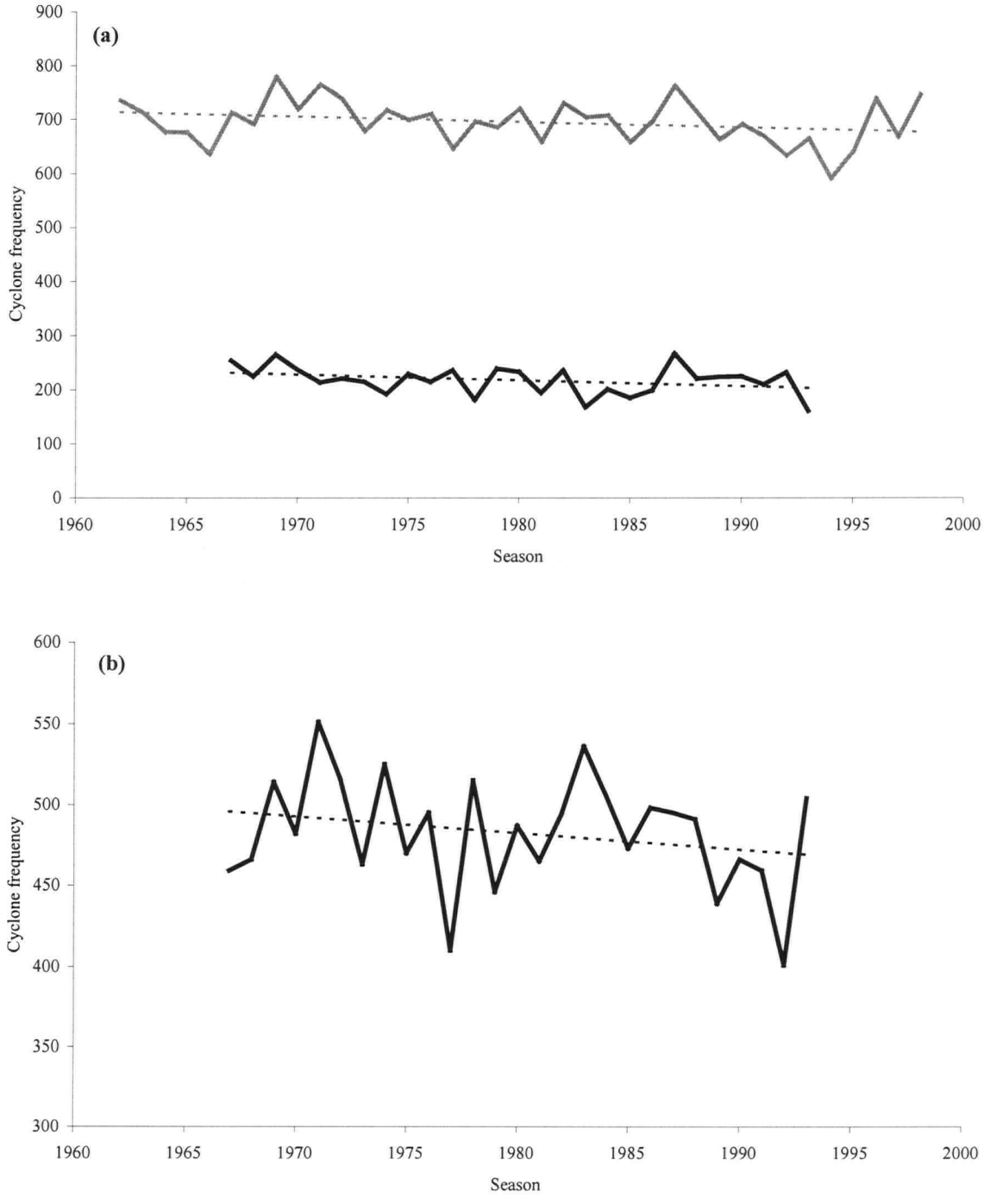

Figure 3.6 – North America/North Atlantic combined (30°N to 80°N, 120°W to 0°) NDJFMA cyclone frequency: (a) shows cyclone frequencies: GISS data (1961/62-1997/98) are represented by grey lines, while the dark lines represent ARCSS data (1966/67-1992/93); and (b) shows the difference in frequency observed between the two datasets. Thin, dashed lines represent a linear regression trend in each case.

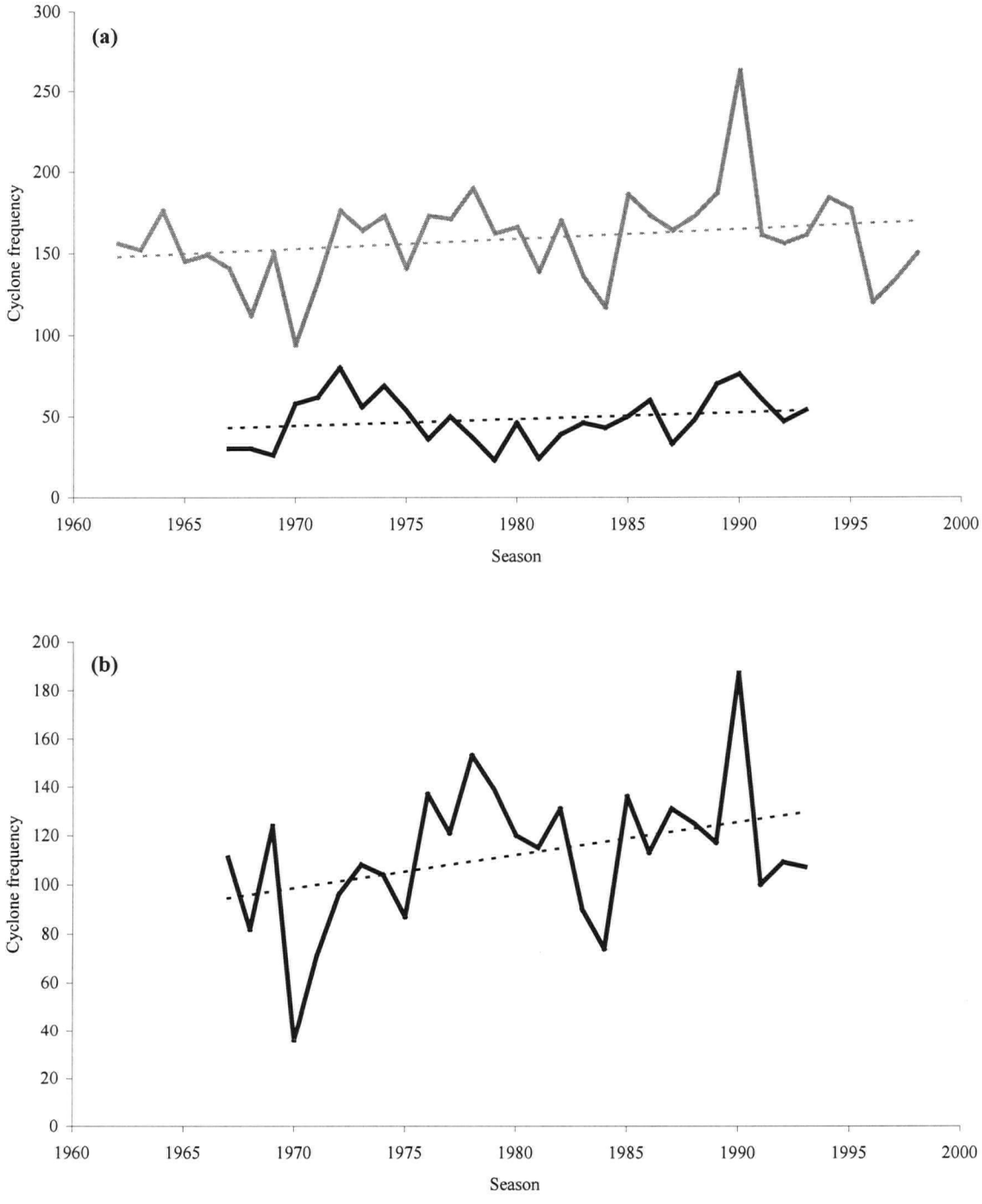

Figure 3.7 – North America/North Atlantic combined (30°N to 80°N, 120°W to 0°) NDJFMA intense cyclone (<980hPa) frequency: (a) shows cyclone frequencies: GISS data (1961/62-1997/98) are represented by grey lines, while the dark lines represent ARCSS data (1966/67-1992/93); and (b) shows the difference in frequency observed between the two datasets. Thin, dashed lines represent a linear regression trend in each case.

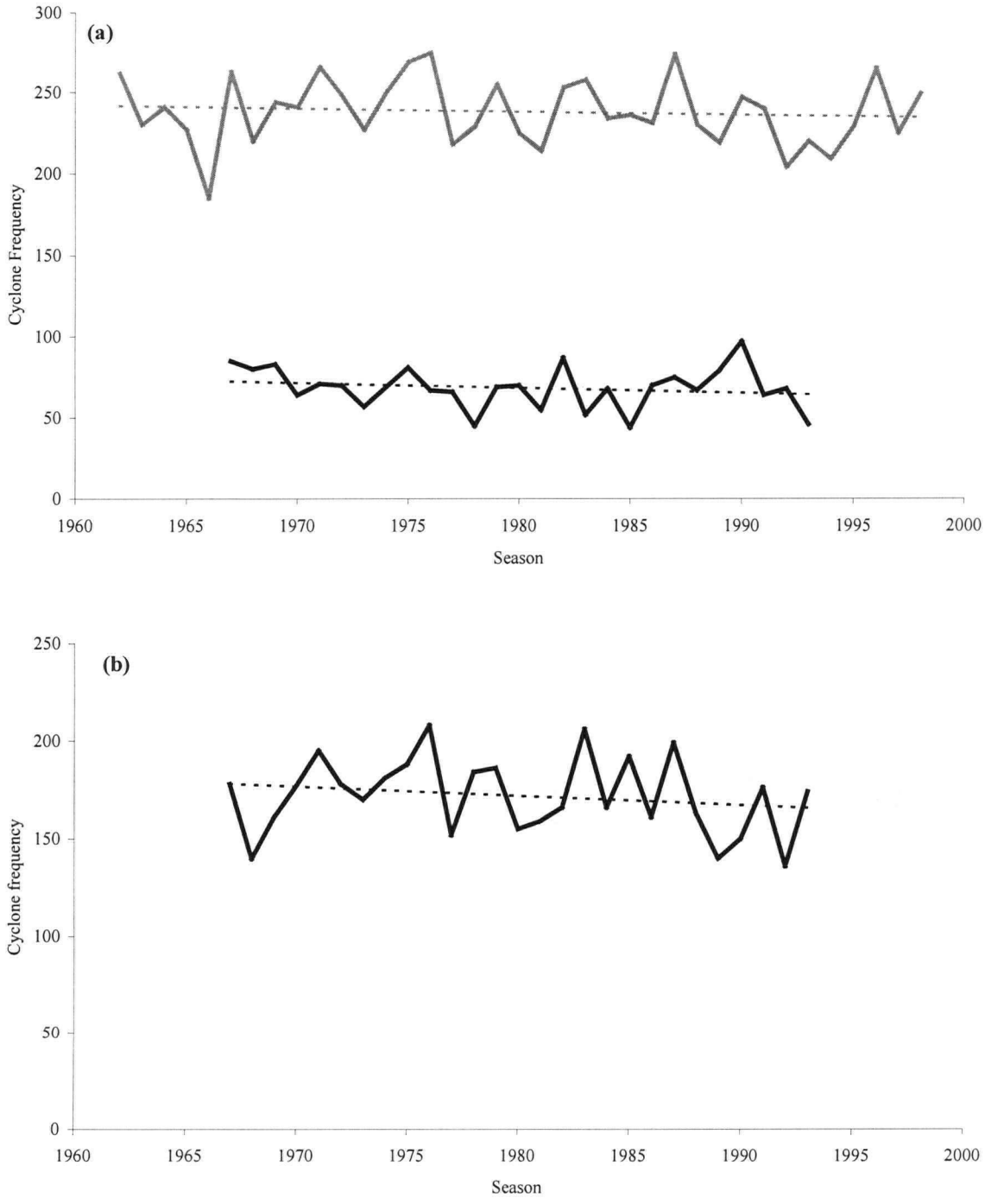

Figure 3.8 – North American (30°N to 80°N, 120°W to 70° W) NDJFMA cyclone frequency: (a) shows cyclone frequencies: GISS data (1961/62-1997/98) are represented by grey lines, while the dark lines represent ARCSS data (1966/67-1992/93); and (b) shows the difference in frequency observed between the two datasets. Thin, dashed lines represent a linear regression trend in each case.

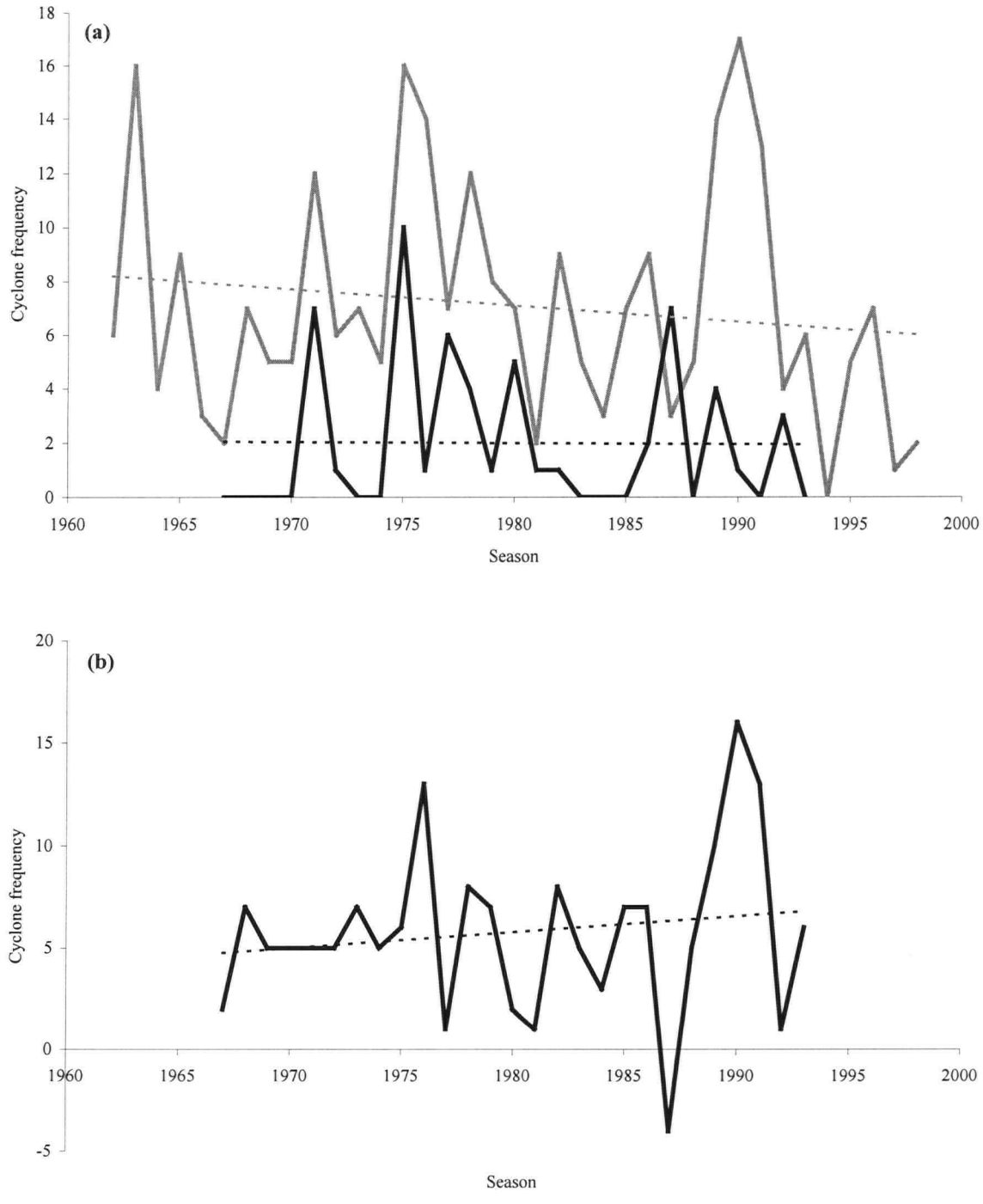

Figure 3.9 – North American (30°N to 80°N, 120°W to 70° W) NDJFMA intense cyclone (<980hPa) frequency: (a) shows cyclone frequencies: GISS data (1961/62-1997/98) are represented by grey lines, while the dark lines represent ARCSS data (1966/67-1992/93); and (b) shows the difference in frequency observed between the two datasets. Thin, dashed lines represent a linear regression trend in each case.

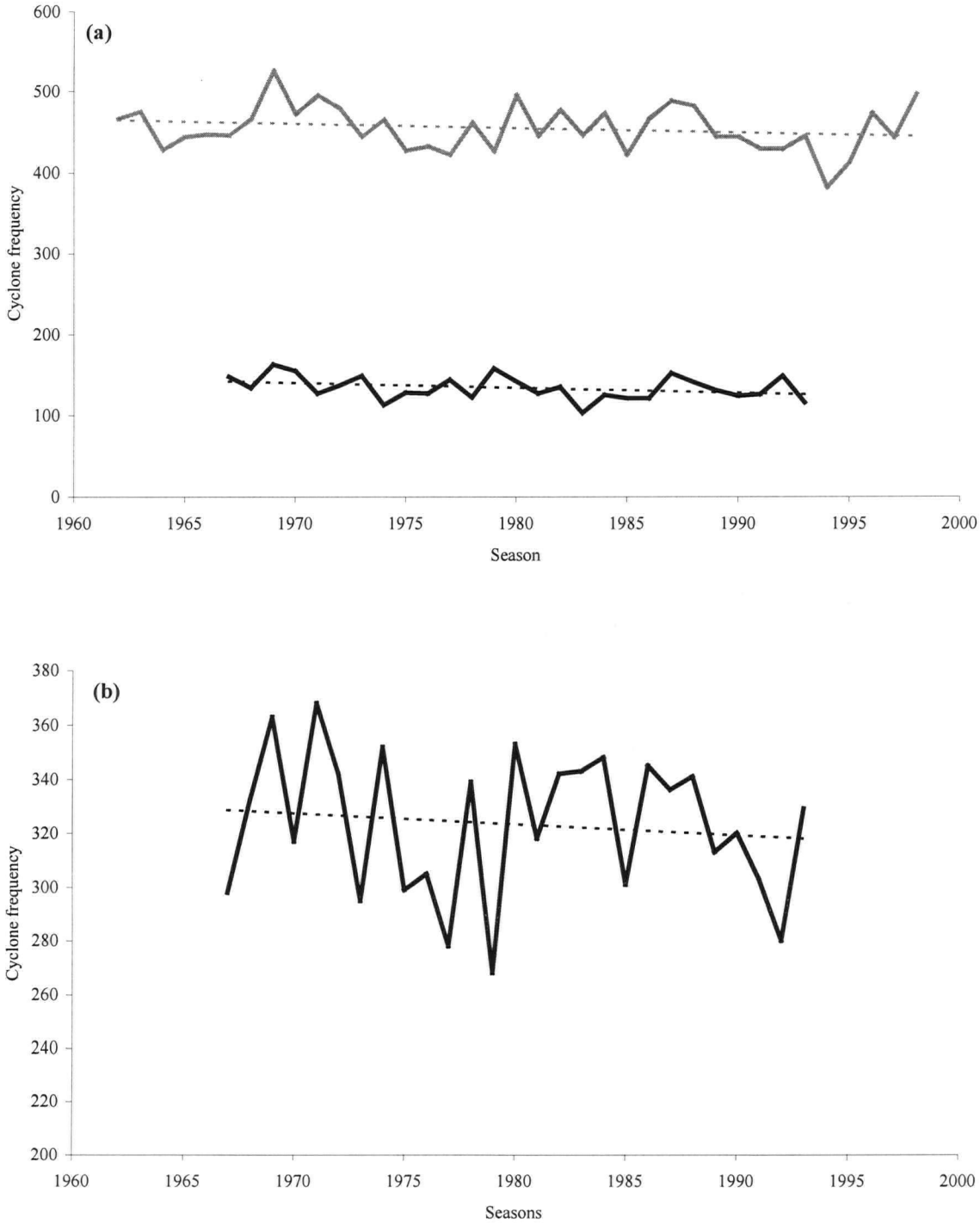

Figure 3.10 – North Atlantic (30°N to 80°N, 70°W to 0°) NDJFMA cyclone frequency: (a) shows cyclone frequencies: GISS data (1961/62-1997/98) are represented by grey lines, while the dark lines represent ARCSS data (1966/67-1992/93); and (b) shows the difference in frequency observed between the two datasets. Thin, dashed lines represent a linear regression trend in each case.

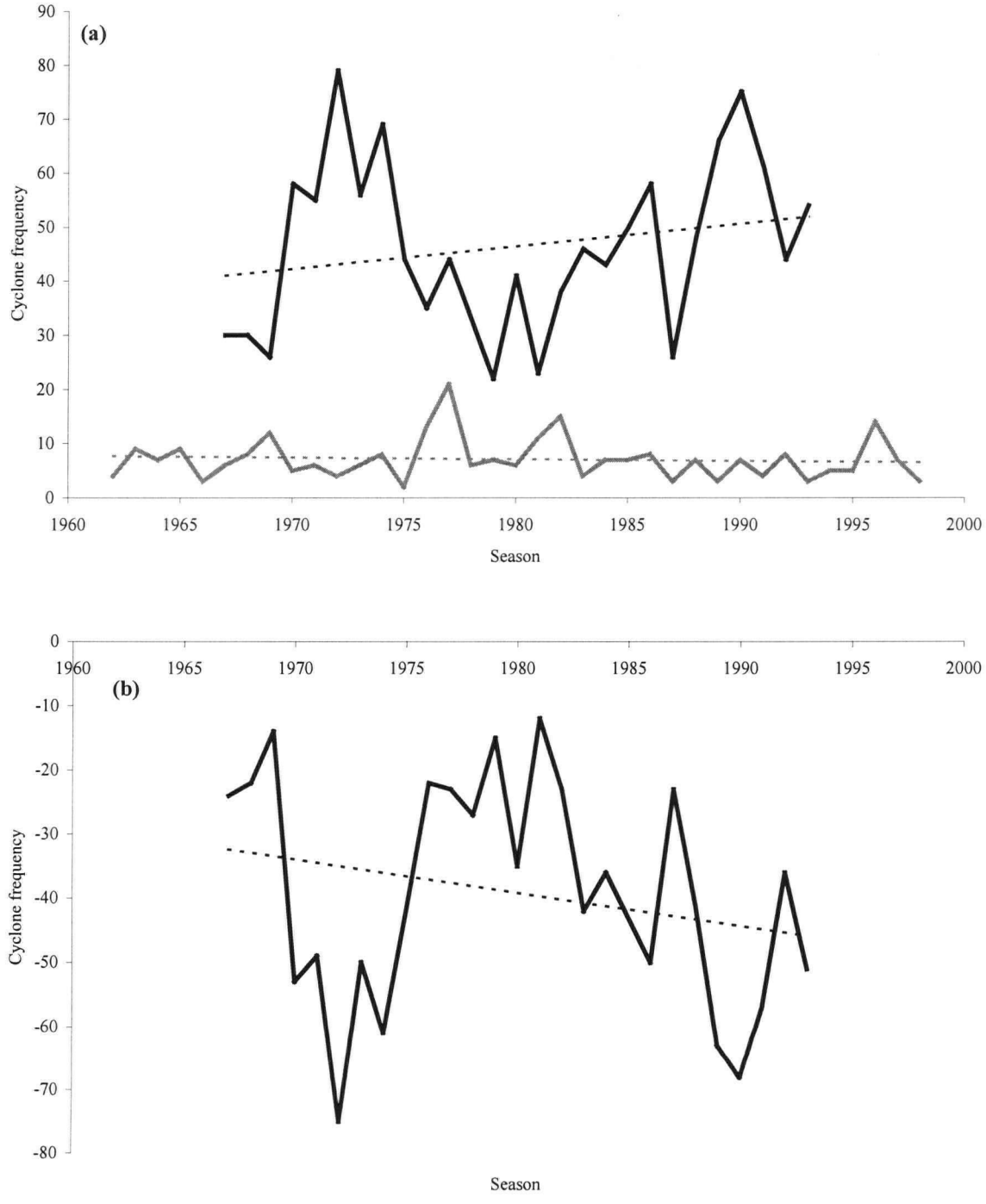

Figure 3.11 – North Atlantic (30°N to 80°N, 70°W to 0°) NDJFMA intense cyclone (<980hPa) frequency: (a) shows cyclone frequencies: GISS data (1961/62-1997/98) are represented by grey lines, while the dark lines represent ARCSS data (1966/67-1992/93); and (b) shows the difference in frequency observed between the two datasets. Thin, dashed lines represent a linear regression trend in each case.

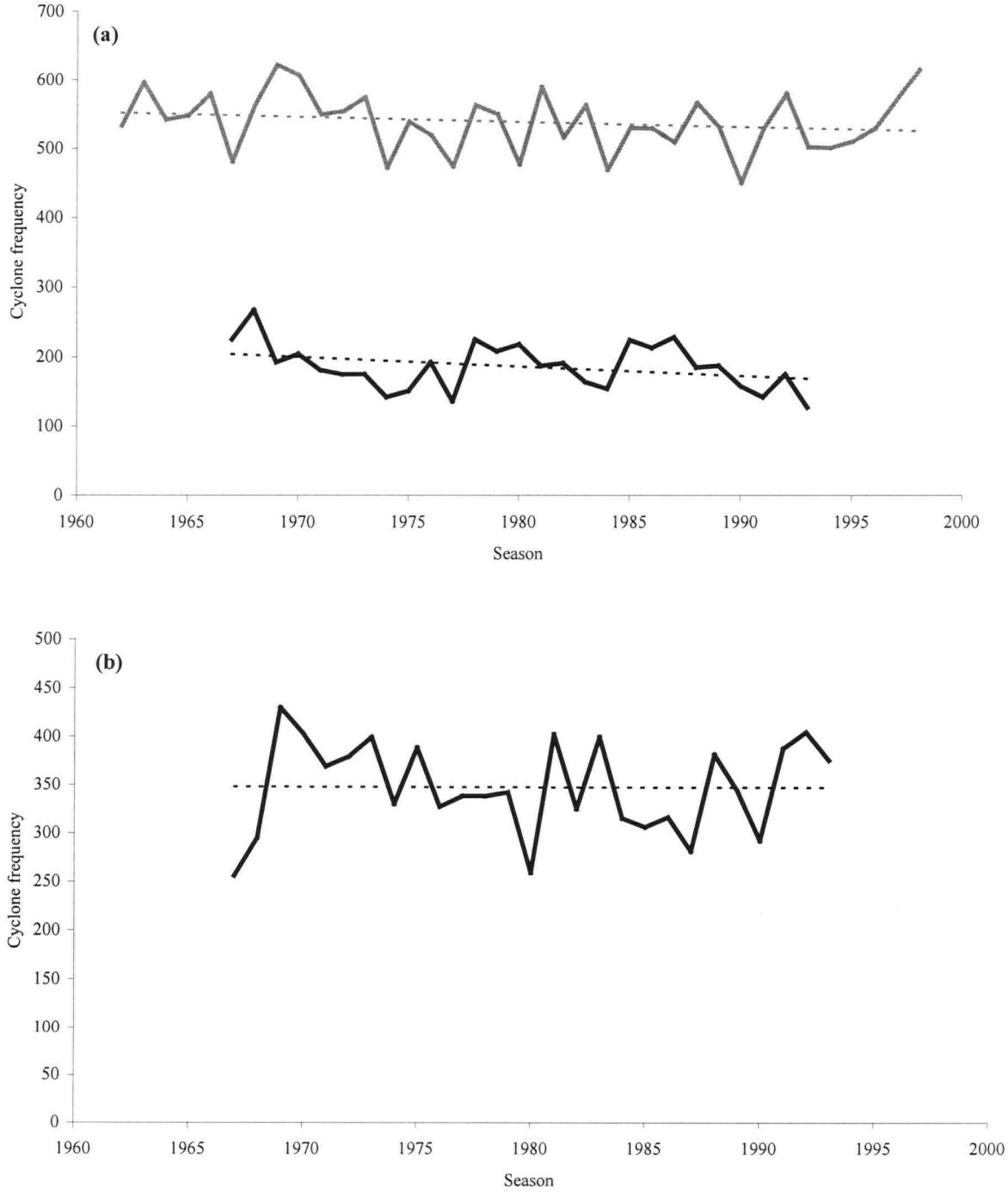

Figure 3.12 – Europe/Asia (30°N to 80°N, 0° to 135°E) NDJFMA cyclone frequency: (a) shows cyclone frequencies: GISS data (1961/62-1997/98) are represented by grey lines, while the dark lines represent ARCSS data (1966/67-1992/93); and (b) shows the difference in frequency observed between the two datasets. Thin, dashed lines represent a linear regression trend in each case.

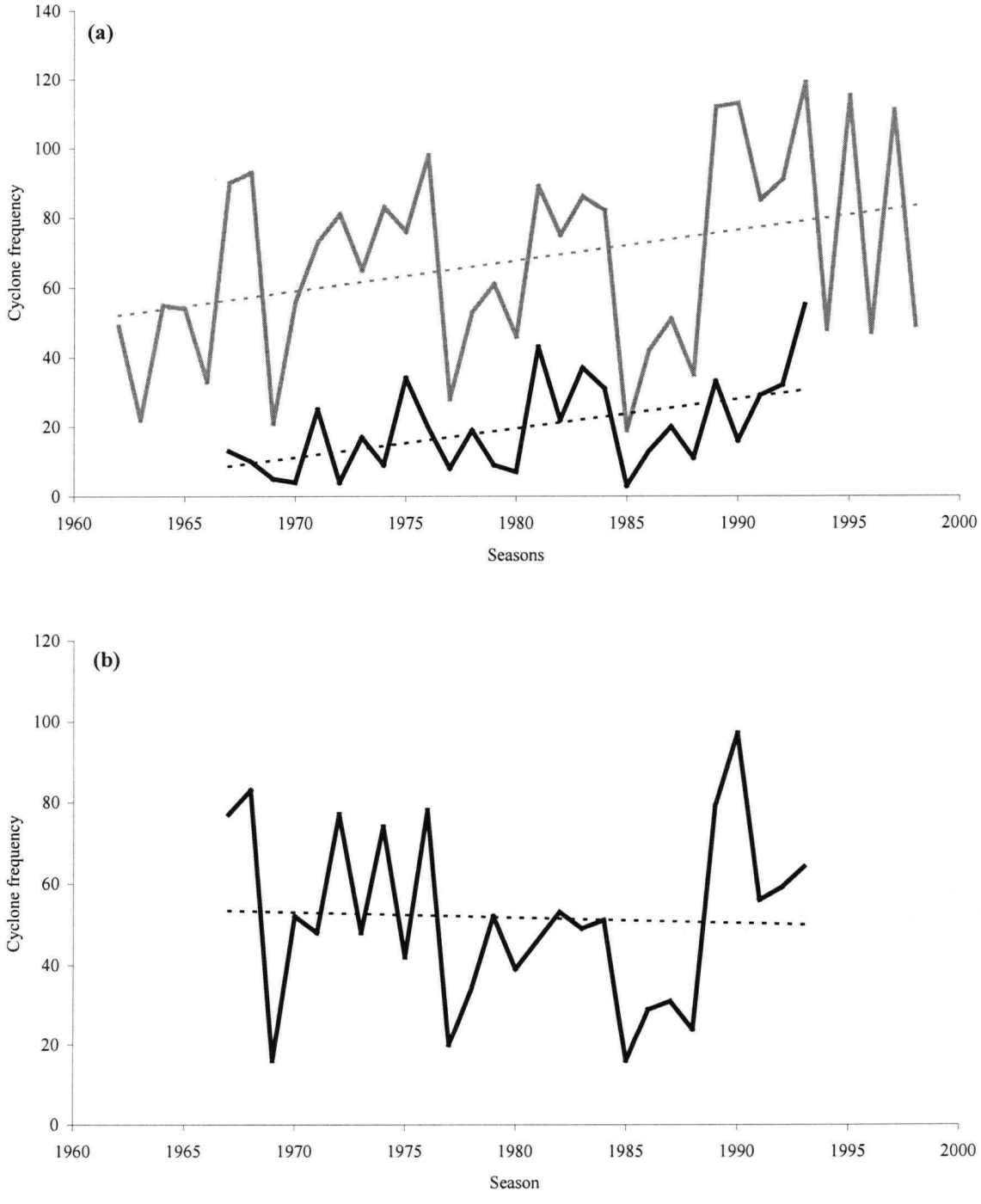

Figure 3.13 – Europe/Asia (30°N to 80°N, 0° to 135°E) NDJFMA intense cyclone (<980 hPa) frequency: (a) shows cyclone frequencies: GISS data (1961/62-1997/98) are represented by grey lines, while the dark lines represent ARCSS data (1966/67-1992/93); and (b) shows the difference in frequency observed between the two datasets. Thin, dashed lines represent a linear regression trend in each case.

While other periods of positive and negative anomaly also exist, none of these is as consistent between both sets of data as the 1976/77 negative cyclone anomaly. The consistency with which this anomaly occurs in all regions of the Northern Hemisphere can be seen in figure 3.14.

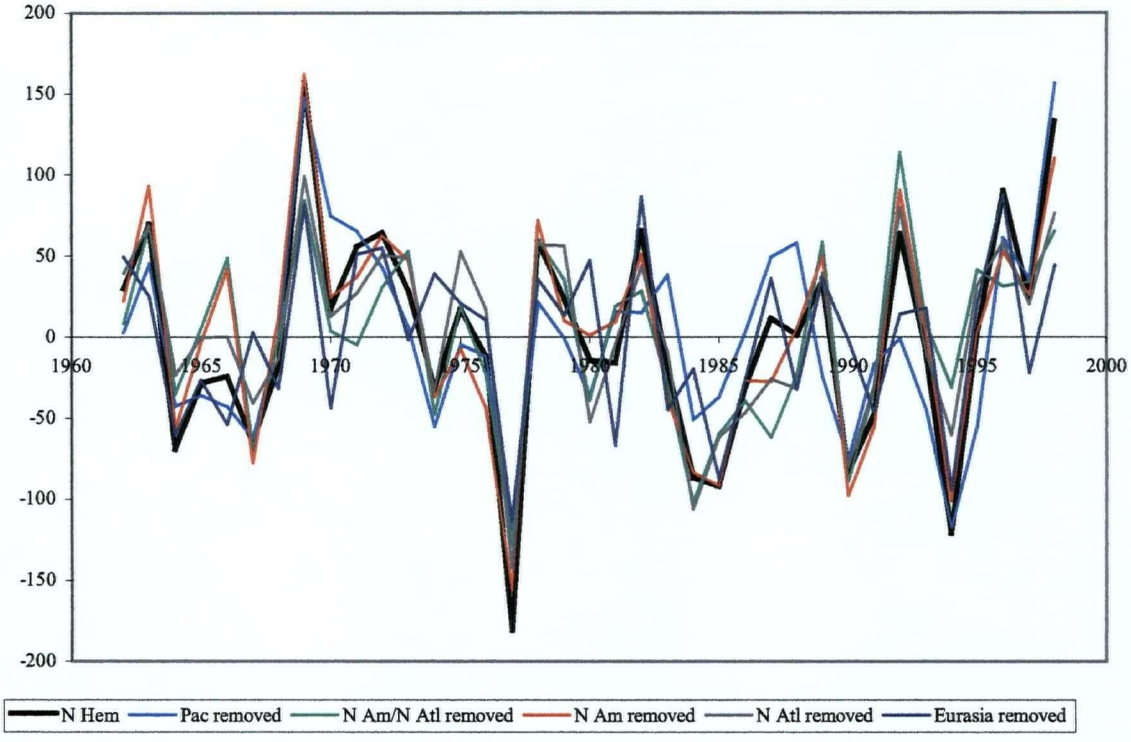

Figure 3.14 – Regional anomaly-removed indices. Indices represent Northern Hemisphere cyclone frequency anomalies from GISS data with various regional anomalies removed from 1961/62 to 1997/98 (refer to text for more details). The thick black line shows the full Northern Hemisphere cyclone anomalies; light blue line shows Northern Hemisphere anomalies with Pacific anomalies removed; green line shows combined anomalies from North American and the North Atlantic; red line shows North American anomalies; grey line shows North Atlantic anomalies; and the thin dark blue line shows Eurasian anomalies removed.

Figure 3.14 shows various indices for Northern Hemisphere cyclone frequency with specific regions removed separately for each index. For example, the "Pacific removed" index shows the Northern Hemisphere cyclone frequency with the Pacific cyclone record removed (linear trend is also removed in all cases). The result is an index which shows the degree to which anomalies in the region in question contribute to the total Northern Hemisphere anomaly record. Indices that are least similar to the full record indicate regions which are the primary influence in the anomaly observed in the full record at that time.

From figure 3.14 it can be seen that the peak anomaly season in the Northern Hemisphere record which is echoed in every other region to the greatest degree is the 1976/77 event. A positive

anomaly event during 1968/69 shows a similar degree of uniformity throughout Northern Hemisphere regions, but not as precisely as the 1976/77 event. Interestingly, the 1968/69 event corresponds to a large negative anomaly in the North Atlantic Oscillation (NAO, see figure 3.16). The coincidence of the cyclone and NAO anomalies during 1968/69 differs from the 1976/77 in that the latter event does not correspond to as significant anomaly in the NAO or other similar climate mechanisms investigated here. The 1976/77 event does, however, occur near the beginning of an extended phase of positive anomaly in the NAO.

Other peak anomalies in the record are predominantly influenced by specific regions. For example, the negative anomaly during 1993/94 is observed in all indices, but to varying degrees. The North American/North Atlantic anomaly record shows the largest difference from the main record, so it is likely that the cause for that anomaly in the full record occurred mainly in those regions.

Similarly, a peak in 1988/89 in the full record is accompanied by similar peaks in all indices except for the Pacific record. This suggests that this anomaly, and possibly what has been suggested as a climate regime shift, is primarily a North Pacific regional event and not hemispheric in nature. In fact, Northern Hemisphere cyclone anomalies in the latter half of 1980's appear to be largely the result of North Pacific variability. This can also be seen in a comparison to the regional cyclone records presented above. Another period of singular-region 'forcing' occurs during the mid-1960's. In this case the North American and North Atlantic regions appear to be primarily responsible for the state of Northern Hemisphere variability. The 1976/77 event, however, is prevalent in all indices, suggesting that the difference between this and other seasons exhibiting a significant anomaly in cyclone frequency, is that this event was of a hemispheric nature with respect to cyclone occurrence.

This means that the Northern Hemisphere winter season coinciding with the 1976/77 climate regime shift was accompanied by a large, hemisphere-wide decrease in cyclone frequency. The reasons for this decrease are not clear, but will be discussed in following chapters. Since it appears that the event is of a global, or at least hemispheric nature it is likely that there was something about that particular season which suppressed cyclone, or eddy development in the Northern Hemisphere's mean atmospheric flow. Possible explanations could be a variation in meridional temperature gradient modulating the need for mid-latitude eddies to transport energy poleward, a change in ocean circulation or a change in a combination of climatic phenomena such as those which influence other large scale indices like the AO or PDO.

Figure 3.15 shows the same analysis in the case of Northern Hemisphere intense cyclone anomalies.

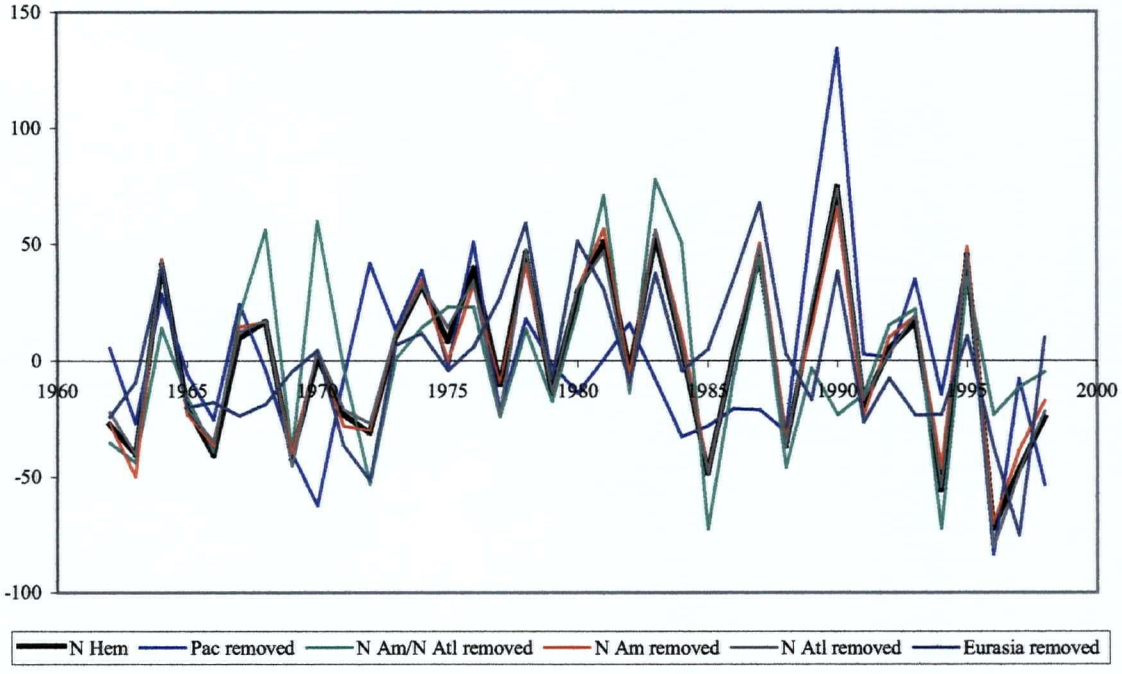

Figure 3.15 – Regional anomaly-removed indices for intense cyclones. Indices represent Northern Hemisphere intense (<980hPa) cyclone frequency anomalies from GISS data with various regional anomalies removed from 1961/62 to 1997/98 (refer to text for more details). The colour scheme for different regions is the same as in figure 3.14.

The 1976/77 regime shift is not apparent in the intense cyclone anomaly record. Although, it can be noted that for that season anomalies in Eurasian intense cyclones appear to be the most influencing factor in the record. Eurasian intense cyclones are also the most prominent throughout the late 1960's. This is in contrast to the full record in figure 3.14 where anomalies in North American and North Atlantic cyclones were mostly responsible for anomalies in the Northern Hemisphere record. In the case of intense cyclones, North American and North Atlantic cyclone anomalies influence the Northern Hemisphere record most prominently in the early 1970's instead.

Intense cyclones in the North Pacific region still account for most of the variability in the Northern Hemisphere record throughout the 1980's and over the 1988/89 peak, although in the middle part of the 1980's an influence by Eurasian intense cyclones can also be observed. This could suggest that the anomalous intense cyclone frequency in the Pacific around this time is due to storms originating in the Asian region. However, seeing as other observations presented here

point to very few intense cyclones occurring in the Asian portion of the Eurasian continent (refer to the analysis of Gobi Desert region cyclones at the end of this chapter) this scenario is less likely than the increase in Pacific and Eurasian intense cyclone frequency merely being coincidental.

Significant periods of negative anomaly were found in cyclone frequency during the early to mid 1980's in the Pacific region that were similar to those observed by Nakamura et al. (2002), who related changes there over the 1980's and 1990's to variability in the Aleutian Low and Siberian High (following Trenberth, 1994). In that study, using data from 1979 to 1995 the authors also found a tendency for mid-winter storm activity to increase through this period. Though, from comparison of figure 3.4a, it is possible this trend is an effect of that analysis beginning just before the extended 1980's period of low winter cyclone frequency in the northern hemisphere Pacific region.

Interestingly, despite the better agreement of the two data sets in the latter half of the record, the ARCSS data does not exhibit the extended 1980's cyclone anomaly. The ARCSS data also show a large negative anomaly in the Northern Hemisphere and Pacific records in the early 1970's, although it is unclear to what this anomaly might be related.

To an extent, a period of negative anomalies in cyclone frequency similar to the 1980's Pacific event can also be observed in GISS data in the North American and Atlantic regions during the 1990's. This coincides with an extended positive phase of the NAO (figure 3.16).

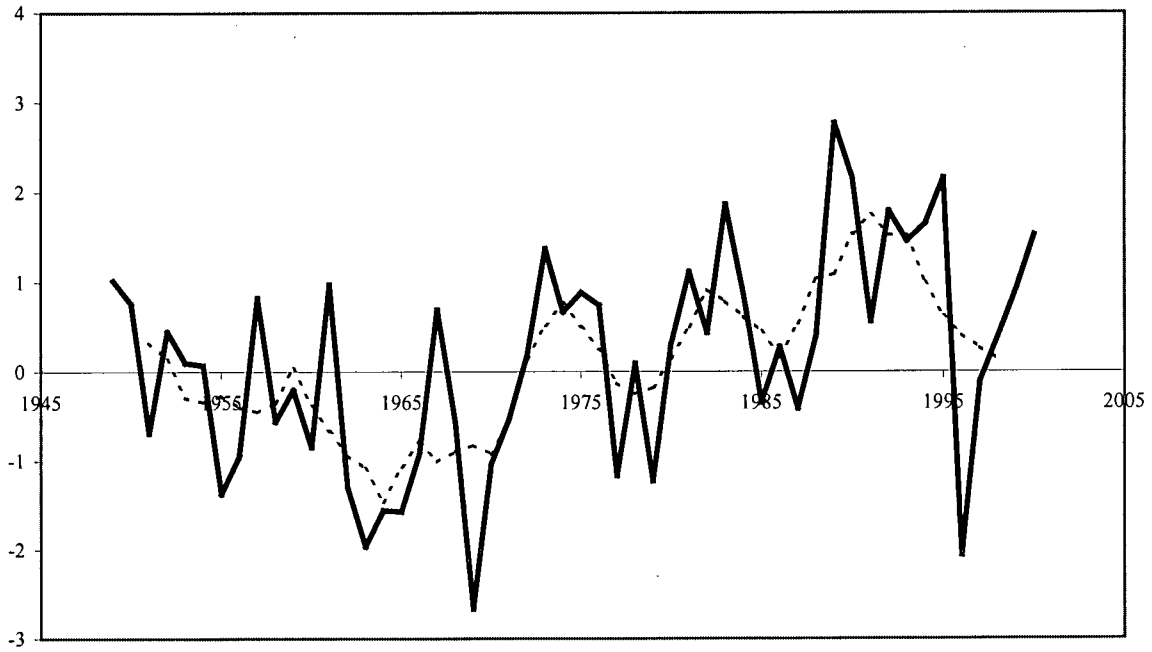

Figure 3.16 – Mean winter (Dec-Mar) values of the North Atlantic Oscillation, 1949 - 2003 (Hurrell, 1995 – completed using updated values from http://tao.atmos.washington.edu/data_sets/nao/). The dashed line represents a five-year running mean.

From the time series analyses and associated dataset difference figures (part (b) of figures 3.2 through 3.13), it is apparent that in all cases except for Pacific region the GISS data show a higher cyclone frequency. This difference is echoed for intense cyclone frequency in all cases except in the North Atlantic analysis. In this instance, while a greater number of storms are observed in the full record in the GISS analysis, the ARCSS analysis produces a higher frequency of intense cyclones. This could indicate a bias towards more severe storms in the far North Atlantic in the ARCSS algorithm. Mean SLP tends to be lower at higher latitudes, so it is possible that the ARCSS algorithm does not adequately compensate for this.

The sign of the trends in difference between regions is not consistent throughout all analyses either. On one hand, this might indicate that there is not a problem due to missed storms in any parts of the records. On the other hand, it could suggest the existence of anomalous situations not being adequately recognised by the algorithms or that there are additional spatial and temporal variations in the effectiveness of the algorithms with respect to the representation of certain situations. Such an example of this would be the 'blocking' of cyclone paths in the north-east Pacific discussed earlier in this chapter.

A notable feature of the difference analyses which re-occurs in several cases is a 'spike' in difference between the datasets around 1990. This spike is predominantly due to an increase in GISS cyclone frequency that is not matched in the ARCSS data.

As observed in figure 3.14, 1976/77 is often a point of minimum difference in many of the analyses. That is, variability which might be associated with the 1976/77 regime shift is well represented in both datasets. An exception to this is intense cyclone frequency in the North American/North Atlantic record.

Much of the cyclone frequency variability observed during significant episodes in the Northern Hemisphere record is also observed in northern hemisphere Pacific region cyclones. The other regions are much less similar, except for a negative Northern America/North Atlantic anomaly event in the GISS record around the mid-1990's.

In contrast to other analyses presented here, this suggests that most of the variability in the Northern Hemisphere record occurs in the north Pacific region. If the GISS record is assumed to be more accurate, then this Pacific influence on the Northern Hemisphere record is despite the combined North American/North Atlantic record recording a higher frequency of cyclones.

From the GISS analyses, Pacific cyclone frequency is only marginally higher than North Atlantic cyclone frequency. This provides motivation to focus attention in the following chapters on the Pacific region.

From the analysis of ARCSS data there appear to be peak periods in the frequency of intense cyclones during the early 1970's and early 1990's. These seem to be predominantly represented in the North Atlantic records and coincide with a rare negative phase of the NAO in the 1990's (see figure 3.16).

Another feature of intense cyclone frequency in the Eurasian region from the GISS data, is a 'capacitor-like' pattern throughout much of the record. At semi-regular periods there exists a peak, or culmination of a positive trend at 1968/69, 1976/77 and 1984/85. In at least the latter two instances this is followed by a period of negative anomaly which, in the case of the 1967/77 and 1984/85 'crashes', lasts several years. This pattern resembles a scenario where storm intensity, or frequency of intense storms, increases in the mean flow until some, unstable threshold point is reached. At this point the intensity of storms, or eddy development in the mean flow would break down before slowly building up again, in much the same fashion as a capacitor on an electrical circuit board stores energy.

Observations of events in intense cyclone frequency are not as intuitive as the clearer distinction of events in the complete cyclone record, so analysis therein is primarily statistical and covered in the remainder of the chapter.

3.2. Climate regime shift in cyclone frequency time series analysis.

Distinct changes in the nature of trends in cyclone frequency can be observed in the time series analyses (see figures 3.17 through 3.27). Interestingly, these changes in trend are more widespread in the analyses than significant changes in mean cyclone occurrence either side of the 1976/77 regime shift (see table 3.2). That is, during different climate regime phases the nature of cyclone frequency anomaly in many regions of the Northern Hemisphere maintains a similar magnitude of cyclone variability across the different regimes, despite changes in trend or frequency.

Not all records with a significant change in cyclone frequency are accompanied by a change in trend. This is the case, for instance, in the GISS analyses for all North Pacific region cyclones. A notable occurrence of change in trend around the 1977 regime shift, which is also accompanied by a significant change in frequency, is observed in the full Northern Hemisphere analysis. This change in trend varies between analyses, with the GISS data showing a near zero trend becoming positive after 1976/77 (figure 3.17a) and the ARCSS data showing a negative trend becoming near zero (figures 3.17b and 3.18b). While both changes in trend are still positive, the trends observed in the frequency of intense cyclones differ from those in the full record, with positive trends followed by near zero trends in all analyses. These trends are more also uniform across the different sets of data. In the case of intense cyclone frequency from the GISS analysis and in all analyses of ARCSS data, the trends observed in the Northern Hemisphere are similar to those observed in the North Pacific, further highlighting the significance of this region a 'hotspot' of cyclone activity and suggesting relevance of the variability in this region to climate in the rest of the Northern Hemisphere.

Some degree of evidence for changes in cyclone trend influenced by climate regime shift can be seen in other regions of the Northern Hemisphere analysed, however while the changes are readily observable, they are not as robust as those observed in the Northern Hemisphere or north Pacific regions.

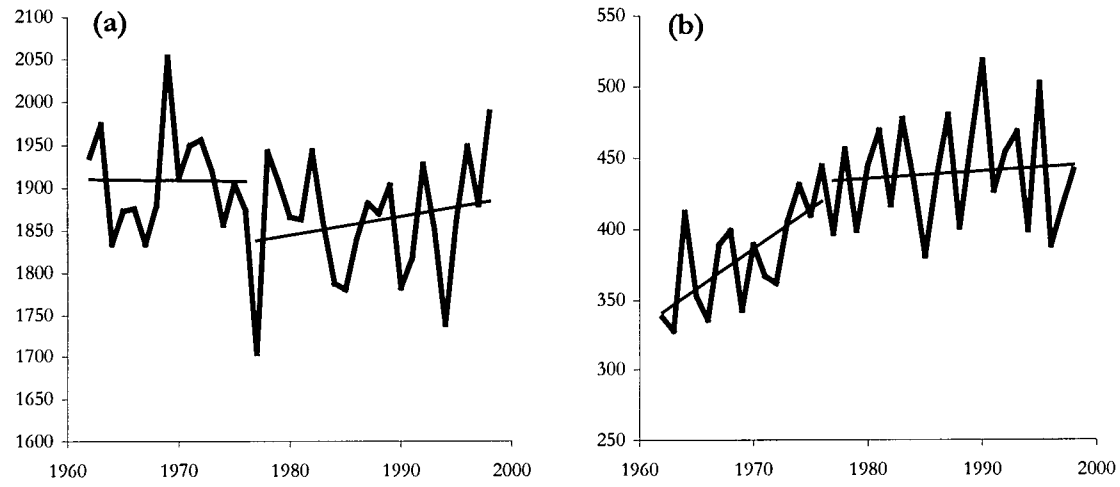

Figure 3.17 – Northern Hemisphere NDJFMA (a) cyclone frequency; and (b) intense (<980hPa) cyclone frequency; with split regression analyses around 1976/77. Data from the GISS dataset, 1962/63 – 1997/98.

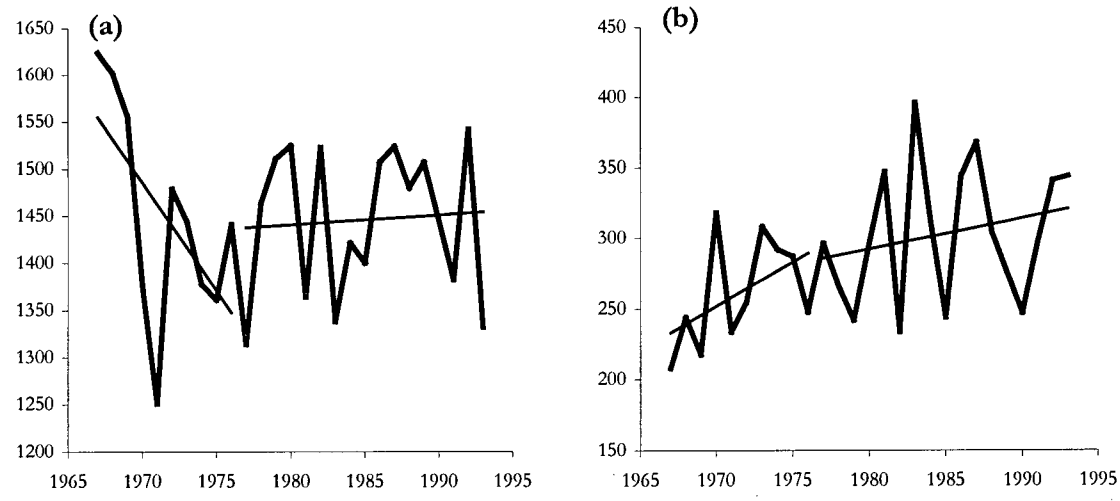

Figure 3.18 – Northern Hemisphere NDJFMA (a) cyclone frequency; and (b) intense (<980hPa) cyclone frequency; with split regression analyses around 1976/77. Data from the ARCSS dataset, 1966/67 – 1992/93.

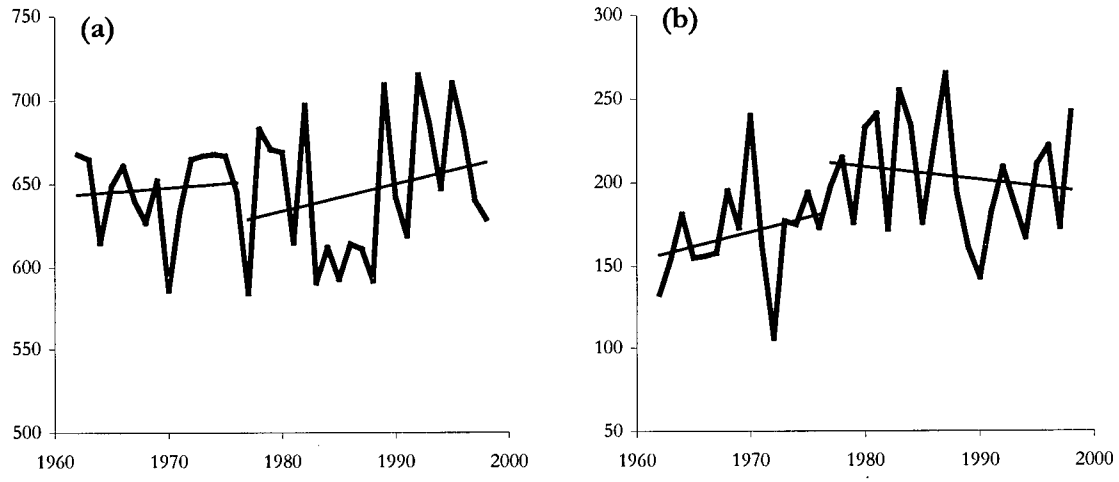

Figure 3.19 – North Pacific (30°N to 80°N, 135°E to 120°W) NDJFMA (a) cyclone frequency; and (b) intense (<980hPa) cyclone frequency; with split regression analyses around 1976/77. Data from the GISS dataset, 1962/63 – 1997/98.

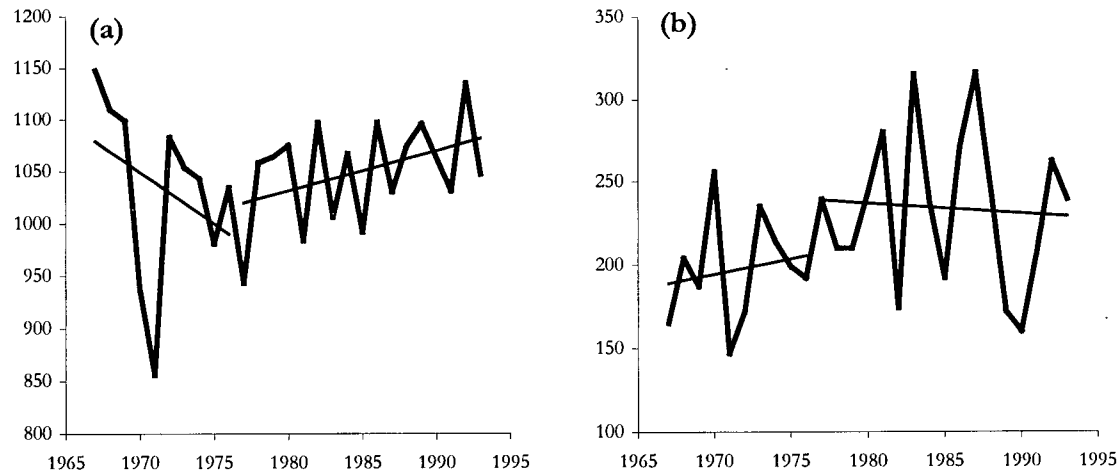

Figure 3.20 – North Pacific (30°N to 80°N, 135°E to 120°W) NDJFMA (a) cyclone frequency; and (b) intense (<980hPa) cyclone frequency; with split regression analyses around 1976/77. Data from the ARCSS dataset, 1966/67 – 1992/93.

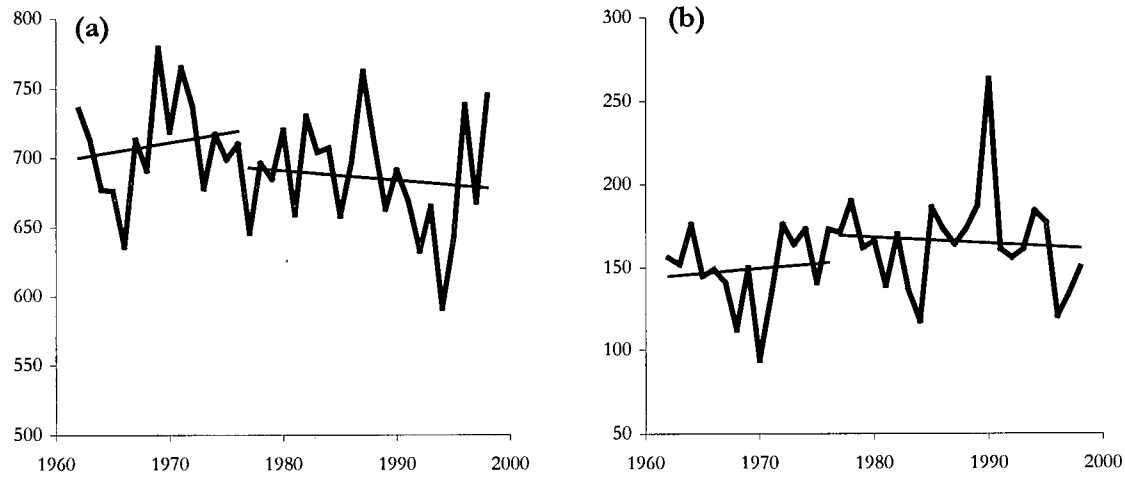

Figure 3.21 – North America/North Atlantic combined (30°N to 80°N, 120°W to 0°) NDJFMA (a) cyclone frequency; and (b) intense (<980hPa) cyclone frequency; with split regression analyses around 1976/77. Data from the GISS dataset, 1962/63 – 1997/98.

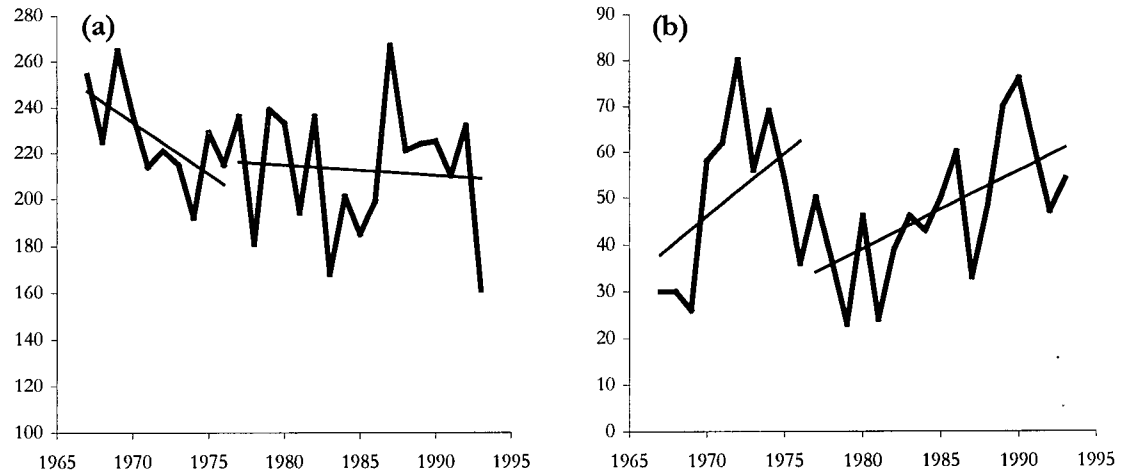

Figure 3.22 – North America/North Atlantic combined (30°N to 80°N, 120°W to 0°) NDJFMA (a) cyclone frequency; and (b) intense (<980hPa) cyclone frequency; with split regression analyses around 1976/77. Data from the ARCSS dataset, 1966/67 – 1992/93.

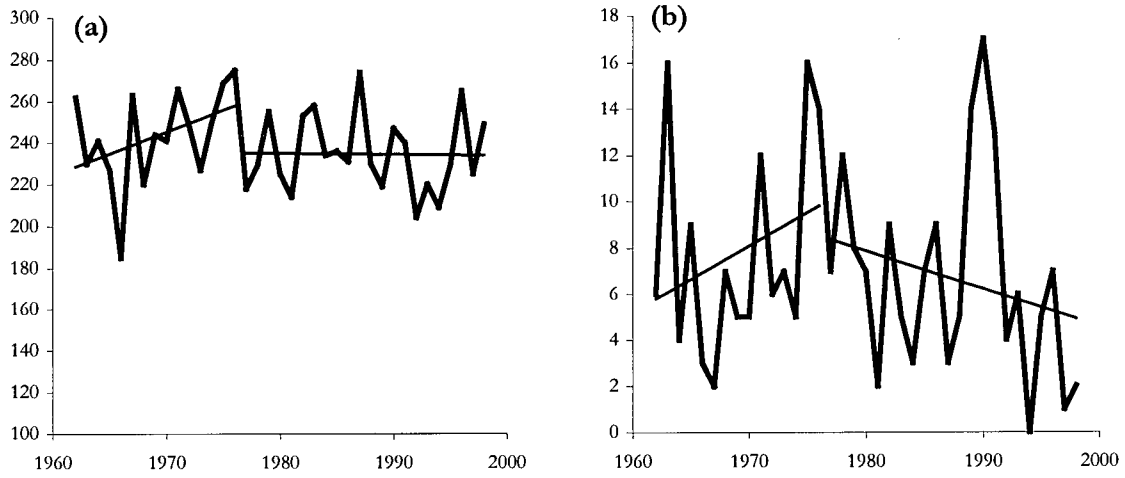

Figure 3.23 – North American (30°N to 80°N, 120°W to 70° W) NDJFMA (a) cyclone frequency; and (b) intense (<980hPa) cyclone frequency; with split regression analyses around 1976/77. Data from the GISS dataset, 1962/63 – 1997/98.

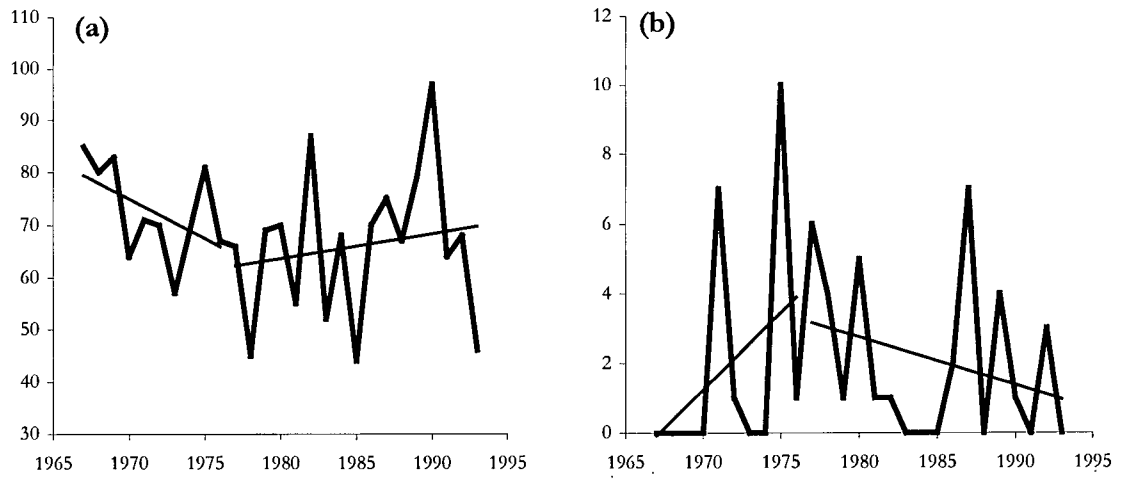

Figure 3.24 – North American (30°N to 80°N, 120°W to 70° W) NDJFMA (a) cyclone frequency; and (b) intense (<980hPa) cyclone frequency; with split regression analyses around 1976/77. Data from the ARCSS dataset, 1966/67 – 1992/93.

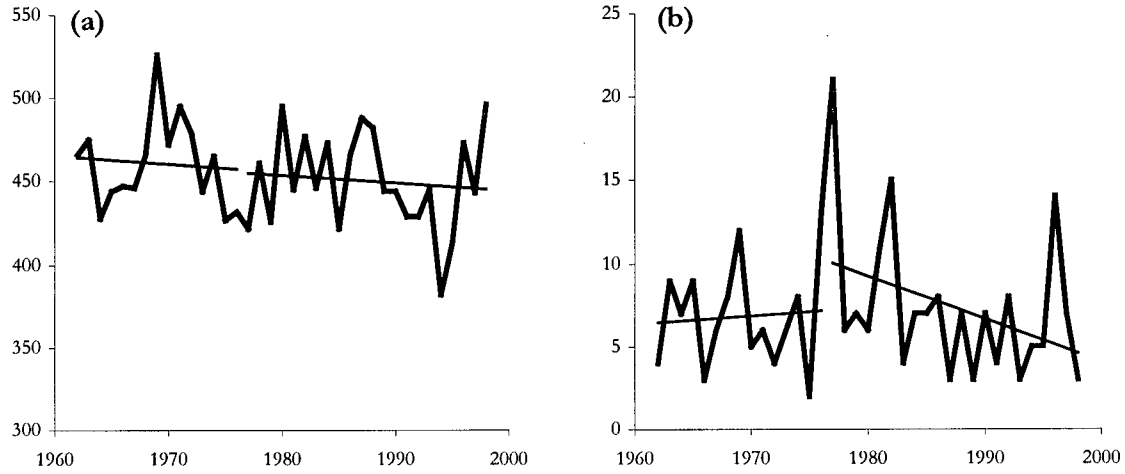

Figure 3.25 – North Atlantic (30°N to 80°N, 70°W to 0°) NDJFMA (a) cyclone frequency; and (b) intense (<980hPa) cyclone frequency; with split regression analyses around 1976/77. Data from the GISS dataset, 1962/63 – 1997/98.

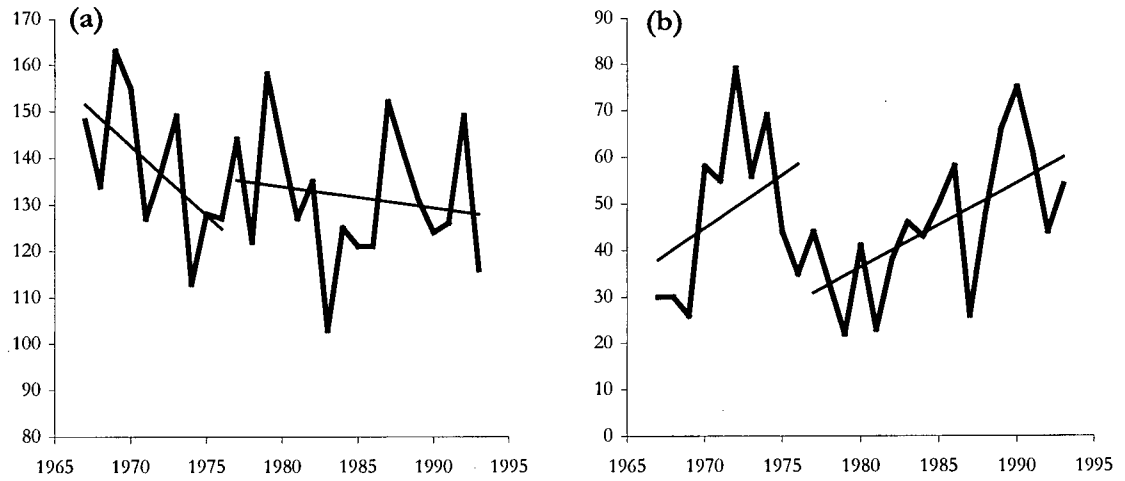

Figure 3.26 – North Atlantic (30°N to 80°N, 70°W to 0°) NDJFMA (a) cyclone frequency; and (b) intense (<980hPa) cyclone frequency; with split regression analyses around 1976/77. Data from the ARCSS dataset, 1966/67 – 1992/93.

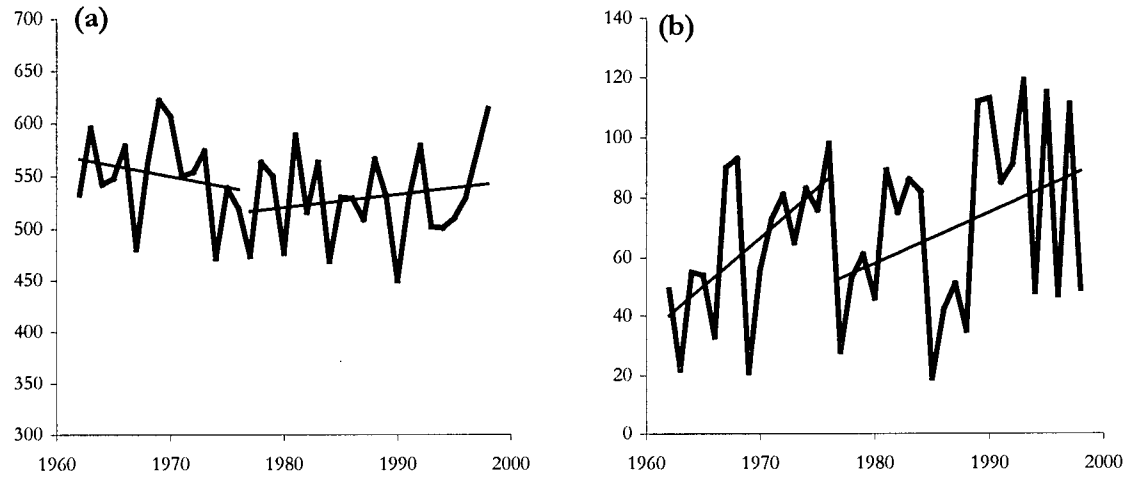

Figure 3.27 – Europe/Asia (30°N to 80°N, 0° to 135°E) NDJFMA (a) cyclone frequency; and (b) intense (<980hPa) cyclone frequency; with split regression analyses around 1976/77. Data from the GISS dataset, 1962/63 – 1997/98.

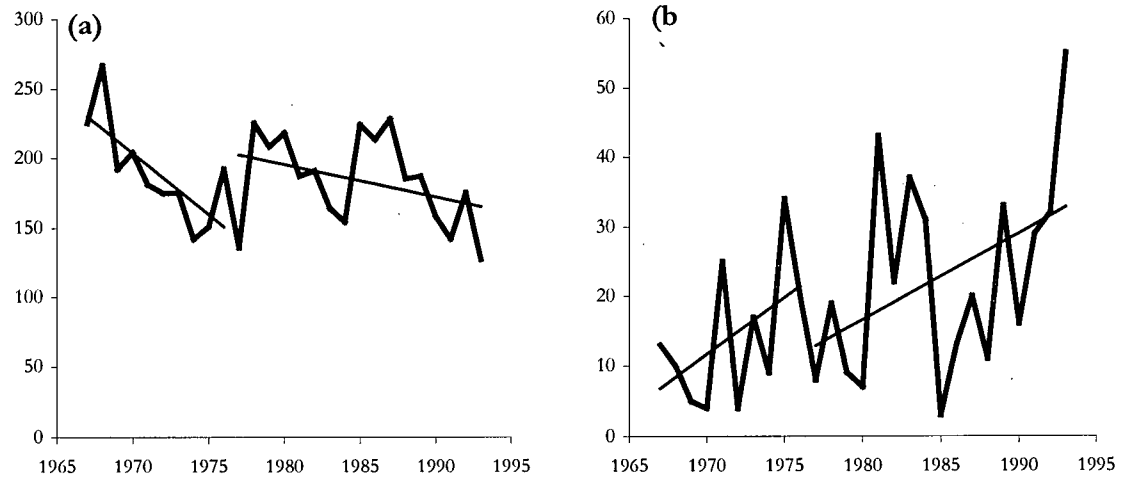

Figure 3.25 – Europe/Asia (30°N to 80°N, 0° to 135°E) NDJFMA (a) cyclone frequency; and (b) intense (<980hPa) cyclone frequency; with split regression analyses around 1976/77. Data from the ARCSS dataset, 1966/67 – 1992/93.

Tables 3.2a to 3.2f show the statistical significance of the difference on cyclone frequency in various regions of the Northern Hemisphere for the different classifications of climate regime change (refer to Chapter 2 for regime definitions).

Table 3.2 – Significance of difference (z-statistics) in NDJFMA cyclone frequency between phases of variously defined climate regimes, for: (a) Northern Hemisphere; (b) North Pacific (30°N to 80°N, 135°E to 120°W); (c) North America (30°N to 80°N, 120°W to 70° W); (d) North Atlantic (30°N to 80°N, 70° W to 0°); (e) North America and North Atlantic combined (30°N to 80°N, 120°W to 0°); and (f) Europe and Asia (30°N to 80°N, 0° to 135°E) for both ARCSS (1966/67-1992/93) and GISS (1961/62 – 1997/98) analyses. Dark shading denotes a trend which is significant at the 95% level – orange for significant positive and blue for significant negative. Pale shading denotes significance at the 90% level.

(a) **Nth Hemisphere Frequency**

	ARCSS		GISS	
Regime	**Full**	**980**	**Full**	**980**
PDO	-0.65	3.78	-1.25	1.99
77 regime	-0.13	2.5	-2.23	4.74
77/89 regime	-0.01	1.59	-1.65	1.81

(b) **Nth Pacific Frequency**

	ARCSS		GISS	
Regime	**Full**	**980**	**Full**	**980**
PDO	-0.48	4.59	-1.78	5.21
77 regime	0.53	2.76	-0.12	3.31
77/89 regime	-0.3	2.4	-2.11	3.4

(c) **Nth America Frequency**

	ARCSS		GISS	
Regime	**Full**	**980**	**Full**	**980**
PDO	-2.72	0.13	-1.15	-2.76
77 regime	-1.47	0.13	-1.17	-0.77
77/89 regime	-1.65	0.42	-0.02	-0.78

(d) **Nth Atlantic Frequency**

	ARCSS		GISS	
Regime	**Full**	**980**	**Full**	**980**
PDO	-0.59	-1.06	0.43	1
77 regime	-1.09	-0.41	-1.15	0.42
77/89 regime	-0.43	-2.36	0.64	1.3

(e) **Nth America/Atlantic Frequency**

	ARCSS		GISS	
Regime	**Full**	**980**	**Full**	**980**
PDO	-1.47	0.13	-0.52	-0.86
77 regime	-1.48	0.13	-1.89	1.87
77/89 regime	-0.75	0.42	0.31	0.58

(f) **Europe/Asia Frequency**

	ARCSS		GISS	
Regime	**Full**	**980**	**Full**	**980**
PDO	0.28	0.89	-0.05	-1.06
77 regime	-0.49	0.32	-1.58	0.82
77/89 regime	1.17	-0.35	-1.09	-2.01

In this analysis, a significant positive difference corresponds to a higher frequency of cyclones occurring during phases of climate regimes which were designated as positive and vice versa in the case of a negative significance of difference. As outlined in Chapter 2, the positive and negative designation of regime phases is based upon positive and negative phases of the PDO. The analyses show results that vary widely across the various regions for different regime definitions. In general, there is no significant difference in cyclone frequency in the Northern Hemisphere from analysis of ARCSS data cyclone statistics. The exception is over the North American continent, where there is a significant negative difference between phases of the PDO. Although this result is not echoed in the GISS analysis, it does compliment the findings of Mantua et al. (1997). In that study, correlations were drawn between North American precipitation and decadal oscillations in North Pacific SSTs. Precipitation is often associated with cyclone occurrence.

Similarly, a significant negative difference between pre-1976/77 and post-1976/77 cyclone frequency in the whole Northern Hemisphere observed in the GISS analysis is not found in the parallel ARCSS analysis. Minor differences (significant at the 90% level) exist in the Northern Hemisphere between 77/89 regime phases (GISS analysis), in the combined North American/North Atlantic region either side of the 1976/77 regime 'flip' (GISS analysis) and in the North American region between 77/89 regime phases (ARCSS analysis).

The strong relationship shown here between positive regime phases and increases in intense cyclone frequency in the North Pacific and Northern Hemisphere might also partly explain the positive trends observed in these regions over the time investigated. Though, this association does not seem to exist in the case of North American or North Atlantic cyclones.

Furthermore, and in a similar manner to the trend analyses, most of the variability in Northern Hemisphere and North Pacific cyclone frequency between climate regime phases can be observed in intense cyclones. Again, the similarity between the positive regime phases and positive change in trend in intense cyclone frequency coinciding in the latter part of the cyclone record in some regions of the Northern Hemisphere suggests that the trends observed are perhaps a factor of the timing of the regime phases with respect to the time period analysed.

However, in order to better assess the degree to which the trend is reliant upon this factor, a more detailed analysis of cyclone frequency with a longer data record would be required.

3.3. Gobi Desert cyclone frequency.

While the GISS and ARCSS data sets are generally in good agreement on regional and global scales in terms of spatial variability in cyclone statistics, in some more localised regions of important cyclone occurrence there is almost no uniformity. An example of such a region is the Gobi Desert region of northern China/southern Mongolia (40°N to 50°N, 100°E to 110°E). Figures 3.28a and 3.28b show mean cyclone frequency for the Eurasian region from ARCSS and GISS data sets respectively.

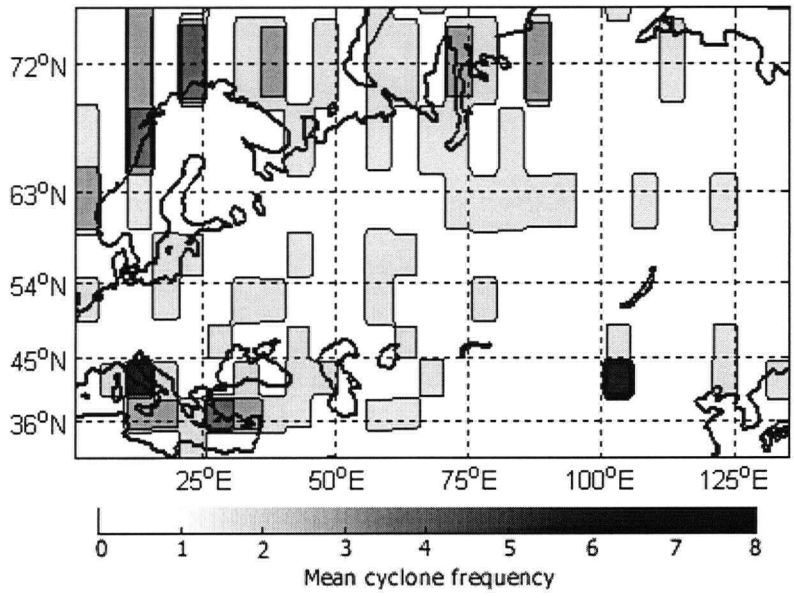

Figure 3.28a – Mean NDJFMA cyclone frequency from ARCSS data for the Europe/Asia region (30°N to 75°N and 0° to 135°E), 1966/67-1992/93. Cyclone frequency is calculated in 5° x 5° latitude-longitude squares.

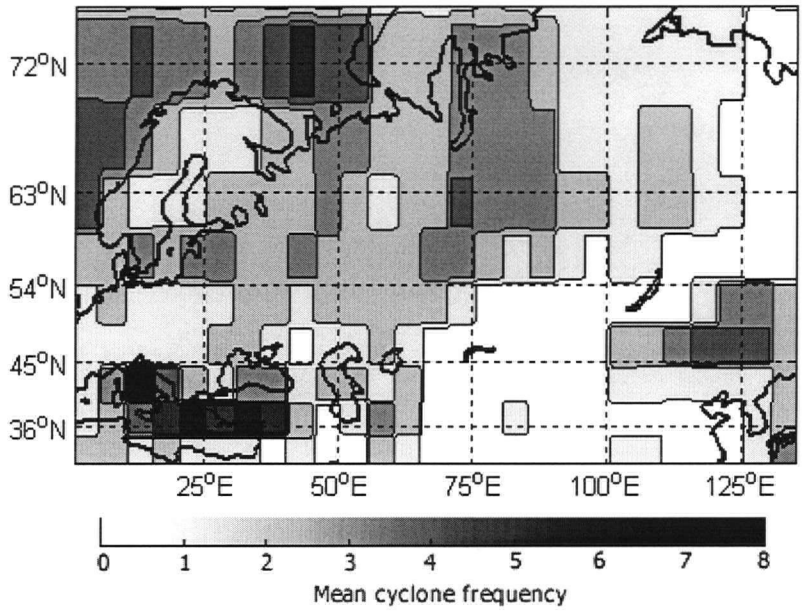

Figure 3.28b – Mean NDJFMA cyclone frequency from GISS data for the Europe/Asia region (30°N to 75°N and 0° to 135°E), 1962/63-1997/98. Cyclone frequency is calculated in 5° x 5° latitude-longitude squares.

As noted in the northern hemisphere analysis, cyclone coverage over this region appears to be more complete, or smoother, in the GISS data. In both datasets, however, a maximum in cyclone frequency can be observed around 40°N to 50°N, 100°E to 110°E.

In the ARCSS analysis, the high frequency of cyclones over the Gobi Desert occurs as a distinct maximum which is not supported by a significant amount of cyclone activity in the surrounding 5° x 5° squares. In the GISS analysis, the region is 'connected' with north-west Pacific cyclones. As with the Northern Hemisphere analysis, whether this represents a greater accuracy in GISS data or is a product of cyclone identification algorithm smoothing is ambiguous. Despite the discrepancies between datasets in the Eurasian region, what is apparent from both datasets is that the Gobi Desert area is one of significant cyclone activity in north-east Asia.

Figures 3.29a and 3.29b show time series analyses of cyclone frequency in the Gobi Desert region from ARCSS and GISS datasets respectively.

The time series analyses highlight a surprising degree of difference between the two datasets. While the ARCSS analysis shows a significant positive trend in cyclone frequency ($z = 6.03$, 1.96 is significant), a significant negative trend ($z = -12.59$) can be found using GISS data.

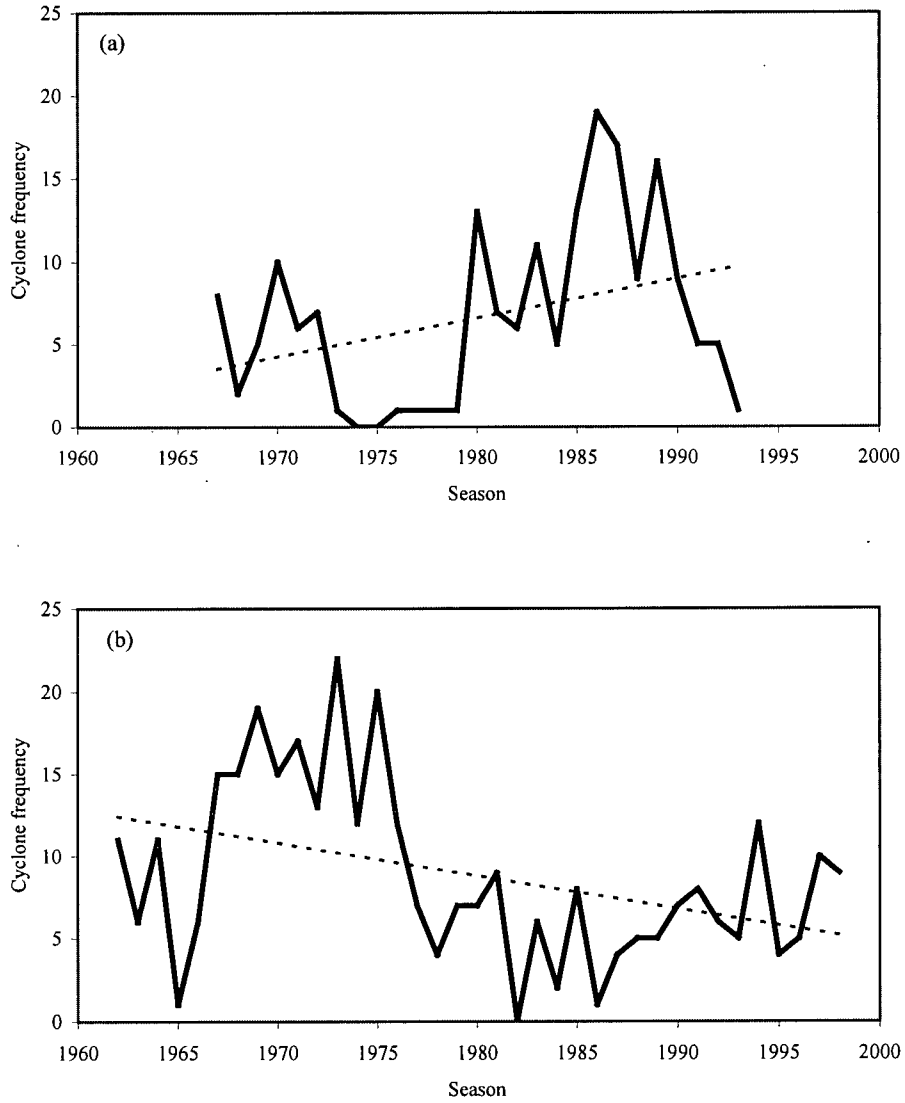

Figure 3.29 – Gobi Desert region (40°N to 50°N, 100°E to 110°E) mean NDJFMA cyclone frequency, from: (a) ARCSS data, 1966/67-1992/93; and (b) GISS data, 1962/63 – 1997/98.

The GISS data show a large period of high cyclone frequency during the late 1960's to the mid 1970's. The ARCSS data show a higher frequency period through most of the 1980's. An analysis of cyclone frequency anomalies in the region by removing the linear trend from both time series reveals that after the early 1970's, anomalies in frequency in the two analyses are almost inverse. Prior to this, the large positive anomaly period in the GISS data is only partly represented in ARCSS data.

The time series analysis from the GISS data is more similar to the analysis conducted by Qian et al., 2002. However, this is to be expected to a degree given that the cyclone data used in that

study was also Re-analysis based. The GISS data are also more consistent with the frequency of dust storm days in that region also included in the Qian et al. study. Qian et al. (2002) found a positive correlation between dust storms and cyclone frequency in that region.

The reasons why the ARCSS data yield such a different result are unclear. It could be that the ARCSS data are simply not as accurate over the time period analysed in this region, despite the agreement between datasets in location of the cyclone frequency maxima. Although this can not be concluded with certainty due to the possible existence of the common data source issue.

The results of statistical analyses of cyclone frequency variability in this region with respect to the PDO and different definitions of climate regime change are summarised in table 3.3.

Table 3.3 – Significance of difference in Gobi Desert region (40°N to 50°N, 100°E-110°E) NDFJMA cyclone frequency between different phases of various climate regime indices.

	Gobi Desert Frequency			
	ARCSS		GISS	
Regime	Full	980	Full	980
PDO	1.86 *		-2.93	
77 regime	2.27	N/A	-4.45	N/A
77/89 regime	1.65 **		-4.12	

* significant to 90% CI and significant for 45-50N, 100-105E

** 95% significant for 45-50N, 100-105E

The GISS data show a significant decrease in cyclone frequency following the 1977 climate regime flip. Significantly less cyclones are also observed during positive phases of the PDO and during positive years from the regime index constructed using the two regime change events (1976/77 and 1989) in the GISS analysis. The difference is more significant between regime phases than during positive and negative phases of the PDO. This suggests that while there is a negative relationship between cyclone frequency in this region and the PDO, there is a different, or additional degree of relationship between cyclone frequency and the mechanisms associated with the climate regime phase changes. It also alludes to the possibility that the climate regime shifts might also exist outside of the immediate Pacific region.

The cyclone variability time series in both analyses resemble variability in the Siberian High (see figure 3.30) in different ways.

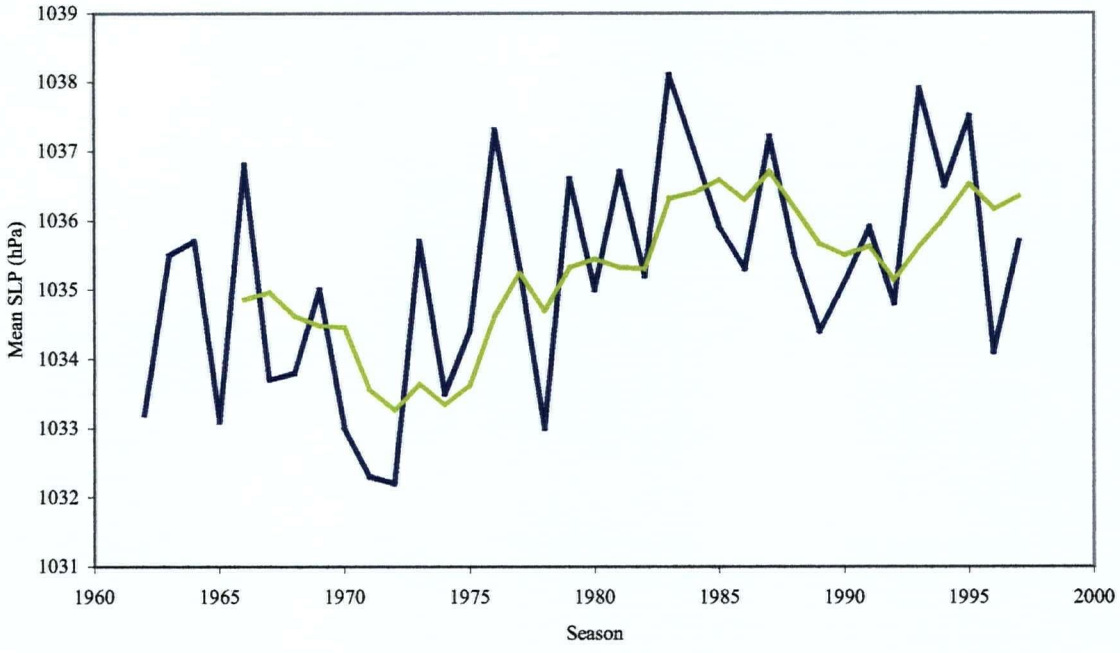

Figure 3.30 – Siberian High Index (SHI), 1962/63 to 1997/98 with 5-year running mean (green line). Refer to Chapter 5 for a detailed explanation and analysis of Siberian High variability.

Although neither cyclone time series correlates with seasonal mean values of the Siberian High at the 95% level, similarities can be observed with respect to significant periods of positive and negative anomaly in the data and the GISS cyclone analysis shows a significant correlation with the Siberian High Index (SHI) at the 90% level. For example, a low anomaly period in the SHI in the 1970's corresponds partly to fewer cyclones in the ARCSS analysis and to a high anomaly period in the GISS data. Likewise, during a period of positive anomaly in the SHI during the mid to late 1980's, GISS data show a generally lower frequency of cyclones in the region while the ARCSS analysis during that part of the time series echoes the positive SHI.
Other studies relating to cyclone variability related to the Siberian High are summarised in Nakamura et al., 2002.

3.4. Analysis of Pacific cyclogenesis from ARCSS data.

As has already been noted, cyclone statistics in the ARCSS dataset are best represented in the Pacific region. This is also the case in the analysis of cyclogenesis events.

Figure 3.31 shows mean Northern Hemisphere NDJFMA cyclogenesis events from 1966/67 to 1992/93, calculated from ARCSS data. The plot shows that according to the ARCSS data, a large enough difference exists between the number of seasonal Pacific cyclogenesis events and those in all other regions that mean cyclogenesis does not appear on the Northern Hemisphere map outside of the Pacific region. This supports the notion that the north Pacific is a crucial region of cyclone formation and poleward energy transport in the Northern Hemisphere (after van Loon and Williams, 1979).

It should also be noted that no cyclogenesis events are observed in the north Atlantic region. This region contains one of the more active storm tracks of the Northern Hemisphere. In reality, the north-west portion of the Atlantic region should show a major centre of cyclogenesis. The fact that it doesn't here suggests that the ARCSS data set does not accurately represent cyclone occurrence in the Atlantic region.

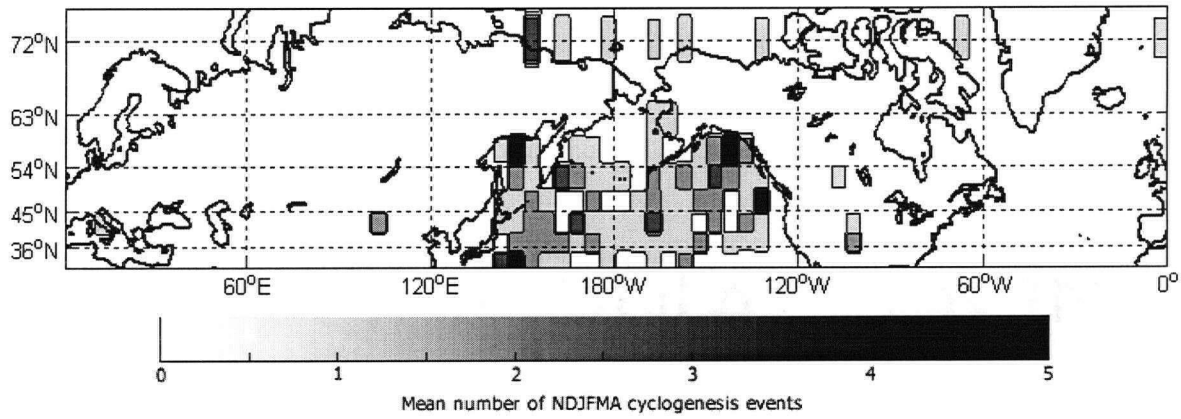

Figure 3.31 – Mean Northern Hemisphere NDJFMA cyclogenesis events from ARCSS data, 1966/67-1992/93.

Seeing as literature reviewed, climate indices used and the nature of investigation here focuses on the northern hemisphere Pacific region, the existence of a greater number of Pacific cyclogenesis events in the ARCSS data provides motivation to focus an analysis of cyclogenesis in this context on the Pacific region. The ARCSS data are used as the primary source for

analysis here as the GISS dataset contains no specific designation for observations of cyclogenesis events.

The mean seasonal analysis of the Pacific identifies two major regions of cyclogenesis. One of these is in the north-west Pacific. This region itself contains multiple regional maxima. One intense region of north-west Pacific cyclogenesis can be observed over the Sea of Okhotsk (around 55°N, 150°E). The other zone of higher cyclogenesis appears along the Kurishio/Oyashio Extension (around 30°N to 50°N and 135°E to 160°E).

The other region of higher cyclogenesis forms in the far north-east Pacific. One explanation for a maximum in mean cyclogenesis occurring in this region might be that storms here, which travel across the North American continent, are 'seeded' by cyclonic systems remaining in this region following propagation across the North Pacific. This might be related to the phenomenon of eddies from Pacific storms seeding Atlantic cyclones (after Chang and Yu, 1999) used by Chang and Fu (2002) to partly explain similarities in interdecadal variability between those two regions.

The number of cyclone forming in the Northern Hemisphere from 1966/67 to 1992/93 decreased significantly (table 3.4 and figure 3.32a).

Table 3.4 – Significance of trend (z-statistic) in NDJFMA cyclogenesis in the North Pacific region from ARCSS data (1966/67-1992/93). Events are also counted for Eastern (40°N to 65°N, 165°W to 135°W) and Western (40°N to 65°N, 145°E-155°E) regions of the North Pacific. Shading denotes a trend which is significant at the 95% level.

	z-statistic
N Pacific	-7.57
W Nth Pacific:	-9.39
E Nth Pacific:	-0.71

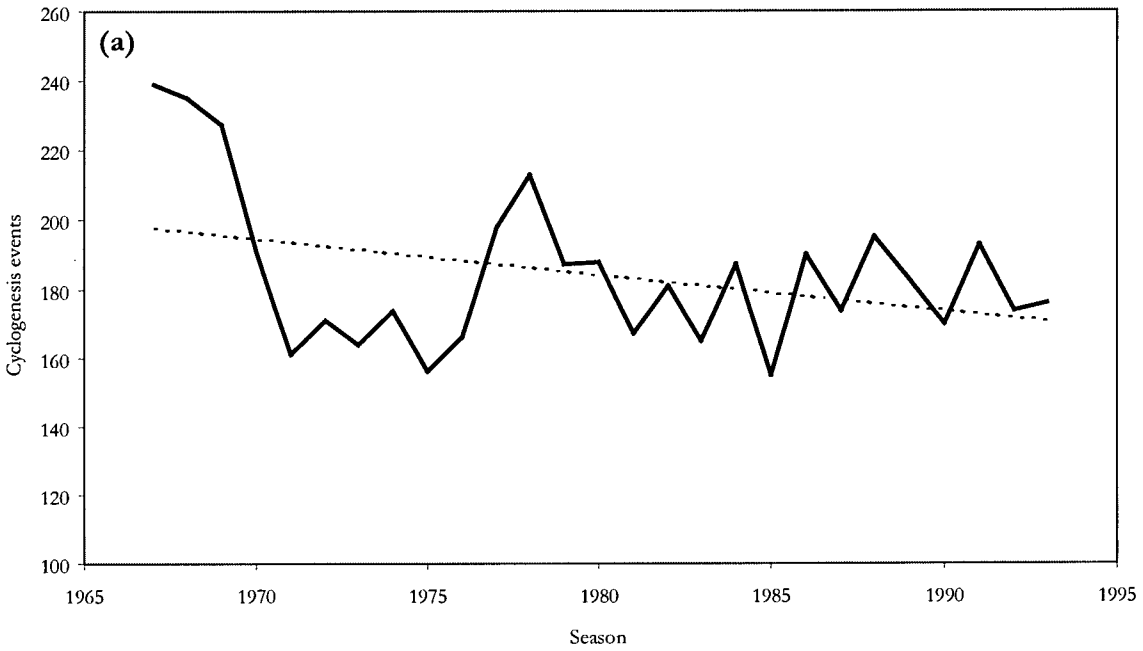

Figure 3.32a – North Pacific (30°N to 80°N, 135°E to 120°W) NDJFMA cyclogenesis events from ARCSS data, 1966/67 to 1992/93.

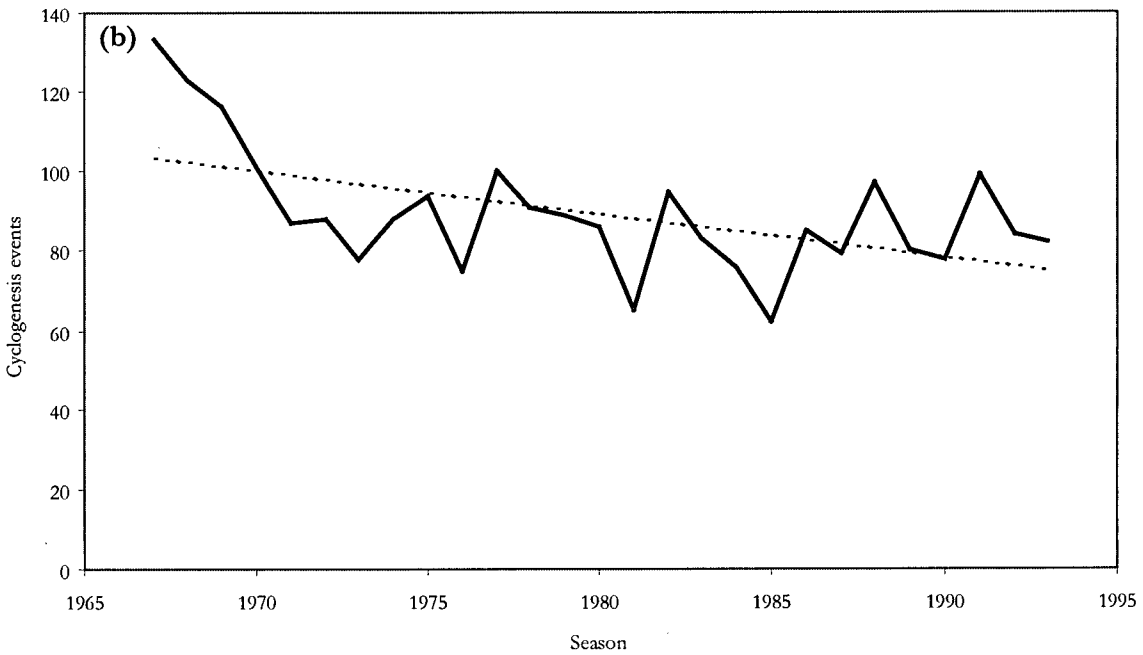

Figure 3.32b – Western North Pacific (40°N to 65°N, 145°E-155°E) NDJFMA cyclogenesis events from ARCSS data, 1966/67 to 1992/93.

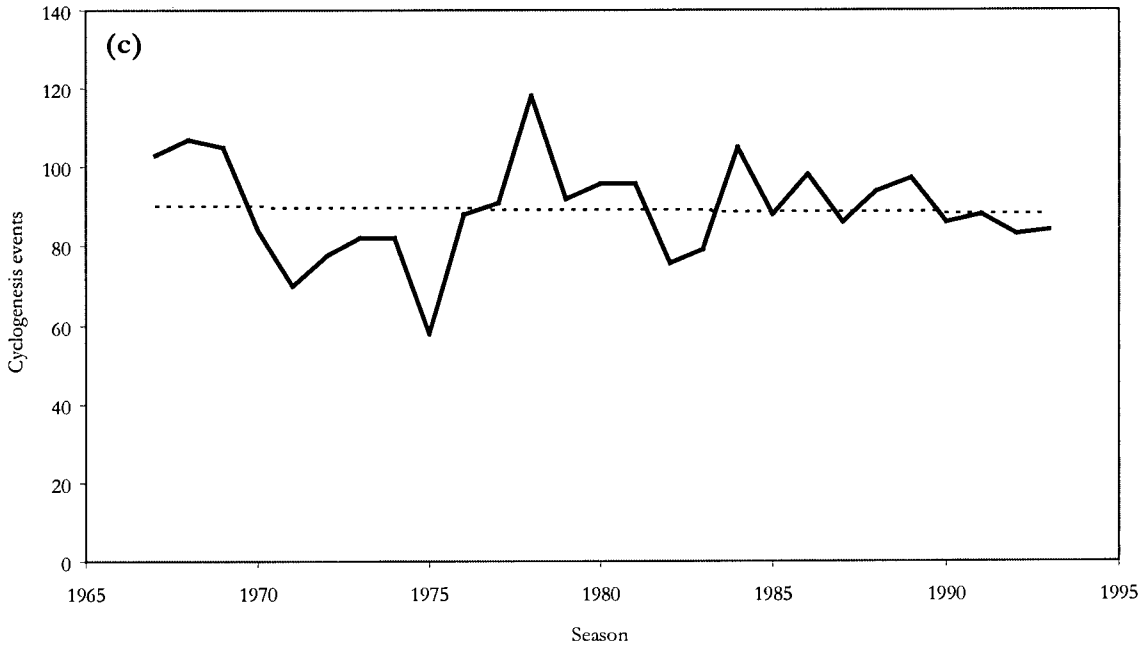

Figure 3.32c – Eastern North Pacific (40°N to 65°N, 165°W to 135°W) NDJFMA cyclogenesis events from ARCSS data, 1966/67 to 1992/93.

From table 3.4 and figures 3.32a-c, it is clear that most of the negative trend observed in the North Pacific is due to a similar negative trend in the western portion of the region. In the western North Pacific the number of cyclogenesis events decreases from a much larger number of events compared with the eastern North Pacific, to a similar value in the time period investigated. Meanwhile, very little change is observed in the general number of eastern North Pacific events. In addition to supporting the hypothesis that much of the variability in the North Pacific cyclone occurrence stems directly from variability in the north-west Pacific, this also adds justification for this region becoming a focal point for further analysis.

In all three Pacific cyclogenesis time series, there exists a prominent period of lower cyclogenesis through much of the 1970's. This negative anomaly period ends around the date of 1976/77 climate regime change.

Interestingly, despite the trend in overall North Pacific cyclogenesis apparently resulting from the negative trend in the western North Pacific, the positive anomaly immediately following the 1976/77 regime change is better represented in the eastern North Pacific record. Eastern North Pacific cyclogenesis correlates better with the North Pacific record on interannual time scales

also, correlating significantly at the 95% level. Interannual western North Pacific cyclogenesis variability does not correlate significantly with variability in the whole North Pacific.
While there is no significant difference in the number of cyclogenesis events in the entire North Pacific region between phases of any of the climate regime indices investigated between 1966/67 and 1992/93, there were differences between regimes in the individual regions within the North Pacific (see table 3.5).

Table 3.5 – Significance of difference (z-statistics) between phases of various climate regime indices in the western North Pacific (40°N to 65°N, 145°E-155°E) and eastern North Pacific (40°N to 65°N, 165°W to 135°W) from ARCSS data between 1966/67 and 1992/93. Dark shading denotes a trend which is significant at the 95% level – orange for significant positive and blue for significant negative. Pale shading denotes significance at the 90% level.

West Nth Pacific		East Nth Pacific	
Regime	ARCSS	Regime	ARCSS
PDO	-1.84	PDO	-1.37
77 regime	-1.66	77 regime	-1.22
77/89 regime	-2.85	77/89 regime	-2.07

Although it is difficult to assess changes over decadal time scales from such a short period of data with a large degree of confidence, significant differences were found in the number of cyclogenesis events occurring during positive and negative phases of the 77/89 regime index. Interestingly, this result is not observed between phases of the PDO or around the 1976/77 regime flip, with no significant results in the eastern North Pacific and differences only being significant at the 90% level in the western North Pacific. In disagreement with earlier hypotheses that the PDO is merely a representation of the regime shifts, this suggests that to a fair degree the shifts observed in general climate properties in the North Pacific region are not entirely explained by the PDO. It also provides evidence for the existence of the 1989 regime shift in the context of Pacific regional variability.

4. Analysis of north-west Pacific cyclones.

Observations made using various atlases of Northern Hemisphere cyclone occurrence (eg. GISS Atlas of Extratropical Cyclones, http://www.giss.nasa.gov; Mariner's Weather Log, National Weather Service, http://www.nws.noaa.gov) and analyses detailed in the previous chapter illustrate the north-west Pacific region as a major 'birthing' ground of North Pacific cyclones. In accordance with this observation, it is reasonable to hypothesize that variables affecting cyclone formation in that area could hold significance for storms in the entire North Pacific region. This region could also be more readily influenced by features in regional-scale circulation and mean flow 'upstream' of the Pacific, providing a link between non-Pacific climate variability and North Pacific cyclone frequency.

4.1. Variability in the occurrence of cyclones in the north-west Pacific region.

The frequency of cyclones in the north-west Pacific region exhibits a significant negative trend between 1961/62 and 1997/98 (figure 4.1).

From the time series analysis, four events of major change or anomaly can be observed. The most extreme of these corresponds to the 1982/83 El Niño event. From the Southern Oscillation Index (SOI; Troupe, 1965 - figure 4.2), it can be seen that this event was the most extreme El Niño event during the time period investigated. Trenberth and Hurrell (1994) discussed mechanisms linking ENSO variability and changes in North Pacific storm tracks.

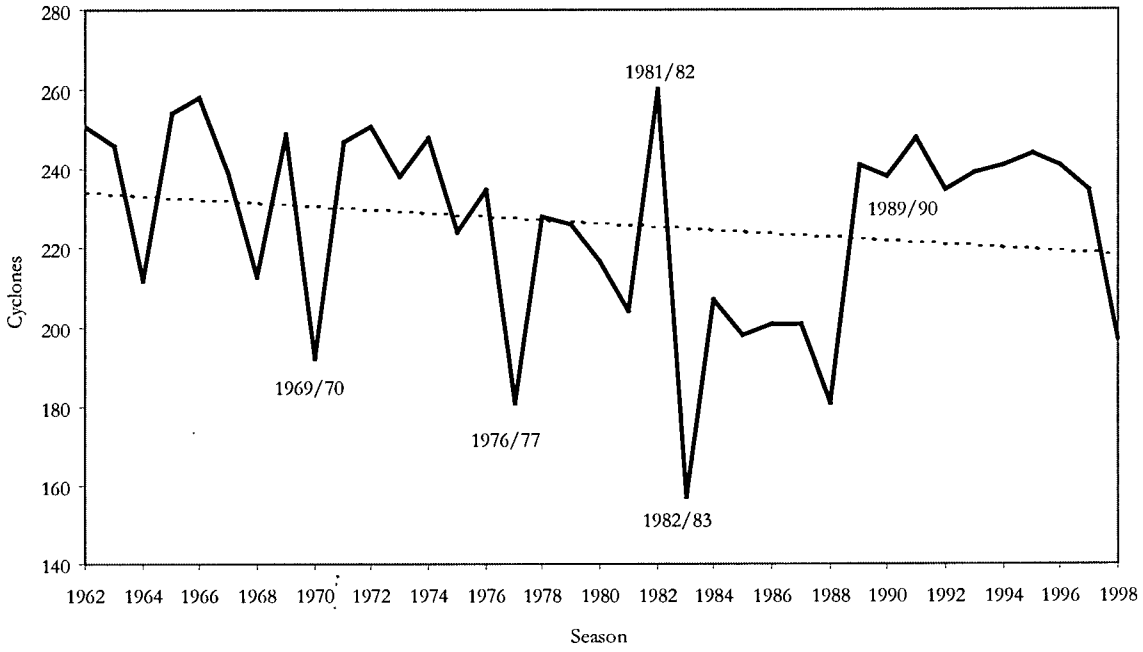

Figure 4.1 – NDJFMA cyclone frequency in the north-west Pacific region (30°N to 60°N, 130°E to 170°E), 1961/62-1997/98.

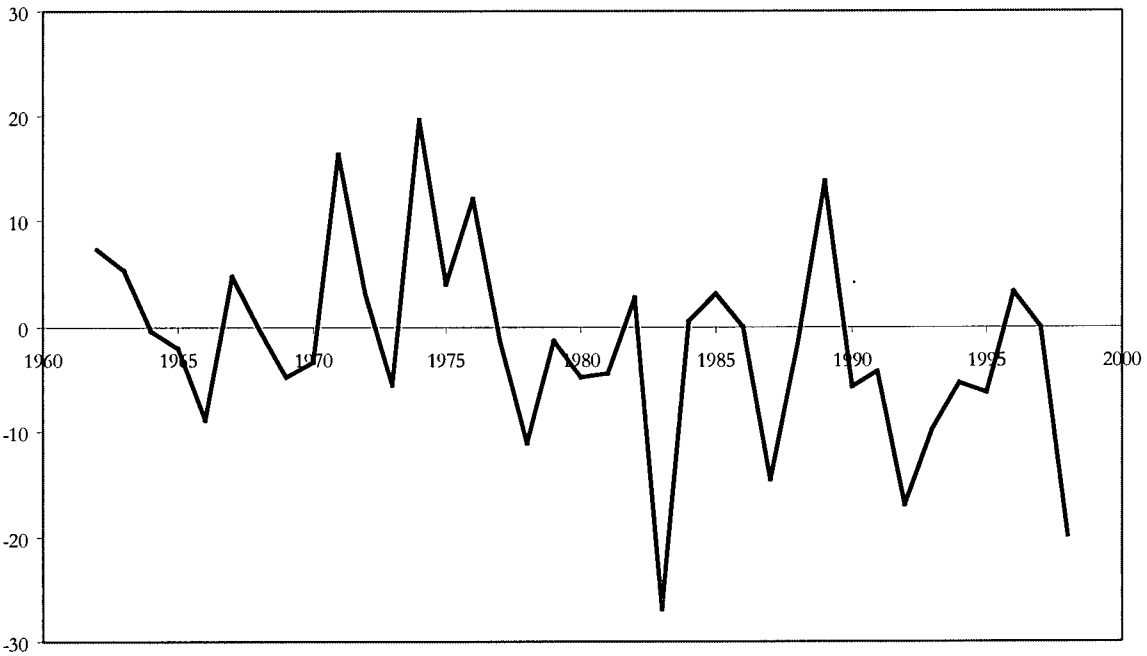

Figure 4.2 – NDJFMA mean Southern Oscillation Index (SOI), 1961/62 to 1997/98.

While some of the extreme events noted in the cyclone record appear to correspond to severe ENSO events, suggesting an influence on north-west Pacific cyclone occurrence by tropical SSTs, the relationship is not immediately obvious in all cases. For example, while the 1982/83 and 1989/90 events in the cyclone record correspond to ENSO events, others such as the 1969/70 event do not. Interestingly, the 1969/70 event coincides with the end of a phase of downward trend, and low anomaly, in the NAO (see figure 3.16). Additionally, all extreme events other than 1982/83 correspond to dates which have previously been linked to dates around which there have been observed changes in climate 'regime' (Chang and Fu, 2002 and Harnik and Chang, 2003 also observed a change in the general state of the North Pacific storm track after 1970). Gershnov and Barnett (1998) observed an interdecadal modulation of ENSO–related teleconnections and patterns in North Pacific variables that correspond to previous studies of Pacific decadal climate variability, such as that by Mantua et al. (1997). So it is likely that an additional explanation to similarities between the SOI and north-west Pacific cyclones is to be found, in part, to be due to both phenomena being influenced in a like manner by interdecadal variability in the background climatic state of the Pacific region.

The change in storm track noted by Chang and Fu (2002) during the early 1970's corresponds with the changes noted in the previous chapter in cyclone frequency and trends in a number of regions of the Northern Hemisphere, and also with a change around the same time in the Siberian High (see Chapter 5 for further analysis of this). Seeing as cyclones in the north-west Pacific region form in the mean flow 'downstream' of the Siberian High (eg. Chang, 2001), an additional influence from non-Pacific forced aspects of this climatic feature could perhaps explain the lack of a straightforward relationship between cyclone frequency in this region, the ENSO cycle and other mechanisms of interdecadal Pacific variability. This will be investigated more thoroughly later in this chapter.

There were significant differences observed in cyclone frequency between phases of all indices of climate variability examined (table 4.1). Unlike the analysis of cyclogenesis occurring in the north-west Pacific (refer to section 3.4), the difference in cyclones observed in the region between phases of the PDO is significant. This is likely due to the current analysis taking in a greater, better defined number of storms forming in or passing through the far north-west Pacific (the spatial sample areas are slightly different).

Table 4.1 – Z-statistic values for significance of difference in NDJFMA cyclone frequency between different phases of various climate indices (regimes) for the north-west Pacific area (30°N to 60°N, 130°E to 170°E), 1961/62 to 1997/98. Shading signifies values significant at the 95% level.

Regime	z-statistic
PDO	-4.04
77 regime	-2.42
77/89 regime	-3.78

The sample area is in the proximity of a centre of PDO-related SLP variability (see Mantua et al., 1997), meaning that the PDO should be a major factor in cyclone variability in this region. This analysis also allows for a greater influence from the Siberian High and mean flow variability 'upstream' of the north-west Pacific region by including cyclones entering the sample area from regions directly under the effect of the 'upstream' phenomena.
In this case, the relationship between the PDO and cyclones could also signify a relationship between the PDO and Siberian High, but this will be more fully analysed in Chapter 5.

4.2. Upper level wind variability and cyclone frequency in the north-west Pacific.

An analysis of the north-west Pacific region shows only small areas where there are significant correlations between vertical wind shear and cyclone frequency. It can be noted, however, that the correlations between cyclone frequency in the region and 200hPa winds are slightly stronger than those with vertical wind shear. This might imply that it is the upper level winds that are the influence on cyclone frequency and vertical wind shear is merely an unrelated variable which is also reliant on 200hPa winds.
However, given the lack of significant correlations in the region, it can be assumed that cyclone frequency in the region is not entirely related to the amount of vertical wind shear present.

An Empirical Orthogonal Function (EOF) analysis of 200hPa winds in the north-west Pacific region suggests that the PDO is a primary influence. The first EOF of 200hPa u-direction wind in the north-west Pacific accounts for 63.2% of the November-April variability. This component correlates well with the PDO, Southern Oscillation Index and variability in the Siberian High (SH) (see table 4.2), but both the SOI and SH exhibit interdecadal modes associated with

mechanisms of interdecadal variability such as those represented by the PDO (eg. Elliot and Angell, 1988; Power et al., 1999). The differences in magnitude of correlations between the relevant climate indices shown in table 4.2 supports the notion that first EOF variability in 200hPa winds relating to the SH and ENSO/SOI are a PDO 'echo'.

The spatial variability in the first u-direction 200hPa wind EOF implies that a centre of variability lies to the north-east of the region (see figure 4.4). This is less in keeping with patterns of variability associated with the PDO (Mantua et al., 1997) than the SST signature of the Interdecadal Pacific Oscillation (IPO) described by Power et al. (1999), but is still similar enough that the PDO will be used here as an index for analysis. The pattern also closely resembles that of areas of significant correlation between the PDO and 200hPa zonal wind (figure 4.5).

Table 4.2 – z-values for correlation between EOF modes of NDJFMA 200hPa zonal wind velocity and various climate indices in the north-west Pacific region (30°N to 60°N, 130°E to 170°E). Shading indicates values significant at the 95% level.

EOF (% variability)	PDO	SOI	SH	AO	AO (DJF)
1 (63.2%)	6.6	4.2	2.3	-1.63	-1.67
2 (21.1%)	0.59	0.14	-0.5	1.04	-2.05

The second EOF of 200hPa zonal wind variability (figure 4.6) correlates negatively at the 95% level with the December-February Arctic Oscillation (AO). There is no significant correlation with the November-April AO, probably due to the wintertime effect of the AO being at its peak in mid-winter. The spatial pattern of variability in the second EOF shows a quasi-AO pattern, with a skewed north-south pattern of variability. It is possible this pattern could be skewed due to the influence of the Kurishio/Oyashio current and its effect on SSTs and SLP in the region (for examples, see Miller and Schneider, 2000).

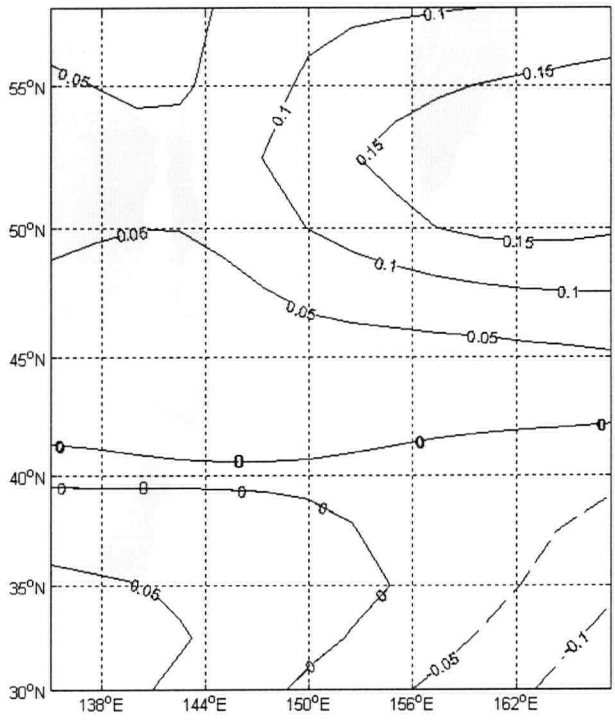

Figure 4.4 – First EOF of variability in NDJFMA 200hPa zonal wind in the north-west Pacific region (30°N to 60°N, 130°E to 170°E), 1961/62-1997/98.

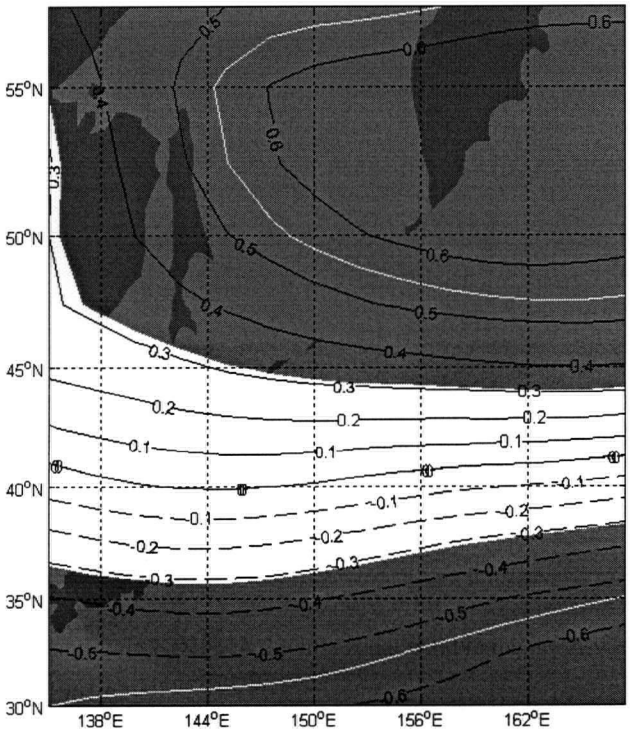

Figure 4.5 – Correlation between NDJFMA 200hPa zonal wind and the PDO in the north-west Pacific region (30°N to 60°N, 130°E to 170°E), 1961/62-1997/98. Shaded areas are significant at the 95% level.

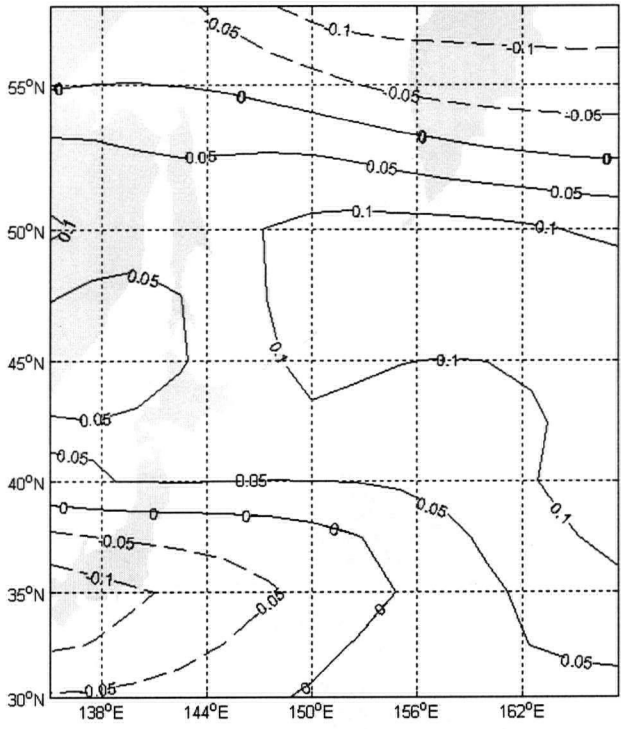

Figure 4.6 – Second EOF of variability in NDJFMA 200hPa zonal wind in the north-west Pacific region (30°N to 60°N, 130°E to 170°E), 1961/62-1997/98.

Relationships found previously are likely due purely to both cyclone development and vertical wind shear sharing a common relationship with meridional temperature gradient. Thermal wind theorem provides that baroclinic instability is dependant upon vertical wind shear (refer to Holton, 1992) and eddies in baroclinic flow result from instability in that flow.

Strong correlations between November-April cyclone frequency and the PDO exist in the northern and southern portions of the region. While this resembles, to an extent, an Arctic Oscillation pattern, an EOF analysis of cyclone frequency shows the first EOF most likely represents a PDO influence (table 4.3). While the AO also correlates significantly with the first EOF, the nature of the correlations suggests that this is due to a PDO signal in the AO. Again, the peak winter December-January signal correlates better than the full seasonal mean AO.

Table 4.3 - z-values for correlation between EOFs of NDJFMA cyclone frequency and various climate indices in the north-west Pacific region (30°N to 60°N, 130°E to 170°E). Shading indicates values significant at the 95% level.

PC (% variance)	PDO	SOI	SH	AO (NDJFMA)	AO (DJF)
1 (57.3%)	-5.08	0.15	-2.8	2.36	2.52
2 (18%)	0.6	-2.3	-0.54	1.04	1.36
3 (12%)	-1.4	2.99	0.63	-1.34	1.89

There is also an element of the first EOF analysis that correlates to variability in the Siberian High. The following chapter outlines a significant difference in mean SLP under the mean, mid-winter position of the Siberian High before and after 1976/77. If the PDO is a physical representation of the climate regime shift, then it follows that a substantial PDO signal will exist in Siberian High variability, explaining the correlation here between cyclones and the Siberian High as coincidental. However, a spatial analysis of the correlation between north-west Pacific cyclones and the Siberian High (figure 4.8) shows that the correlations exist slightly further poleward than the correlations with the PDO (figure 4.7) found in the southern-most part of the north-west Pacific region.

Chang (2001) described how variability in the Siberian High affects eddy growth 'downstream' of the feature in the north-west Pacific region. This is supported by the correlations shown in figure 4.8, and makes sense given previous work detailing relationships between eddy development and variability in mid-latitudinal mean flow (eg. Lau, 1988). Additional effects on Siberian High variability, such as those from the NAO (Rogers, 1997), Eastern European teleconnection patterns (Gong and Ho, 2002) and variability in East Asian monsoon circulation could explain the slight difference between Siberian High and PDO effects on the region's cyclone frequency. Although, it is possible that any region showing a relationship between the Siberian High and cyclone frequency will also have a significant component of variability related to the PDO and any slight shifts in the spatial spread of correlation are due to other, lesser, non-Pacific influences on the Siberian High.

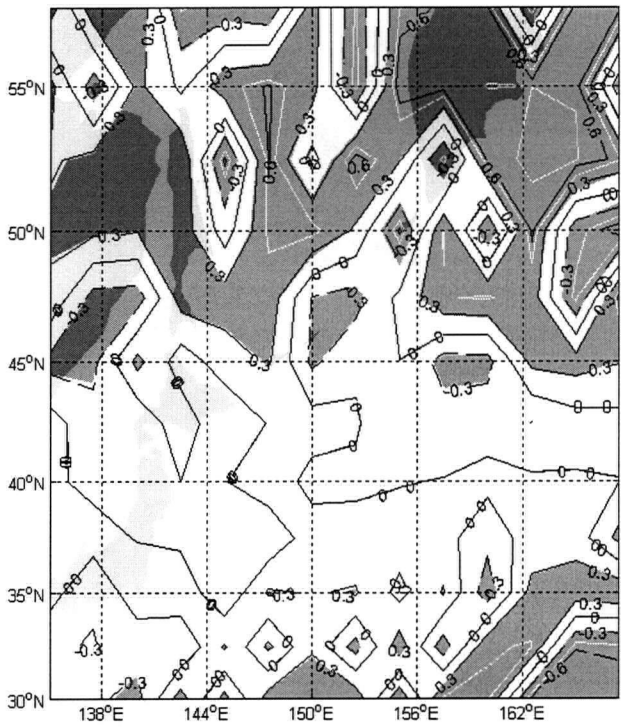

Figure 4.7 – Correlation between NDJFMA cyclone frequency in the north-west Pacific region (30°N to 60°N, 130°E to 170°E) and the PDO, 1961/62-1997/98. Shaded areas are 95% significant.

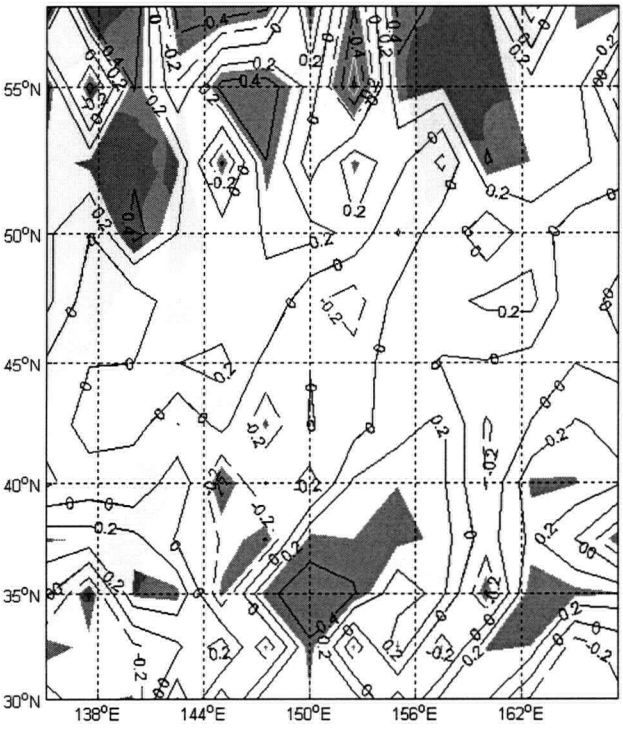

Figure 4.8 - Correlation between NDJFMA cyclone frequency in the north-west Pacific region (30°N to 60°N, 130°E to 170°E) and variability in the mean January position of the Siberian High, 1961/62-1997/98. Shaded areas are 95% significant.

It is also possible that changes in the mean flow downstream of the Siberian High are primarily responsible for variability in storms forming in the North Pacific and that the state of atmospheric and oceanic variables in that region serve to enhance or dampen the variability. In this case, eddy development downstream of the Siberian High would encounter either favourable or unfavourable conditions for formation and propagation depending on the state of Pacific regional climate, such as those represented by the PDO or variations in meridional conditions as represented by the AO. Seeing as such states of the region have been observed to affect climatic features in the mean flow such as the Aleutian Low (eg. Mantua et al., 1997), it would also be reasonable to postulate the existence of an effect on storm track location (eg. in Cayan et al., 1995; as reviewed by Miller and Schneider, 2000).

A spatial analysis of cyclone frequency in the north-west Pacific reveals that differences in location of the storm track between PDO phases and Siberian High variability are not significant (figures 4.9a-4.9d), meaning that the primary PDO/Siberian High discrepancy here is in actual cyclone numbers, rather than mere shifts in the north-west Pacific storm track. So, while effects on cyclone variability in the region occur in different places depending on the state of various North Pacific and Eurasian climate phenomena, there is no major change in the location of the storm track.

Table 4.3 also shows that the second and third EOFs (accounting for 18% and 12% or the variance, respectively) correlate significantly with the SOI. What is interesting to note here, is that while the second storm frequency EOF correlates negatively with the SOI, the third EOF shows a positive correlation. Since the positive phase of the SOI corresponds to La Niña conditions in the equatorial Pacific, a negative correlation suggests that there is a positive relationship between variability in north-west Pacific cyclone frequency represented by the second EOF and El Niño events.

ENSO teleconnections produce a positive relationship between ENSO events and conditions related to SST and SLP in the north-west Pacific region (Halpert and Ropelewski, 1992; among others). Given a relationship between such variables and atmospheric states affecting eddy development (eg. Lau and Nath, 1991), this could explain the positive relationship between phases of the ENSO and cyclone frequency here.

In the case of the third EOF from the north-west Pacific storm analysis, which shows an opposite relationship to the second EOF, increases in cyclone frequency in the region are associated with a La Niña phase of ENSO. This does not fit well with traditionally accepted effects on north-west Pacific conditions related to ENSO teleconnections. La Niña events are characterised by

warmer than normal SSTs in the western equatorial Pacific Ocean. This study found no significant relationship between vertical wind shear in either the western equatorial Pacific region, nor in the immediate north-west Pacific region. Therefore, remaining hypotheses concerning mechanisms to cyclone variability relating to western equatorial SST anomalies include changes in the meridional, hemispheric temperature gradient or direct SST influences in the north-west Pacific.

The nature of the meridional temperature gradient and poleward energy transport is associated with eddy growth in the mean, wave-like baroclinic flow (eg. Lau and Nath, 1991). If western equatorial Pacific SSTs increase during a La Niña event, then it is feasible that around western Pacific longitudes the meridional temperature gradient changes also. In this case, eddy growth could be affected to compensate. In this scenario, cool SSTs in the eastern Pacific that are related to La Niña events might also result in the meridional temperature gradient changing there to a degree, but in a way which hinders or shifts eddy propagation. A stumbling block with this hypothesis is that La Niña teleconnection patterns tend to result in positive SST anomalies which extend sufficiently poleward in the western North Pacific (after Halpert and Ropelewski, 1992; with additional observations using NOAA National Weather Service data and analyses, http://www.nws.noaa.gov) to disallow changes in the temperature gradient significant enough to cause enhanced eddy formation.

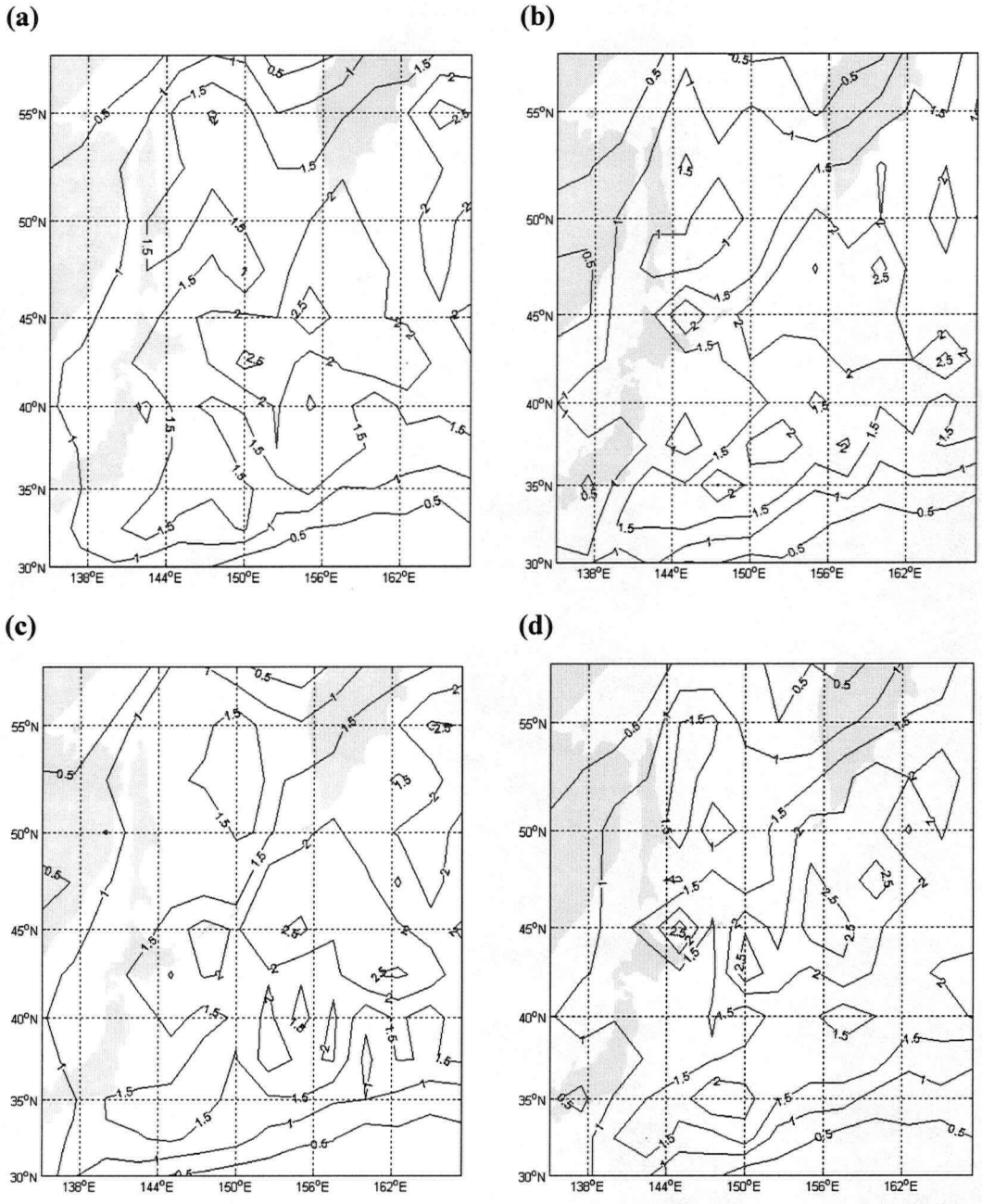

Figure 4.9 – North-west Pacific (30°N to 60°N, 130°E to 170°E) mean NDJFMA cyclone frequency from 1961/62 to 1997/98 during: (a) negative PDO phase seasons; (b) positive PDO phase seasons; (c) negative SHI anomaly seasons; and (d) positive SHI anomaly seasons.

In the absence of significant meridional temperature gradient effects, another explanation could lie in the direct influence of the state of atmospheric properties associated with SSTs in the north-west Pacific region. Part of the Siberian High record shows a good relationship to the phase of ENSO (see Chapter 5). It is also likely that the relationship here between ENSO and the third EOF occurs via ENSO-forced affects on SLP in the region of the Siberian High. By

this mechanism, the variability in the Siberian High would translate to changes in the nature of the mean flow, in which eddies form, downstream of the Siberian High. An effect similar to this is the case of mid-winter 'peak' storm occurrence as discussed by Nakamura et al. (2002).

As to the nature of the effect on cyclones occurring in the north-west Pacific and whole North Pacific region by ENSO, it appears that both phases affect cyclone frequency in the same way. Hence, any discernable variability in cyclone frequency would be dependent upon the severity of individual El Niño or La Niña events.

It is also possible that the effect that an ENSO event has on anomalies in cyclone behaviour in the region depends on the state of other influential variables. This would be similar, in principle, to the modulation of the impact ENSO has on various regional climates depending on the background state of Pacific climate (eg. Gershunov and Barnett, 1998; McCabe and Dettinger, 1999; Power et al., 1999; Grant and Walsh, 2001). The identification of such a modulation in this case would require a more specific study.

5. Evidence for climate regime shift in Northern Hemisphere mean flow and the Siberian High.

The Siberian High is a semi-permanent anticyclone usually positioned over the north-western region of Asia (see figure 5.1). It is the most prominent feature of atmospheric circulation over the Eurasian continent and is a primary influence on climate in that region. The state of the Siberian High also has a major effect on Northern Hemisphere circulation and climate. For example, Cohen et al. (2001) showed that anomalies in the dominant mode of wintertime SLP and surface temperature in the Northern Hemisphere partly originate in the Siberian High region.

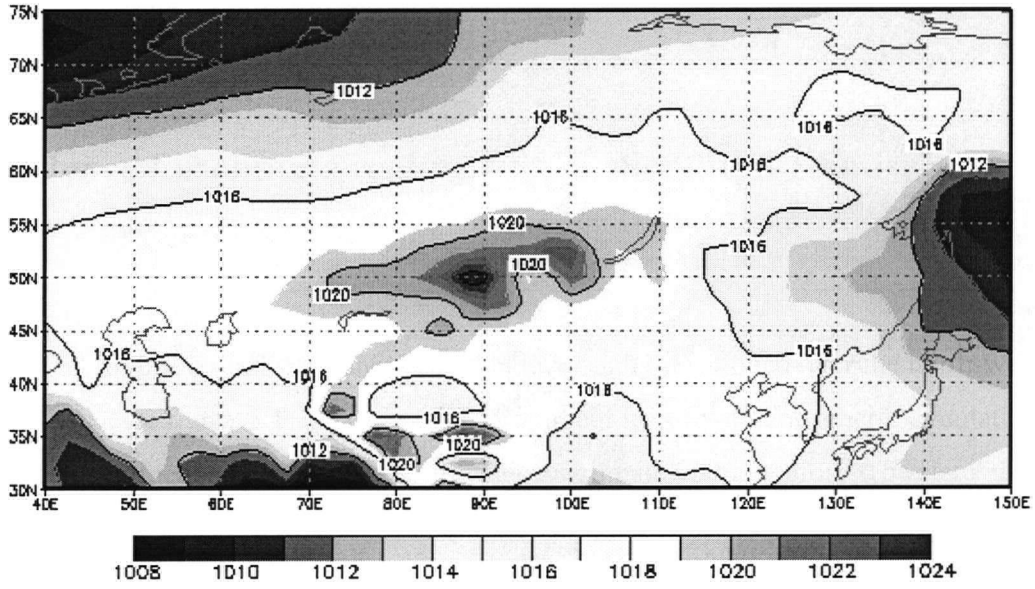

Figure 5.1 – Mean January Sea Level Pressure (SLP), 1948/49 - 2002/2003; indicating the usual mid-winter location of the Siberian High over Eurasia. Plot created online using NCEP Reanalysis data provided by the NOAA-CIRES Climate Diagnostics Centre, Boulder, Colorado, USA (http://www.cdc.noaa.gov).

Baroclinic instability theory allows for cyclonic and anticyclonic synoptic systems to be viewed as eddies in the mean flow (eg. Simmons and Hoskins, 1978). Eddy activity, or synoptic weather systems, form most readily 'downstream' of major permanent and semi-permanent wave features of the mean flow, such as the Siberian High (eg. Blackmon et al. 1977; Blackmon et al. 1984; Chang, 2001). It then follows that variations in the mean flow will also produce variability in storm tracks. It can also be expected that prominent, quasi-permanent features in

the mean flow will also exhibit the variability. If this is the case, then variability in the nature of North Pacific storm track could be preceded, or accompanied by, variability observed in the Siberian High. In this way, additional influences to non-Pacific forced aspects of the Siberian High could help explain the lack of a straightforward relationship between cyclone frequency in this region, the ENSO cycle and mechanisms of interdecadal Pacific variability (refer to Chapter 3).

5.1. The effects of Pacific region climate phenomenon on the Siberian High.

Figure 5.2 shows the Siberian High Index (SHI), constructed using mean sea level pressure values taken from NCEP/NCAR Re-analysis data (see Chapter 2 for details regarding the Re-analysis data used).

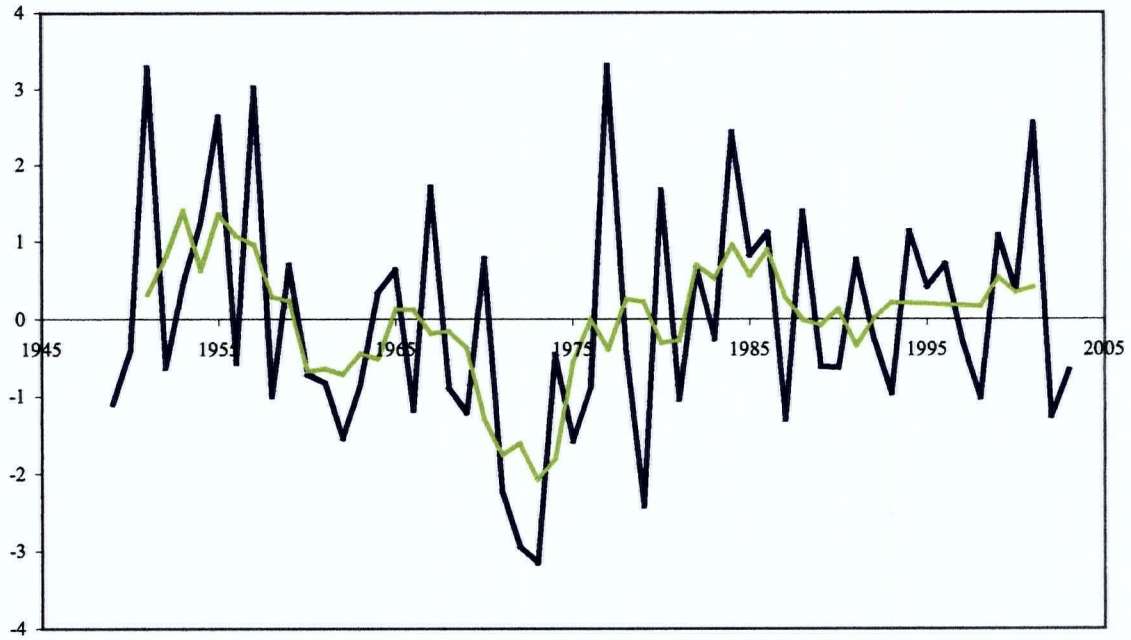

Figure 5.2 – Siberian High Index (SHI), 1948/49 – 2002/2003 with 5-year running mean (green line) and linear trend removed. The index was constructed from mean NDJFMA derived SLP values from NCEP/NCAR Reanalysis data at 50°N, 90°E. This point was located as the mean January position of the Siberian High. Data obtained from the NOAA-CIRES Climate Diagnostic Centre (CDC) Reanalysis website (http://www.cdc.noaa.gov).

A noticeable feature of the Siberian High Index is its apparent PDO-like interdecadal scale variability. From the 5 year moving average in figure 5.2, it can be seen that the 1950's were predominantly in a phase of positive anomaly. Following this was a mostly negative phase which persisted until around 1976/77. At this time the index returns to a predominantly positive phase until the end of the record. In a similar manner to the PDO (figure 2.2), this positive phase was broken only by a minor negative interlude in the late 1980's/early 1990's.

The 1976/77 season also coincides with the largest positive anomaly in the mean seasonal pressure record. The other largest positive anomaly is during the 1951/52 season. This does not correspond to a change in the general state of the PDO, but does coincide with the beginning of an extended negative NAO (see figure 3.16). This point in time also coincides with the most negative value of the Interdecadal Pacific Oscillation (IPO) index, constructed by Power et al. (1999) and based on low-pass filtered northern and equatorial Pacific SSTs and other variables. This suggests a possible change in Northern Hemisphere climate around this time that is not completely explained by the PDO and north Pacific climate conditions alone.

Since the PDO signal observed in North Pacific climate phenomena is closely linked to the mean atmospheric flow (observed in features such as the Aleutian Low; Mantua et al., 1997), it is possible that the mean flow itself might show the same signal and that such a signal would also be observable as a modulation of the Siberian High. One reason for this, could be related to the effect of PDO-forced mechanisms on the Siberian High and other such features of the mean flow (eg. Hurrell and van Loon, 1997).

While there is a significant difference between the mean SLP in the region of the Siberian High during different phases of the PDO at the 90% level, the differences in SLP are not significant at the 95% level. Nor are the correlations between SHI and PDO variability significant. While similarities in the general state of the two indices can be observed throughout the 1970's, 1980's and 1990's, change prior to that in the general state of the Siberian High is not observed in the PDO. That is, major changes in the location and/or strength of the Siberian High do not always correspond to changes in the PDO.

The occurrence of seasons with a significant anomaly in the SHI appears to be better related to the phase of the PDO in the middle part of the record than the early or latter periods. The extended negative anomaly periods of the SHI occur during extreme negative phases of the PDO, although available degrees of freedom here are not sufficient to conduct a viable statistical analysis to substantiate or disprove these observations. It can also be noted, however, that many of the negative Siberian High anomaly seasons are also negative PDO phase seasons, and vice

versa. In addition to this, and despite only being significant at the 90% level, the analysis of the difference between mean SLP of the Siberian High during different PDO phases shows that the mean seasonal intensity of the Siberian High is higher in positive phases of the PDO. The analysis also shows that during the part of the record when the SHI shows similarities to the PDO, the significance of this difference is slightly greater than the difference associated with different phases of climate regime. On one hand, the fact that the values of significant difference are only slightly different could mean either that the primary influence in Siberian High variability is the state of North Pacific climate, or that Northern Hemisphere zonal mean flow varies as a whole. Then again, the fact that a difference exists in this and other analyses presented here might suggest additional, non-Pacific influences on the Siberian High and could explain some of the 'noise' in the climate regime/PDO/North Pacific cyclone relationships shown in previous chapters.

Further evidence for a decadal scale variability in the intensity of the Siberian High that is not related to the PDO comes from an EOF analysis of mean SLP data in the Siberian High region. Figure 5.3 shows the first EOF of mean November-April SLP in an area encompassing the usual mid-winter location of the Siberian High (40°N to 60°N, 60°E to 110°E).

In a similar manner to the SHI record, the 5 year running mean analysis of the first EOF (62% of the variance) shows periods of a multi-annual to decadal phase which resemble the PDO in the middle part of the record, but not the early or latter parts. Despite the limited north-south scope of the area sampled, the Arctic Oscillation (AO) is still the primary mode of variability of SLP, with the first EOF correlating negatively with the AO at the 95% level.

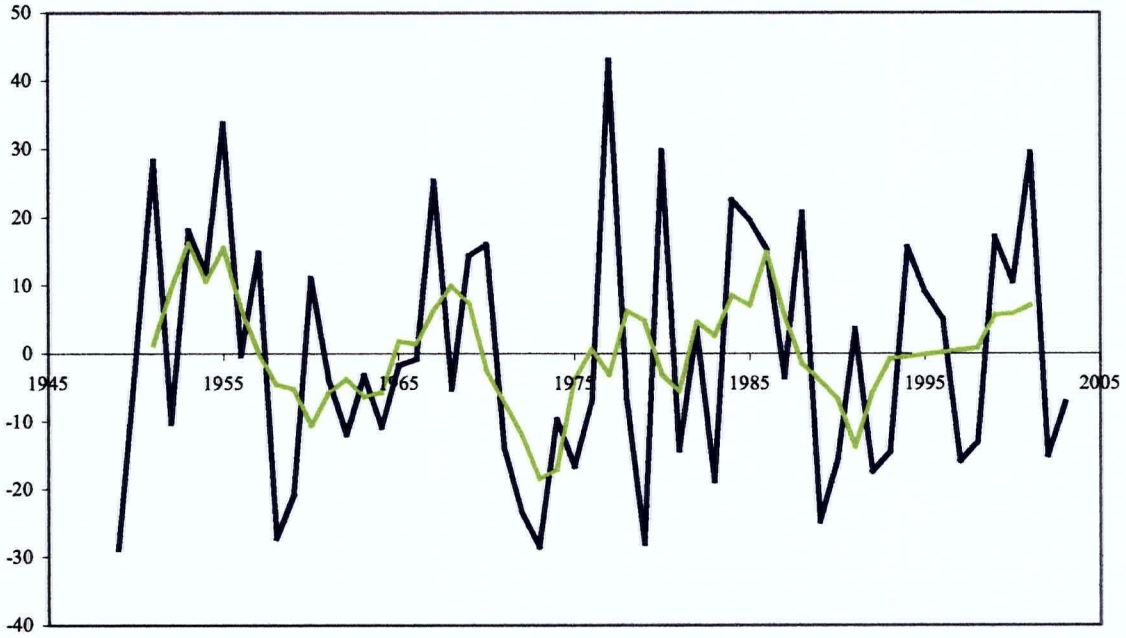

Figure 5.3 – First EOF (approximately 62% of the variance) of mean NDJFMA SLP (linear trend removed) in the immediate region of the usual winter time position of the Siberian High (40°N to 60°N, 60°E to 110°E), 1961/62-1997/98. The green line represents a 5 year moving average. The Position of the Siberian High during the Northern Hemisphere winter was located with data obtained from the NOAA-CIRES CDC Reanalysis on their website (http://www.cdc.noaa.gov).

Another interesting feature worth noting in the first EOF, and perhaps warranting future investigation, is the rare, prolonged periods of one particular phase. Examples are the two periods of consecutive negative SHI anomaly in the early 1970's and 1990's. Both are periods noted for distinct changes in the nature of the North Pacific storm track and/or climate and end around times usually associated with shifts in climate regime (see Chang and Fu, 2002; and Hare and Mantua, 2000 for summaries of changes in cyclone frequency and climate regime shift respectively).

The second EOF (accounting for 21.3% of the variance – see figure 5.4) better illustrates a link between the Siberian High and Pacific regional climate, significantly correlating with the SOI (t-statistic = -2.7, above 95% confidence level) over the time period investigated. However, further analysis of separate periods of the time series indicates that this significant correlation between the SOI and SHI does not hold for the entire record. As shown in Table 5.1, the middle part of the record shows a strong, negative correlation. It is this influence which 'forces' the overall

correlation obtained in the initial analysis. The early and latter parts of the Siberian High record show no relationship to the SOI.

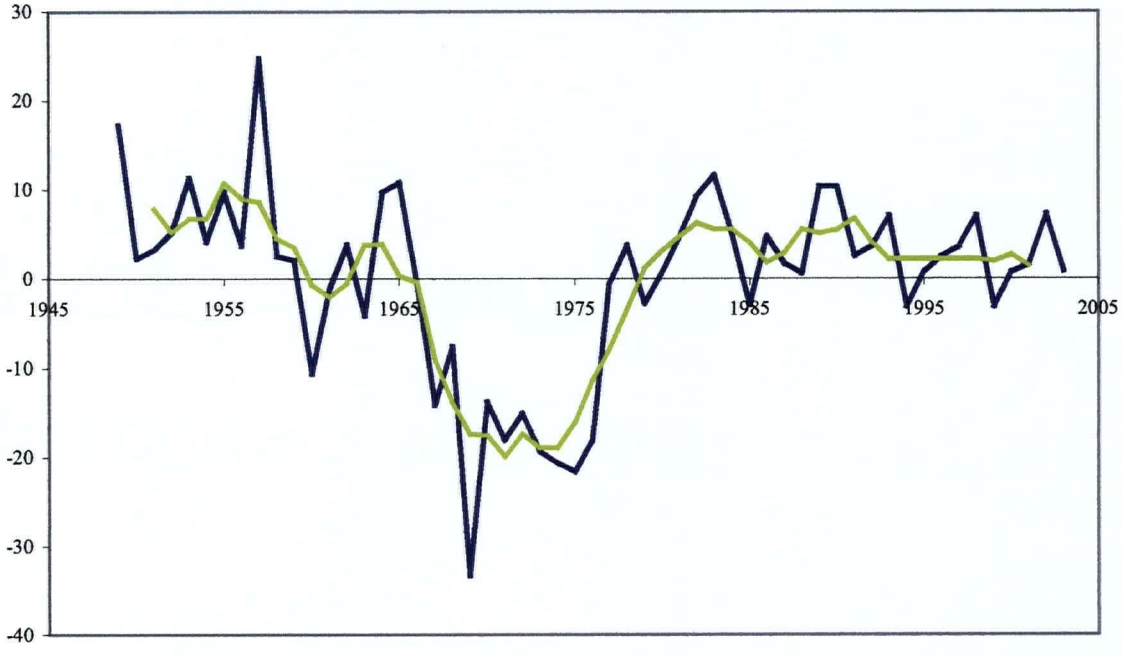

Figure 5.4 - Second EOF (approximately 21.3% of the variance) of mean NDJFMA SLP (linear trend removed) in the immediate region of the usual winter time position of the Siberian High (40°N to 60°N, 60°E to 110°E), 1961/62-1997/98. The green line represents a 5 year moving average.

Table 5.1 – Correlation between the Siberian High Index (SHI) and Southern Oscillation Index (SOI) for different periods of the 1948/49 – 2002/2003 time period examined. Correlations significant at the 95% level are shaded.

Period	Correlation
1948/49 - 1966/67	-0.17
1966/67 - 1985/86	-0.5
1985/86 - 2002/03	-0.15

It is possible that the effect of ENSO teleconnections on the Siberian High region are affected to varying degrees by different climate regimes, or parts of different climate regimes, in a similar manner to the varying effect of ENSO on north-west Pacific cyclone frequency discussed in the

previous chapter. There is also the possibility that the correlation between the SHI and Pacific climate variability is associated with the existence of the shift in climate regime. In this scenario, a relationship would not usually exist. However, the period encompassing a hemispheric climate regime shift would involve a change of a magnitude sufficient to affect a range of climate parameters in a similar manner.

The second EOF also appears to better represent the multi-annual to decadal time scale signal of the Siberian High, with the 5 year running mean analysis outlining distinct periods of positive and negative anomaly. A major feature represented in the second EOF time series, is a reduction in mean SLP (or weakening of the Siberian High) caused by this mode of variability during the late 1960's into the 1970's. This coincides with a strengthening of the Aleutian Low which occurred over the same time period (Nitta and Yamada, 1989; Trenberth, 1990). Given the correlation between the SOI and second EOF during this time, it is likely that both the Siberian High and Aleutian Low were affected to a similar degree. An intriguing possibility here is that the coincidence of the weakening of the Siberian High and strengthening of the Aleutian Low, with no direct correlation existing between North Pacific decadal-scale climate indices and the second EOF, could suggest that the effects of the 1970's event were not limited to the Pacific region. Rather, the effects were linked to an event of a global or hemispheric nature that ended around the 1976/77 date. This latter theory is supported by the finding of significant periods of time in the record where there is no relationship between the SOI and second EOF.

One possibility is that this event was directly linked to properties of the mean, Northern Hemispheric atmospheric flow and that multi-decadal climate variability in the Pacific region, represented in part by the PDO, was merely the response to this hemispheric event in the North Pacific region.

Such an effect could be achieved via direct forcing from atmospheric conditions on the major North Pacific mean flow features. Another means could be an indirect effect via 'downstream' transport of the variability. These would include changes to the nature of the mean flow affecting, for example, cyclone occurrence and/or storm track variations.

Another possibility lies in changes in the meridional temperature gradient. Previous links between the AO and first EOF could support this hypothesis.

Another interesting feature of the SHI, is the apparent discontinuity in the record centred around the 1976/77 season (see figure 5.5).

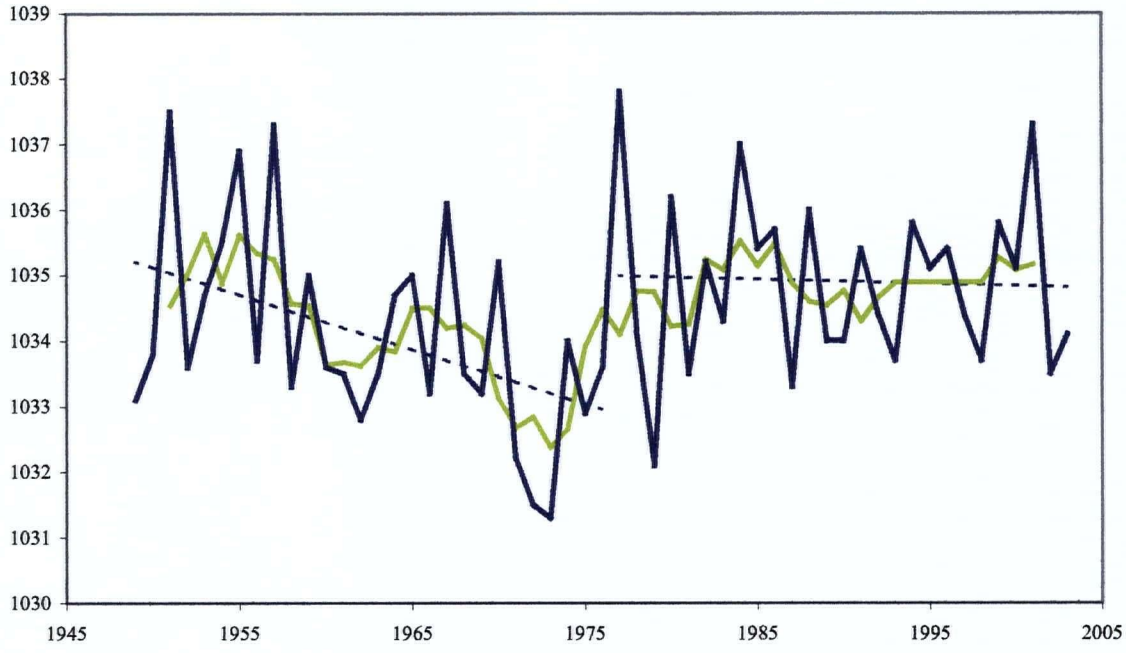

Figure 5.5 – Siberian High Index with split regression analyses either side of 1976/77, 1948/49-2002/2003.

Before 1976/77, mean NDJFMA SLP in the area underneath the Siberian High shows a negative trend. After 1976/77, there is a significant change in trend with the remainder of the record showing a near-zero (slightly negative) trend. There is also a change in the mean SLP associated with the wintertime Siberian High, although this change is only significant at the 90% level. While this change is similar to the changes observed in many of the cyclone analyses (see chapter 3), the change in trend also appears to be closely linked to the extended 1960's/1970's period of negative anomaly preceding the climate regime shift. Nevertheless, the similarities between the change in trend between this and the cyclone analyses suggests a link between cyclone and Siberian High variability, or at least links to a common mode of climate variability. The existence of such a link supports the previous postulation that cyclone frequency in the region is significantly different between regime phases and it seems likely that this difference is associated in some way with the mean atmospheric flow.

The change in trend is of identical nature (but of varying magnitude) to most cyclone trend analyses conducted using ARCSS data and is also similar, but of inverse sign, to trend changes observed in North American cyclone frequency as well as North Pacific and Northern Hemisphere intense cyclone frequency from GISS analyses.

It should also be noted that the degree of significance of change in mean SLP more closely resembles the degree of change found in the GISS analysis, suggesting that the GISS data are a more accurate representation of cyclone frequency and that the findings of moderate relationships between cyclone frequency and the Siberian High here and in previous studies (eg. Nakamura et al., 2002) can be honoured. However, as discussed previously, dissimilarities between the GISS data and mean SLP-based SHI and the ARCSS analysis should be noted with caution seeing as both the GISS and mean SLP datasets are derived from Re-analysis products. The prominent existence of the 1976/77 regime shift in Siberian High intensity in the absence of a significant relationship to the PDO further suggests that the regime shift was not an event limited to the North Pacific region. In this case, the regime shift can be assumed to also affect the global mean flow in the Northern Hemisphere. This supplies more evidence that the 1976/77 regime shift was a hemispheric phenomenon and that the PDO merely represents the signal of the shift in the Pacific region.

The second 1989 regime shift is not as prominent here, with no significant change in trend or mean SLP around this date. Combined with the positive period of the PDO following this part of the record, it is likely that this regime shift is merely related to separate interdecadal variability in the North Pacific region and not a hemispheric event, as the 1976/77 event appears to be. It is also possible that the second 1989 event is related to the 'extended' El Niño in the early 1990's (see Latif et al., 1997 for further analysis of this event) or the existence of separate modes of interdecadal variability associated with regime shift in the North Pacific (Minobe, 1999).

6. Conclusions

Despite a fair degree of variation between sets of data used in this analysis, the storm climatology and location of major storm tracks in the North Pacific region is in fairly good agreement with observations and findings presented in previous studies. In regions other than the North Pacific, however, it appears that cyclones are not as accurately represented in one of the datasets used. This is specifically noted as being the case in the North Atlantic region. Points in time where the different datasets are in agreement occur during periods of major climate shift. That is, major modes of climate variability are more consistent across datasets than minor changes.

Significant trends were found in cyclone frequency and intense cyclone frequency in nearly all the regions analysed. However, these trends varied in sign depending on region and type of cyclone. For the entire Northern Hemisphere, a significant negative trend was observed from 1961/62 to 1997/98. This negative trend was echoed in the North American/North Atlantic and Eurasian regions. Conversely, a positive trend was observed over the same time period in the Northern Hemispheric Pacific region.

In nearly all cases, and despite the general occurrence of negative trends in total cyclone frequency, a significant positive trend was observed in intense cyclone frequency. The only exception to this was in the North Atlantic region from the analysis of GISS data, where a significant negative trend was found. In all regions of the Northern Hemisphere except for over the North American continent, the trend in intense cyclones is significantly more positive than that found in full cyclone records. This implies that the percentage of cyclones that reach an 'intense' degree of severity has increased over the time period investigated. The positive trend predominantly occurring in intense cyclones might suggest that the changes in poleward energy transfer associated with a global warming scenario might affect the intensity of Northern Hemisphere cyclones to a greater degree than the total number of cyclones.

Intense cyclone trends in the North American region were more significantly negative than trends in overall cyclone frequency.

Evidence for interseasonal and interdecadal variability in cyclone frequency in various regions of the Northern Hemisphere was also found. Apart from variability observed in the time series analyses, the most obvious example of decadal variations observed here were changes in cyclone frequency associated with different phases of various modes of climate variability. Changes on these time scales were also more prominent in the intense cyclone record, rather than in all cyclones. Fewer such relationships were found in the complete cyclone record, save for a couple of instances. Using GISS data, a significant decrease in storms in the entire Northern Hemisphere was observed after 1976/77, although it does not appear that this change is most apparent in any one, particular region. The closest that a change of this nature occurs primarily in any of the regional analyses is in the combined North America/North Atlantic GISS-based analysis. However, in this case the change is not significant at the 95% level. A negative relationship is also found in the full ARCSS data record between the PDO and North American cyclones.

From an analysis of the degree to which anomalies in the Northern Hemisphere are influenced by different regions at various times during the record, it is apparent that not all major changes in Northern Hemisphere cyclone climatology are similar. For example, while some readily observable events to anomalous cyclone behaviour in specific region, other major events remain a Hemispheric phenomenon with all regions being affected. Such an event is the 1976/77 climate regime shift. While there was no significant change in overall cyclone frequency around this event for the most part, the season during which this event occurred does coincide with the lowest cyclone frequency and largest magnitude anomaly in the full Northern Hemisphere record. It was shown that the 1976/77 event affected cyclone frequency in all regions of the Northern Hemisphere to a similar degree. That is, the 1976/77 event was of a Hemispheric nature.

Further evidence for the existence of the 1976/77 regime shift in cyclone frequency is found from the 'split' regression analysis of cyclone records. In most cases, regression analyses of cyclone frequency before and after the 1976/77 shift yield a significant change in trend. In some cases trends are heavily influenced by large, anomalous events either later or earlier in the record. But in other cases the change in trend stands statistically on its own.

The change in trend around the 1976/77 regime shift was also found in non-cyclone data. The possibility of change in the mean, zonal flow of the Northern Hemisphere was identified from analysis of a major feature in the mean flow, the Siberian High. In the case of the Siberian High there is a very distinct change from a negative trend pre-1976/77 to a near-zero trend with

significantly higher mean SLP after 1976/77. It is likely this change in trend and mean SLP represents a sharp change in general nature of the Siberian High, and possibly the mean atmospheric flow in the Northern Hemisphere, that coincides with the 1976/77 climate regime shift.

Cyclones occurring in the Gobi Desert and north-west portion of the North Pacific were also investigated. Both these regions are located where cyclones which propagate into the North Pacific region are formed.

While there was an extraordinary amount of variability between datasets in the case of the Gobi desert, good relationships were still found between Gobi region cyclones and various indices of regime shift and interdecadal climate variability. Analysis of GISS data showed a large positive trend in the cyclone record and significantly less cyclone occurring after 1976/77. This analysis also yielded a negative relationship between mean cyclone frequency and phases of the PDO and 77/89 regime shifts. On the other hand, Gobi region analyses conducted using ARCSS data showed a large positive trend over the duration of the record and a significantly positive increase in mean cyclone frequency after 1976/77. Positive relationships were also found here with the other climate indices, but these were not significant at the 95% level.

Although a statistically significant relationship between Gobi Desert cyclones and the Siberian High was not found, similarities were observed with respect to general states of phase of both variables.

Cyclones forming in the north-west Pacific were identified as having a major influence on cyclone variability in the whole North Pacific region. This was typified by a large, negative trend in North Pacific cyclogenesis being primarily due to the trend observed in cyclogenesis occurring in the north-western Pacific region.

A significant difference between the mean number of November-April cyclogenesis events during phases of the 77/89 regime index was found. The nature of this relationship was such that positive phases of the 77/89 regime shift coincided with a lower rate of cyclogenesis in the North Pacific. Similar relationships to this were also found in the north-west Pacific for the other climate regime indices, but these were not significant at the 95% level. The existence of a relationship here between Pacific cyclogenesis but not cyclone occurrence elsewhere in the Northern Hemisphere suggests that the 1989 regime shift event is only prevalent in variables associated with Pacific regional climate and was not a hemispheric-wide event. This postulation

is further supported by the lack of evidence for a climate regime shift around 1989 in the SHI, considered here as a proxy index for global circulation properties in the Northern Hemisphere. Minobe (1999) noted that only part of the inter- to multi-decadal variability observed in North Pacific SLP and SSTs, the 15-20 year mode, explains the existence of the 1989 shift. There is a possibility that this mode is the North Pacific link to the existence of various states of climate in that region while the longer mode is more indicative of the global/hemispheric influence. However, much more work is needed for these conjectures to be assessed any further.

Cyclone frequency in the north-west Pacific and the possibility of a relationship to vertical wind shear in that region was also investigated.

Significant correlations between north-west Pacific cyclone frequency and vertical wind shear/upper level u-direction winds were not found except for within a few, small areas. An EOF analysis of north-west Pacific upper level winds indicated that the PDO is a primary influence on variability. Other indices such as the SOI and SHI also correlated with the first north-west 200hPa wind EOF, but it is assumed that this is due to the existence of the PDO signal in those indices. The second EOF indicated that the peak winter-time AO is also an important factor in upper level u-wind variability.

Some significant events in north-west Pacific cyclone frequency were observed to coincide with specific events in regional and global scale climate, some of which have been found previously to have a relationship with cyclone climatology in the North Pacific storm track. For instance, as with other Northern Hemisphere regions, the 1976/77 regime shift is observed as a large negative anomaly in cyclone frequency. Likewise, the extreme 1982/83 El Niño is also observed as an even larger negative anomaly.

A link is found here during certain periods of the record between ENSO and the Siberian High. Further relationships found between the Siberian High and north-west Pacific cyclone frequency suggest the possibility of additional ENSO-related effects on Pacific cyclones transmitted via the mean atmospheric flow 'downstream' of the Siberian High.

While it is difficult to separate the Siberian High signal from the PDO in the north-west cyclone frequency analysis, subtle differences were observed suggesting additional, non-Pacific effects on cyclone frequency via the Siberian High/mean flow. For example, a slight variation in spatial patterns of correlation was observed between PDO and SHI correlations with cyclone frequency. This difference was such that cyclone variability associated with the SHI occurred slightly poleward of the southern portion of variability associated with the PDO. An EOF analysis of

north-west Pacific cyclone variability showed that the SHI is indeed correlated with the first EOF, however once again it is not clear how much of this relationship can be attributed to the PDO signal in the SHI.

A spatial analysis of the patterns of correlation between cyclone frequency and the SHI/PDO revealed that differences in location of the storm track between PDO phases and variability in the Siberian High are not significant, meaning that the PDO/Siberian High-related variability probably lies in actual cyclone numbers, rather than shifts in the north-west Pacific storm track. This means that while effects on cyclone variability in the region occur in different places depending on the state of various North Pacific and Eurasian climate phenomena, there is no real change in the location of the storm track. This observation, combined with significant differences observed in cyclone frequency in the region between phases of climate regime and the PDO, leads to the postulation that the reason for this is a dampening, or enhancement, of the formation and/or propagation of cyclones in the mean flow through the Pacific region depending on phase of climate regime and/or the PDO.

A substantial degree of cyclone frequency variability in the north-west Pacific was also attributed to both phases of ENSO, however this relationship was not found to be straightforward. The second and third modes of variability both correlate significantly with different phases of ENSO. The second EOF shows a negative relationship with ENSO, while the third EOF shows a positive relationship. This means that the second mode of variability shows an increase in cyclone frequency during El Niño phases and the third mode shows an increase during La Niña phases.

The negative relationship shown by the second EOF is consistent with teleconnection patterns in SST and SLP in this region and associated atmospheric conditions affecting eddy development which are usually associated with El Niño events.

Parts of the Siberian High Index analysed show a good correlation with the SOI. It is postulated that eddy development in the mean flow downstream of the Siberian High is influenced by the state of ENSO via ENSO-forced pressure anomalies in the region immediately surrounding the Siberian High, and it is this variability which is represented by the third EOF of north-west Pacific cyclone frequency.

While no statistically significant relationship was found between the Siberian High Index and the modes of Pacific interdecadal variability investigated, there were observed interdecadal tendencies in the SHI. Some significant anomalous events in the SHI also coincide with significant periods in other climate indices. For instance, a peak in the SHI during 1951/52

coincides with the beginning of an extended downward trend and negative phase of the NAO as well as the most negative value recorded for the Interdecadal Pacific Oscillation index constructed by Power et al. (1999). An EOF analysis of SHI variability shows that the AO is also a major influence on the state of the Siberian High.

The second EOF also shows a link to Pacific region climate via a good, negative correlation with the SOI. However, the SOI/SHI relationship is only significant in the middle part of the record. The correlation is strongest from 1966/67 to 1985/86. Before and after this period there is no significant relationship between the two indices. This waxing and waning of the SHI/SOI relationship could be the result of variability in the general, background state of climate in the broader region affecting the degree to which the Siberian High is influenced by ENSO.

It is the second EOF of the SHI which also appears to better represent the multi-annual and decadal-scale modes of variability in the Siberian High. A weakening of the Siberian High caused by this mode of variability during the late 1960's and continuing into the 1970's was observed. This coincides with a strengthening of the Aleutian Low which occurred over the same time period.

One possibility is that this event was directly linked to properties of the mean, Northern Hemispheric atmospheric flow and that multi-decadal climate variability in the Pacific region, represented in part by the PDO, is a response to this global event in the North Pacific region.

The interdecadal and regime change-related variability observed here in North Pacific storms is best explained by changes to the mean flow in which the storms are imbedded.

In the absence of Pacific-centred variability which sufficiently describes the spatial and temporal nature of shifts in global climate and circulation regimes, further work is needed to better define, describe and analyse the climate regime shift phenomenon.

The findings presented in here also reaffirm the notion that variability in the mid-latitudinal mean flow, including characteristics within the flow such as extra-tropical cyclones, is very important with respect to influences on Northern Hemisphere climate and could perhaps even be associated with the triggering of large, interdecadal-scale climate changes.

7. References

Blackmon, M., J. Wallace, N.-C. Lau and S. Mullen, 1977. An observational study of the Northern Hemisphere wintertime circulation. *Journal of the Atmospheric Sciences.* **34** 1040–1053.

Blackmon, M., Y. Lee and J. Wallace. 1984. Horizontal structure of 500-mb height fluctuations with long, intermediate, and short time scales. *Journal of the Atmospheric Sciences.* **41** 961–979.

Braithwaite, R. 1994. Thoughts on monitoring the effects of climate change on the surface elevation of the Greenland Ice Sheet. *Global and Planetary Change.* **9** 251-261.

Bromwich, D., F. Robasky, R. Keen and J. Bolzan. 1993. Modelled variations of precipitation over the Greenland Ice Sheet.. *Journal of Climate.* **6** 1253-1268.

Bond, N. and D. Harrison. 2000. The Pacific Decadal Oscillation, air-sea interaction and central north Pacific winter atmospheric regimes. *Geophysical Research Letters.* **27** 731-734.

Cai, M. and M. Mak. 1990. Symbiotic relation between planetary and synoptic scale waves. *Journal of the Atmospheric Sciences.* **47** 2953-2968.

Carnell, R., C. Senior and J. Mitchell. 1996. An assessment of measures of storminess: Simulated changes in Northern Hemisphere winter due to increasing CO_2. *Climate Dynamics.* **12** 467-476.

Cayan, D. and D. Peterson. 1989. The influence of North Pacific atmospheric streamflow in the West. *Aspects of Climate Variability in the Pacific and the Western Americas, Geophysical Monograph.* American Geophysical Union, 375-397.

Cayan, D., A. Miller, T. Barnett, N. Graham, J. Ritchie and J. Oberhuber. 1995. Seasonal-interannual fluctuations in surface temperature over the Pacific: effects of monthly winds

and heat fluxes. *Natural Climate Variability on Decadal-to-Century Time Scales.* National Academy Press, Washington DC. 133-150.

Chang, E. and D. Yu. 1999. Characteristics of wave packets in the upper troposphere. *Journal of the Atmospheric Sciences.* **56** 1708-1728.

Chang, E. 2001. GCM and observational diagnoses of the seasonal and interannual variations of the Pacific storm track during the cold season. *Journal of the Atmospheric Sciences.* **58** 1784-1800.

Chang, E., S. Lee and K. Swanson. 2002. Storm Track Dynamics. *Journal of Climate.* **15** 2163-2183.

Chang, E. and Y. Fu. 2002. Interdecadal variations in Northern Hemisphere winter storm track intensity. *Journal of Climate.* **15** 642-658.

Changong, D., J. Noel and L. Maze. 1995. Determining cyclone frequencies using equal-area circles. *Monthly Weather Review.* **123** 2285-2294.

Chen, T-S, M-C. Yen and S. Schubert. 1996. Hydrologic processes associated with cyclone systems over the United States. *Bulletin of the American Meteorological Society.* **77** 1557-1567.

Chen, Q-S., D. Bromwich and L. Bai. 1997. Precipitation over Greenland retrieved by a dynamic method and its relation to cyclonic activity. *Journal of Climate.* **10** 839-870.

Cohen, J., K. Saito and D. Entekhabi. 2001. The role of the Siberian High in Northern Hemisphere climate variability. *Geophysical Research Letters.* **28** 299-302.

Dettinger, M. and D. Cayan. 1995. Large-scale atmospheric forcing of recent rends toward early snowmelt run-off in California. *Journal of Climate.* **8** 606-623.

Droegemeier, K., J. Smith, S. Businger, C. Doswell, J. Doyle, C. Duffy, E. Foufoula-Georgiou, T. Graziano, L. James, V. Krajewski, M. LeMone, D. Lettenmaier, C. Mass, R. Pielke, P. Ray, S. Rutledge, J. Schaake and E. Zipser. 2000. Hydrological aspects of weather prediction and flood warnings: report of the ninth prospectus development team of the U.S. Weather Research Program. *Bulletin of the American Meteorological Society.* **81** 2665-2680.

Ebbesmeyer, C., D. Cayan, D. McLain, F. Nichols, D. Peterson and K. Redmond. 1991. 1976 step in the Pacific climate: forty environmental changes between 1968-1975 and 1977-1984. *Proceedings of the Seventh Annual Climate (PACLIM) Workshop, April 1990.* J. Betancourt and V. Tharp (Eds.), California Department of Water Resources, Interagency Ecological Studies Program Technical Report 26.

Elliot, W. and J. Angell. 1988. Evidence for changes in Southern Oscillation relationships during the last 100 years. *Journal of Climate.* **1** 729-737.

Enfield, D. and A. Mestas-Nuñez. 1999. Multiscale variabilities in global sea surface temperatures and their relationships with tropospheric climate patterns. *Journal of Climate.* **12** 2719-2733.

Geng, Q. and M. Sugi. 2001. Variability of the North Atlantic cyclone activity in winter analyzed from NCEP-NCAR reanalysis data. *Journal of Climate.* **14** 3863-3873.

Genthon, C. and A. Braun. 1995. ECMWF analyses and predictions of the surface climate of Greenland and Antarctica. *Journal of Climate.* **8** 2324-2332.

Gershnov, A. and T. Barnett. 1998. Interdecadal modulation of ENSO teleconnections. *Bulletin of the American Meteorological Society.* **79** 2715-2725.

Gong, D. –Y. and C. –H. Ho. 2002. The Siberian High and climate change over middle to high latitude Asia. *Theoretical Applied Climatology.* **72** 1-9.

Graham, N. and H. Diaz. 2001. Evidence for intensification of North Pacific winter cyclones since 1948. *Bulletin of the American Meteorological Society.* **82** 1869-1893.

Grant, A. and K. Walsh. 2001. Interdecadal variation in north-east Australian tropical cyclone formation. *Atmospheric Science Letters.* (doi10.1006/asle.2001.0029), http://www.idealibrary.com/links/doi/10.1006/asle.2001.0029/pdf.

Gulev, S., O. Zolina and S. Grigoriev. 2001. Extratropical cyclone variability in the Northern Hemisphere winter from the NCEP/NCAR reanalysis data. *Climate Dynamics.* **17** 795-809.

Haan, C. 1977. *Statistical methods in hydrology.* Iowa State University Press, Ames.

Halpert, M. and C. Ropelewski. 1992. Surface temperature patterns associated with the Southern Oscillation. *Journal of Climate.* **5** 577-593.

Hanna, E., P. Valdes and J. McConnell. 2001. Patterns and variations of snow accumulation over Greenland, 1979-98, from ECMWF analyses, and their verification. *Journal of Climate.* **14** 3521-3535.

Hare, S. and N. Mantua. 2000. Emperical evidence for North Pacific regime shifts in 1977 and 1989. *Progress in Oceanography.* **47** 103-145.

Harnik, N. and E. Chang. 2003. Storm track variations as seen in radiosonde observations and Reanalysis data. *Journal of Climate.* **16** 480-495.

Hayden, B. 1981. Cyclone occurrence mapping: equal area or raw frequencies. *Monthly Weather Review.* **109** 168-172.

Held, I. 1993. Large-scale dynamics and global warming. *Bulletin of the American Meteorological Society.* **74** 228-241.

Hodge, S., D. Trabant, R. Krimmel, T. Heinrichs, R. March and E. Josberger. 1998. Climate variations and changes in mass of three glaciers in western North America. *Journal of Climate.* **11** 2161-2179.

Hoerling, M. and M. Ting. 1994. Organisation of extratropical transients during El Niño. *Journal of Climate.* 7 745-766.

Holton, J. 1992. *An Introduction to Dynamic Meteorology, 3rd ed.* Academic Press, San Diego. 511pp.

Hoskins, B. and D. Karoly. 1981. The steady linear response of a spherical atmosphere to thermal and orographic forcing. *Journal of Atmospheric Science.* **38** 1179-1196.

Hurrell, J. 1995. Decadal trends in the North Atlantic Oscillation: regional temperatures and precipitation. *Science.* **269** 676-679.

Hurrell, J. and H. van Loon. 1997. Decadal variations in climate associated with the North Atlantic Oscillation. *Climatic Change.* **36** 310-326.

Hvidberg, C. 2000. When Greenland ice melts. *Nature.* **404** 551-552.

Iwasaka, Y., H. Minoura and K. Nagaya. 1983. The transport and special scale of Asian dust-storm clouds: A case study of the dust-storm event of April 1979. *Tellus.* **35B** 189-196.

Jones, P. and A. Moberg. 2003. Hemispheric and large-scale surface air temperature variations: An extensive revision and an update to 2001. *Journal of Climate.* **16** 206-223.

Key, J. and A. Chan. 1999. Multidecadal global and regional trends in 1000mb and 500mb cyclone frequencies. *Geophysical Research Letters.* **26** 2053-2056.

Kistler, R., E. Kalnay, W. Collins, S. Saha, G. White, J. Woollen, M. Chelliah, W. Ebisuzaki, M. Kanamitsu, V. Kousky, H. van den Dool, R. Jenne and M. Fiorino. 2001. The NCEP/NCAR 50-year reanalysis. *Bulletin of the American Meteorological Society.* **82** 247-268.

Lambert, S. 1996. Intense extratropical Northern Hemisphere winter cyclone events: 1899-1991. *Journal of Geophysical Research.* **101D** 21,319-21,325.

Latif, M., R. Kleeman and C. Eckert. 1997. Greenhouse warming, decadal variability, or El Niño? An attempt to understand the anomalous 1990's. *Journal of Climate.* **10** 2221-2239.

Lau, N-C. 1988. Variability of the observed midlatitude storm tracks in relation to low-frequency patterns in the circulation pattern. *Journal of the Atmospheric Sciences.* **45** 2718-2743.

Lau, N-C. 1997. Global SST anomalies and the midlatitude atmospheric circulation. *Bulletin of the American Meteorological Society.* **78** 21-33.

Lau, N-C. and M. Nath. 1991. Variability of the baroclinic and barotropic transient eddy forcing associated with monthly changes in the midlatitude storm tracks. *Journal of the Atmospheric Sciences.* **48** 2589-2613.

Lu, J. and R. Greatbatch. 2002. The changing relationship between the NAO and northern hemisphere climate variability. *Geophysical Research Letters.* **29** 52-1 – 52-4.

Mantua, N., S. Hare, Y. Zhang, J. Wallace and R. Francis. 1997. A Pacific interdecadal climate oscillation with impacts on Salmon production. *Bulletin of the American Meteorological Society.* **78** 1069-1079.

McCabe, G. and M. Dettinger. 1999. Decadal variations in the strength of ENSO teleconnections with precipitation in the western United States. *International Journal of Climatology.* **19** 1399-1410.

Metz, W. 1989. Low frequency anomalies of atmospheric flow and the effects of cyclone-scale eddies: a canonical correlation analysis. *Journal of the Atmospheric Sciences.* **46** 1027-1041.

Miller, A. and N. Schneider. 2000. Interdecadal climate regime dynamics in the North Pacific Ocean: theories, observations and ecosystem impacts. *Progress in Oceanography.* **47** 355-379.

Minobe, S. 1997. A 50-70 year climatic oscillation over the North Pacific and North America. *Geophysical Research Letters.* **24** 683-686.

Minobe, S. 1999. Resonance in bidecadal and pentadecadal climate oscillations over the North Pacific: role in climatic regime shifts. *Geophysical Research Letters.* **26** 855-858.

Minobe, S. 2000. Spatio-temporal structure of the pentadecadal variability over the North Pacific. *Progress in Oceanography.* **47** 381-408.

Moore, D. and G. McCabe. 1993. *Introduction to the practice of statistics, 2nd Ed.* W.H. Freeman and Company, New York.

Nakamura, H., T. Izumi and T. Sampe. 2002. Interannual and decadal modulations recently observed in the Pacific storm track activity and East Asian Winter Monsoon. *Journal of Climate.* **15** 1855-1874.

Nitta, T. and S. Yamada. 1989. Recent warming of tropical sea surface temperature and its relationship to the northern hemisphere circulation. *Journal of the Meteorological Society of Japan.* **67** 375-383.

Paciorek, C., J. Risbey, V. Ventura and R. Rosen. 2002. Multiple indices of Northern Hemisphere cyclone activity, winters 1949-99. *Journal of Climate.* **15** 1573-1590.

Peixoto, J. and A. Oort. 1992. *Physics of Climate.* American Institute of Physics, New York. 520pp.

Power, S., T. Casey, C. Folland, A. Colman and V. Mehta. 1999. Interdecadal modulation of the impact of ENSO on Australia. *Climate Dynamics.* **15** 319.

Qian, W., L. Quan and S. Shi. 2002. Variations of the dust storm in China and climatic control. *Journal of Climate.* **15** 1216-1229.

Rogers, J. 1997. North Atlantic storm track variability and its association to the North Atlantic Oscillation and climate variability of northern Europe. *Journal of Climate.* **10** 1635-1647.

Seager, R., Y. Kushnir, N. Naik, M. Cane and J. Miller. 2001. Wind-driven shifts in the latitude of the Kurishio-Oyashio extension and generation of SST anomalies on decadal timescales. *Journal of Climate.* **14** 4249-4265.

Serreze, M. 1996. Arctic cyclone track data set, 1966-1993. Boulder, CO. National Snow and Ice Data Centre. Digital Media.

Serreze, M., F. Carse and R. Barry. 1997. Icelandic low cyclone activity: Climatological features, linkages with the NAO and relationships with recent changes in Northern Hemisphere circulation. *Journal of Climate.* **10** 453-464.

Simmons, A. and B. Hoskins. 1978. The life cycles of some nonlinear baroclinic waves. *Journal of the Atmospheric Sciences.* **35** 414-432.

Straus, D. and J Shukla. 1997. Variations of mid-latitude transient dynamics associated with ENSO. *Journal of the Atmospheric Sciences.* **54** 777-790.

Taylor, K. 1986. An analysis of the biases in traditional cyclone frequency maps. *Monthly Weather Review.* **114** 1481-1490.

Thompson, S. and D. Pollard. 1997. Greenland and Antarctic mass balances for present and doubled atmospheric CO_2 from the GENESIS Version-2 Global Climate Model. *Journal of Climate.* **10** 871-900.

Trenberth, K. 1990. Recent observed interdecadal climate changes in the northern hemisphere. *Bulletin of the American Meteorological Society.* **71** 988-993.

Trenberth, K. and J. Hurrell. 1994. Decadal atmosphere-ocean variations in the Pacific. *Climate Dynamics.* **9** 303-319.

Troup, A. 1965. The Southern Oscillation. *Quarterly Journal of the Royal Meteorological Society.* **91** 490.

van Loon, H. and J. Williams. 1979. The association between latitudinal temperature gradient and eddy heat transport, Part II: Relationships between sensible heat transport by stationary waves and wind, pressure and temperature in the winter. *Monthly Weather Review.* **108** 604-614.

Watts, I. 1969. Climates of China and Korea. *Climates of Northern and Eastern Asia, World Survey of Climatology.* H. Arakawa, Ed., Vol. 8. Elsevier, 1-118.

Wilks, D. 1995. *Statistical methods in the atmospheric sciences: An introduction.* Academic Press, 464pp.

Zhang, Y., J. Wallace and D. Battisti. 1997. ENSO-like interdecadal variability: 1900-93. *Journal of Climate.* **10** 1004-1020.

Zhang, X., J. Sheng and A. Shabbar. 1997. Modes of interannual and interdecadal variability of Pacific SST. *Journal of Climate.* **11** 2556-2569.